The Institute of Paper Chemistry

Appleton, Wisconsin

Doctor's Dissertation

An Evaluation of Column Thermal Diffusion as a Means of Polymer Characterization

David L. Taylor

June, 1962

AN EVALUATION OF COLUMN THERMAL DIFFUSION AS A MEANS OF POLYMER CHARACTERIZATION

A thesis submitted by

David L. Taylor

B.S.E. 1957, Princeton University
M.S. 1959, Lawrence College

in partial fulfillment of the requirements
of The Institute of Paper Chemistry
for the degree of Doctor of Philosophy
from Lawrence College,
Appleton, Wisconsin

June, 1962

TABLE OF CONTENTS

INTRODUCTION

BACKGROUND AND PURPOSE OF STUDY

Thermal diffusion is one of a family of transport phenomena characterized by the migration of particles or molecules under the influence of an externally applied force field. A temperature gradient provides the driving force in thermal diffusion while in the transport processes of sedimentation and electrophoresis the gravitational and electrical fields play analogous roles. In most systems the thermal diffusion effect is weak, and therefore the concentration gradients established in gaseous or liquid solutions exposed to moderate temperature gradients are small.

Thermal diffusion remained a relatively obscure facet of physical chemistry from its initial experimental discovery over one hundred years ago until the invention of the Clusius-Dickel separation tube in the late 1930's. By employing a radial temperature gradient in long concentric vertical tubes, Clusius and Dickel effected dramatic separations of gaseous mixtures (1). The convection currents arising in such an apparatus serve to enhance the thermal diffusion separation in much the same manner that refluxing in a distillation column produces a purer distillate. The process was used to some extent on a large scale as a first-stage separation of uranium isotopes during World War II (2). Thermal diffusion in the liquid phase has received considerable study in recent years, particularly in the petroleum industry (3-5). Attempts to fractionate tall oil from the kraft wood pulping process by thermal diffusion have met with some success (6).

Current interest in thermal diffusion of polymers stems from the work of Debye and Bueche (7) in which it was demonstrated that high polymer solutions

exhibit a rather large thermal diffusion effect and that some fractionation by molecular size occurs in a Clusius-Dickel column. This study has inspired several workers (8-11) to investigate more fully the practicability of thermal diffusion fractionation of high polymers. These recent investigations have largely been of a "screening" nature in that various polymers and modifications of technique have been employed in an effort to discover the extent of fractionation attainable under various conditions. Such an approach is a lengthy one and is likely to leave unrevealed the more fundamental aspects governing the process, knowledge of which would permit a broader answer to the question of the usefulness of thermal diffusion in polymer systems. It is the purpose of this thesis to elucidate the nature of polymer thermal diffusion in a Clusius-Dickel column.

APPROACH AND SCOPE

There are two basic methods of performing a thermal diffusion experiment: a) the static or "cell" method, in which the temperature gradient is established vertically so that there is no convective flow of solution, and b) the "column" method, in which a horizontal temperature gradient induces enriching convection currents as in a Clusius-Dickel column. From the steady state concentration gradient in a thermal diffusion cell, the thermal diffusion constant, α, has been calculated for several polymer-solvent systems (12, 13). The factor α is related to the ordinary diffusion coefficient D and the thermal diffusion coefficient D' by

$$\alpha = -D'T/D \qquad (1)$$

where T is the absolute temperature. The dimensionless grouping of variables in Equation (1) is derived from the integrated, steady state, one dimensional form of the operational equation for mass flux J due to combined ordinary and thermal

diffusion,

$$J = -D\nabla c - D'c\nabla T \qquad (1a)$$

where c is the concentration. The concentration gradient established in a thermal diffusion cell is the result of a balance between the separation tendency due to thermal diffusion and the resultant remixing due to ordinary diffusion, and therefore it is apparent that α, and not D' alone, determines the steady state separation. The cell method has been modified to provide a direct measure of the thermal diffusion coefficient D' through observation of the rate of motion of the boundary between layers of solution and solvent in a temperature gradient (14-16). Although the data obtained concerning α and D' shed significant light on theories of polymer thermal diffusion (12, 17), they cannot be of use in predicting results obtainable in column experiments until more is known about the controlling factors and detailed mechanism of column operation.

The emphasis in the present study was placed on the investigation of a physical process per se rather than on the development of a technique. Hence, a single polymer, polystyrene, was chosen as a test specimen for the entire work. It is expected that general conclusions resulting from the present study regarding the column thermal diffusion of polymers will be valid independent of the chemical nature of the particular polymers involved. Although the precise magnitudes of the various effects differ from system to system, it was hoped that the data obtained would provide the basis for an understanding of the basic mechanisms involved.

The experimental approach to the problem consisted of a systematic study of the behavior of various solutions of well-characterized polystyrene subjected to varying operating conditions in a thermal diffusion column. The resulting data were then interpreted in light of a mathematical analysis and existing theories and data to yield a clearer understanding of the process than has hitherto been available.

THEORETICAL BACKGROUND

THEORY OF POLYMER THERMAL DIFFUSION

THERMODYNAMICS OF IRREVERSIBLE PROCESSES

The General Relations

Classical thermodynamics deals with systems at equilibrium where all gradients of variables of state have vanished. The equilibrium state is characterized by a zero rate of production of entropy, and any deviations from equilibrium can be treated only in terms of inequalities. The concern of the thermodynamics of irreversible processes is the systematic description of the relationships existing between the fluxes, gradients, and entropy production characteristic of nonequilibrium processes.

Associated with any nonequilibrium process is a positive production of entropy as dictated by the Second Law. The rate of production of entropy is always found to be equal to the product of the gradient of a variable of state (the generalized force or "affinity") and the directly associated rate of flow of matter or energy (the "flux"). Thus, it is a matter of experience that

$$\sigma = dS_{irr}/dt = \Sigma_i J_i X_i \qquad (2)$$

where the entropy production rate, σ, is related to the fluxes, $\underline{J_i}$, and affinities, $\underline{X_i}$, characterizing the system at a given time. It is reasonable to assume that near equilibrium the fluxes are linearly related to the affinities and that, in principle, each affinity can contribute to each flux. Hence,

$$J_i = \Sigma_k L_{ik} X_k \qquad (3)$$

where there are k nonequilibrium processes taking place and L_{ik} are the phenomenological coefficients. Assuming the principle of microscopic reversibility, L. Onsager (1) demonstrated that

$$L_{ik} = L_{ki} \quad . \tag{4}$$

The above three equations constitute the groundwork of the thermodynamics of irreversible processes.

The Net Heat of Transport in Thermal Diffusion

Consider a two-component system with a temperature gradient imposed upon it in such a manner that there are no convection currents. The thermal gradient induces a flux of each component as well as a heat flux. The associated affinities, chosen to satisfy Equation (2) are $-\text{grad}(\mu/T)$ for each component where μ is the chemical potential and $\text{grad}(1/T)$ for the heat flow. The fluxes and affinities for each component are related through a mass balance and the Gibbs-Duhem relation so that there need be only two Equations (3) to describe the process. These may be written as

$$J_1 = -L_{11}\,\text{grad}(\mu_1/T) + L_{1q}\,\text{grad}(1/T) \tag{5a}$$

$$J_q = -L_{q1}\,\text{grad}(\mu_1/T) + L_{qq}\,\text{grad}(1/T) \tag{5b}$$

where the subscript 1 refers to mass component and 1 and q to heat transport. The contribution to the mass flux indicated by the L_{1q} term is the thermal diffusion effect, and directly related to it through the Onsager relation is the contribution to the heat flux due to mass flow indicated by the L_{q1} term (the Dufour diffusion-thermo effect). From Equations (5) it can be seen that in the absence of a temperature gradient, the heat flow due to the transport of unit

mass of component 1 is given by

$$J_q/J_1 = L_{q1}/L_{11} \equiv Q_1^* \tag{6}$$

where Q_1^* is defined as the "net heat of transport." Applying the Onsager reciprocal relation (4) to Equation (6) and substituting into (5a) under steady state conditions where J_1 is zero, we have

$$\text{grad}(\mu_1/T) = Q_1^* \text{ grad}(1/T) \tag{7}$$

or, in the one-dimensional case,

$$(\partial\mu_1/\partial N_1)_{T,P}(dN_1/dT) = -Q_1^*/T \tag{8}$$

where N_1 is the mole fraction of component 1. For an ideal solution Equation (8) reduces to

$$d\ \ln N_1/dT = -Q_1^*/RT^2 \tag{9}$$

Thus, the concentration gradient established at steady state in thermal diffusion is directly related to the net heat of transport. Q^* is variously interpreted as

a) That energy carried by the diffusing molecule in excess of its enthalpy at the temperature existing at the origin of the diffusive step (18);

b) That heat which must be absorbed by the region out of which the molecule diffuses to maintain constant the temperature and pressure of that region (19).

Thermodynamics alone can give no further insight into the nature of the net heat of transport.

DRICKAMER DEVELOPMENT

H. G. Drickamer and co-workers have developed expressions for the net heat of transport in liquids starting from molecular interpretations due to Denbigh and including corrections for differences in size and shape of the molecules (20, 21, 12). The Q_1^* (for solute and solvent) are interpreted in terms of the molar activation energy for viscous flow per unit partial molar volume and are related to the experimentally measurable phenomenological coefficients in the following manner.

Writing Equation (8) for both components and combining with the Gibbs-Duhem relation,

$$N_1(\partial\mu_1/N_1) + N_2(\partial\mu_2/N_2) = 0 \tag{10}$$

along with the fact that

$$N_1 + N_2 = 1 \tag{11}$$

we obtain

$$(\text{grad } N_1)/N_1N_2 = ([(Q_2^* - Q_1^*)/N_1(\partial\mu_1/\partial N_1)] \text{ grad } T)/T \tag{12}$$

The phenomenological mass flux equation for component 1 can be written as

$$J_1 = -\rho D \,[\text{grad } N_1 - (\alpha N_1N_2/T) \text{ grad } T] \tag{13}$$

where ρ is the solution density, D is the ordinary diffusion coefficient, and α is the thermal diffusion ratio. At steady state where J_1 is zero, Equation (13) combined with Equation (12) gives the relation

$$\alpha = (Q_2^* - Q_1^*)/[N_1 (\partial\mu_1/\partial N_1)] \tag{14}$$

Drickamer and co-workers have applied their molecular interpretations to (14) and have derived, in the case of polymer solutions (12), the relation that α should be directly proportional to the molecular weight of a polymer in solution at low concentrations.

The thermal diffusion ratio α is a measure of the extent of separation of solute from solution at steady state as expressed by the relation

$$\alpha = (T/N_1N_2)\ \partial N_1/\partial T \qquad (15)$$

derivable from Equation (13). Hence, the Drickamer relations would indicate that a fractionation by molecular weight should occur in a convection free experiment at low concentrations.

KINETIC APPROACH

Debye and Bueche

In the earliest detailed report on thermal diffusion in polymer solutions (7), P. Debye and A. M. Bueche presented a molecular interpretation of thermal diffusion in which the Einstein approach to ordinary diffusion in terms of Brownian motion of the solute particles was extended to the nonisothermal case. It was concluded that the asymmetric character of the transition probability function of the solute molecules in a thermal gradient is the main contributing factor to the thermal diffusion effect, but that the temperature dependence of the ordinary diffusion coefficient is of some importance. Thus, Debye and Bueche considered that a bias in the "random walk" motion of the solute particles, induced by the temperature nonuniformity, is the important underlying effect. The relation of this bias to the molecular weight of dissolved polymer molecules was not discussed.

Theory of Ham

Recently, J. S. Ham has presented a kinetic theory of thermal diffusion in dilute polymer solutions (17). A simple Brownian motion model was adopted as in the treatment of Debye and Bueche, but the diffusive flow was assumed to be separable, in concept, into the individual fluxes of polymer into solution, solvent into solution, and the bulk mass flow necessary to avoid pressure gradients. The superposition of these fluxes to give the net result constituted the main assumption of Ham's theory. Ham's Equation (6) describing the diffusive flux of either component into the solution in terms of the transition probability function is fully equivalent to Equation (7) of the Debye-Bueche treatment, but in the latter case only the polymer flow was considered. In direct contrast to the Debye-Bueche theory, Ham's theory indicates that the asymmetry of the transition probability function is not an essential factor in thermal diffusion, but that the temperature dependence of the mean square of the transition function (which is associated with the diffusion coefficient at low concentrations) is the main contributing factor. The thermal diffusion coefficient, D', was then shown to depend on the difference of two activation energies (for polymer and solvent as in the Drickamer treatment) which are weighted by the diffusion coefficients so that for sufficiently large polymer molecules D' should be independent of molecular weight. Ham's theory also predicts that polymers should always thermally diffuse in the direction of heat flow. The detailed lattice model kinetic approach of Prager and Eyring (22) gave equivalent results.

PHYSICAL INTERPRETATIONS OF THERMAL DIFFUSION

Denbigh noted (23) that if the net heat of transfer is zero--that is, if the diffusing molecule carries no energy in excess of its enthalpy at the origin of

the diffusive step--then no concentration gradient will be established under the influence of a temperature gradient. This implies that only high energy molecules can jump to a neighboring region of different temperature, and they carry their excess energy with them. It is from this point of view that Drickamer and co-workers have developed their theory of thermal diffusion.

If one accepts the above picture of thermal diffusion being an activated process, then the net heat of transfer, if not zero, will be positive because the jumping molecule takes excess heat with it. Then, considering the Le Chatelier principle, the jump will be biased toward the cold regions where the heat can be readily dissipated (24). Hence, a thermal diffusion separation in a multicomponent system results from the differences, among the components, of the general tendency to concentrate in the cold region as borne out by Equation (14). The temperature-density relation for a pure substance may be considered as the special one-component case or as evidence of self-thermal diffusion.

One further interpretation of thermal diffusion has met with some success (25). At a given temperature all components of a solution will have the same mean kinetic energy but the molecules of greatest mass will have the greatest momentum. Hence, a large molecule will penetrate more deeply into cooler regions where its mean square displacement due to Brownian motion is decreased. The molecule is "trapped" in the sense that it will have much less tendency to return to its warmer origin than to proceed even further toward cooler regions. The smaller molecules will be less effectively trapped and a separation will occur.

THEORY OF THE CLUSIUS-DICKEL COLUMN

GENERAL CONSIDERATIONS

The steady-state separations attainable by thermal diffusion in a single convection-free apparatus are small, but by introducing free convection the

separation effect can be greatly enhanced. In a Clusius-Dickel column the temperature gradient is established perpendicular to the gravitational field such that, if the solution under study has a nonzero thermal expansivity, natural convection currents will arise. These currents serve to magnify the thermal diffusion separation occurring in the direction of the temperature gradient in a manner analogous to the improved separation attained in a distillation column through refluxing (1). A Clusius-Dickel column operated with no net material flow through the column corresponds to total reflux distillation. In the usual case of a negative temperature coefficient of density, a solute diffusing in the direction of heat flow in a Clusius-Dickel column will be swept toward the bottom of the column by the cool down-flowing convection stream while the solute-deficient solution remaining near the hot wall will be carried toward the top of the column by the rising warm stream. Thus, a separation in the vertical direction results. At steady state the separation process due to transport of solute between convection streams is balanced against the remixing due to the return of convective flows from the column ends such that there is no net vertical transport of solute. The vertical concentration gradient resulting from thermal diffusion should give rise to an upward transport of solute due to ordinary diffusion, but this transport is easily shown to be negligible in a practical Clusius-Dickel column where the vertical dimension is many times greater than the transverse dimension (Appendix I).

Fractionation of a multicomponent solute would be expected to occur in a Clusius-Dickel column if the rate of transport of the constituents in a temperature gradient differed. As all the constituents participate equally in the convective flow at any point in the column, the fractionation effect should be directly related to the differences in rate of horizontal transport. A complete fractionation cannot be expected because every molecular species must be found at the bottom

of the column, being returned there by the down-flowing convection stream. In principle, however, the distribution of molecular species in the original solute could be calculated from a prior knowledge of the thermal diffusion behavior of the individual species (Appendix II).

MATHEMATICAL TREATMENTS

A rather complete mathematical treatment of the operation of Clusius-Dickel columns has been given by Jones and Furry (26). The separation of gaseous isotopes was of primary concern in the Furry-Jones treatment but recently Emery (27) has introduced into their equations the strong temperature dependencies of viscosity and diffusion in liquids. Because of the extreme concentration dependence of viscosity and diffusion in the case of polymer solutions, it was decided in the present study to employ a detailed mathematical description only in the extreme case of infinitely dilute solutions. In this limit the problem of describing the exact form of the convection velocities can be separated from any concern of solute transport. The problem of describing the concentration gradients established by the diffusive flow of solute molecules can then be treated after the convective flow problem has been solved. Although the Furry-Jones equations could be adapted to the present study, a more direct approach through simple reduction of the general differential transport equations was chosen.

Flow Problem

The general hydrodynamical equation for steady state laminar flow of an incompressible fluid is

$$\nabla \cdot \left\{ \eta(\nabla \vec{v}) + \eta(\nabla \vec{v})' \right\} = \nabla p - \rho \vec{G} \qquad (16)$$

where

η = viscosity

$\underline{\vec{v}}$ = velocity vector

$\underline{p}$ = pressure

ρ = density, and

$\underline{\vec{G}}$ = field forces (e.g., gravity).

We then make the following assumptions which are valid in the case of a long cylindrical vertical column operated with the working solution at infinite dilution:

(a) The temperature gradient is unidirectional in the radial co-ordinate;

(b) All derivatives in the circumferential direction are zero;

(c) There is no radial component of velocity (i.e., ends of column are being ignored);

(d) The viscosity is determined solely by the temperature which implies that the vertical velocity is a function only of the radial co-ordinate.

With these assumptions, Equation (16) expressed in cylindrical co-ordinates $\underline{r}$ and $\underline{z}$, representing radial and vertical directions respectively, becomes

$$(1/r)(d/dr)(\eta r dv_z/dr) = \rho g + dp/dz \qquad (17)$$

where $\underline{v_z}$ is the vertical convection velocity. The quantity $\underline{dp}/\underline{dz}$ differs slightly from the static fluid head gradient because of the convective flows. The boundary and integral conditions to be satisfied are

$$v_z = 0 \quad \text{when} \quad r = r_c, r_h \qquad (18)$$

and

$$\int_{r_c}^{r_h} \rho v_z r dr = 0 \tag{19}$$

expressing no flow at the walls (located at r_c and r_h) and no net flow through the column.

Diffusion Problem

At steady state the transport of solute molecules through any small region of the column by means of thermal diffusion, ordinary diffusion, and bulk convection must give no net change of solute concentration in the region; hence, at steady state we have

$$\nabla\cdot(D'c\nabla T) + \nabla\cdot(D\nabla c) - \nabla\cdot(c\vec{v}) = 0 \tag{20}$$

where c is the concentration and the other terms are as previously defined. Making the same assumptions as in the flow problem and, in addition, assuming that ordinary diffusion in the vertical direction is negligible (see Appendix I for justification), Equation (20) expressed in cylindrical co-ordinates becomes

$$(1/r)(\partial/\partial r)(rD'c\theta + rD\partial c/\partial r) = v_z\, \partial c/\partial z \tag{21}$$

where $\theta = dT/dr$. The temperature gradient θ is constant to the extent that the thermal conductivity of the solution is independent of temperature in the range of the experiment. The boundary and integral conditions to be satisfied are

$$(D'c\theta + D\,\partial c/\partial r)_{r=r_c,\, r_h} = 0 \tag{22}$$

and

$$\int_{r_c}^{r_h} rcv_z dr = 0 \tag{23}$$

expressing the impermeability of the walls to solute transport and the absence of a net vertical transport of solute at any level in the column. Exclusion of the vertical diffusion term allows the independent variables r and z to be separated upon substitution of

$$c = P(r)Q(z) \tag{24}$$

into Equation (21) resulting in

$$\frac{d^2P}{dr^2}\frac{D}{Pv_z} + \frac{dP}{dr}\left[\frac{\theta D'}{v_z P} + \frac{D}{rv_z P} + \frac{\theta}{Pv_z}\frac{\partial D}{\partial T}\right] + \frac{\theta D'}{rv_z} + \frac{\theta^2}{v_z}\frac{\partial D'}{\partial T} = \frac{1}{Q}\frac{dQ}{dz} \tag{25}$$

with Equations (22) and (23) transformed to

$$(D'P\theta/D + dP/dr)_{r=r_c,\, r_h} = 0 \tag{26}$$

and

$$\int_{r_c}^{r_h} rPv_z dr = 0 \tag{27}$$

The left side of Equation (25) is a function of r only and the right side is a function of z only; hence, both sides must be constant, independent of r and z. Therefore, let

$$\gamma \equiv -(1/Q)dQ/dz \tag{28}$$

where γ is the "extinction coefficient" expressing the rate at which the logarithm of the concentration changes in the z-direction along the length of the column. Integrating Equation (28) gives

$$Q = \text{const.}\exp(-\gamma z) \tag{29}$$

which shows that the concentration in the column should vary exponentially with vertical distance for sufficiently dilute solutions. More than one value of γ

will satisfy Equations (25) through (27), the values of γ being the eigenvalues of Equation (25). The concentration as a function of z ought then to be the sum of Q's given by Equation (29) using the various values of γ. However, for values of γ other than the lowest eigenvalue the Q function will more rapidly decrease to zero with increased z, and therefore we can equate experimental measurements of the extinction coefficient with the lowest γ eigenvalue. Substituting Equation (28) into (25) and rearranging gives a more convenient form of the differential equation:

$$\frac{d^2P}{dr^2} + \left(\frac{\theta D'}{D} + \frac{1}{r} + \frac{\theta}{D} \frac{\partial D}{\partial T} \right) \frac{dP}{dr} + \left(\frac{\gamma v_z}{D} + \frac{\theta D'}{rD} \right) P = 0 \qquad (30)$$

The term expressing the temperature dependence of D' has been omitted in Equation (30) as there is available at present no adequate means for estimating this term in the calculations. Computed values of D' will then correspond to some temperature near the middle of the range in a particular experiment.

MATERIALS AND EQUIPMENT

POLYMERS CHOSEN FOR STUDY

Polystyrene was selected as the polymer to be used in the present study because it fulfilled the following criteria: (a) readily soluble in a wide variety of solvents, (b) chemically stable over considerable temperature ranges, (c) chemically uniform linear chain structure, and (d) extensiveness of pertinent literature data available concerning solution properties. The polystyrene samples were prepared and provided by Dr. H. W. McCormick of the Dow Chemical Company and had the following molecular weight characteristics (Table I) as determined by the supplier using an ultracentrifugal sedimentation velocity technique (28):

TABLE I

POLYSTYRENE SAMPLE PROPERTIES

Polymer Designation	Preparative Technique	Weight Av. Mol. Wt.	Wt. Av./Num. Av. Ratio, $\overline{M}_w/\overline{M}_n$
B6	Isothermal Thermal polymerization	434,000	2.85
S102	Szwarc "living polymer"	82,000	1.05
S111	Szwarc "living polymer"	239,000	1.08
S114	Szwarc "living polymer"	3,560,000	1.24

Polymer B6, of very broad molecular weight distribution, was the main polymer of interest in the present study. The three narrow distribution polymers were made available through the International Standard Exchange Program. These polymers are all free of cross-linking and are of the random, atactic configuration. Polymer B6 was found to contain about 2% by weight of volatile material.

Because of the important role which the broad distribution Polymer B6 was to have in the experimental program, the complete molecular weight distribution for

this polymer was determined by ultracentrifugal sedimentation velocity boundary analysis (see Appendix III for details). A Spinco Model E ultracentrifuge with the schlieren optical system was used for the synthetic boundary sedimentation velocity experiments which were performed at 35°C. in cyclohexane. The effects of diffusion were eliminated by extrapolation to infinite time in the manner described by Baldwin (29), and the concentration effect was corrected for analytically by Baldwin's method (30) except that the Johnston-Ogston effect, which is small in polymer systems, was ignored. The concentration correction factors were deduced from literature data on several polystyrene-solvent systems as described in Appendix III. Sedimentation coefficients were converted to molecular weight by means of the relation derived by McCormick (28). The root-mean-square sedimentation coefficient was found to be 8.56 svedbergs, tolerably close to the value 8.59 obtained by McCormick using the full double extrapolation technique of Williams (31). The weight distribution of molecular weight for Polymer B6 is given in Fig. 1.

No measurements of thermal diffusion fractionation of the narrow distribution polymers were to be made, and therefore the ultracentrifuge work was not extended to these polymers.

SOLVENTS USED

The degree of thermodynamic interaction between polymer and solvent largely determines the configuration of the molecules of a particular polymer species in solution (32, p. 424). The molecular configuration in turn strongly affects the magnitude of the molecular transport properties--and thermal diffusion should be no exception. Hence, two solvents representing the thermodynamic extremes have been chosen for the present study.

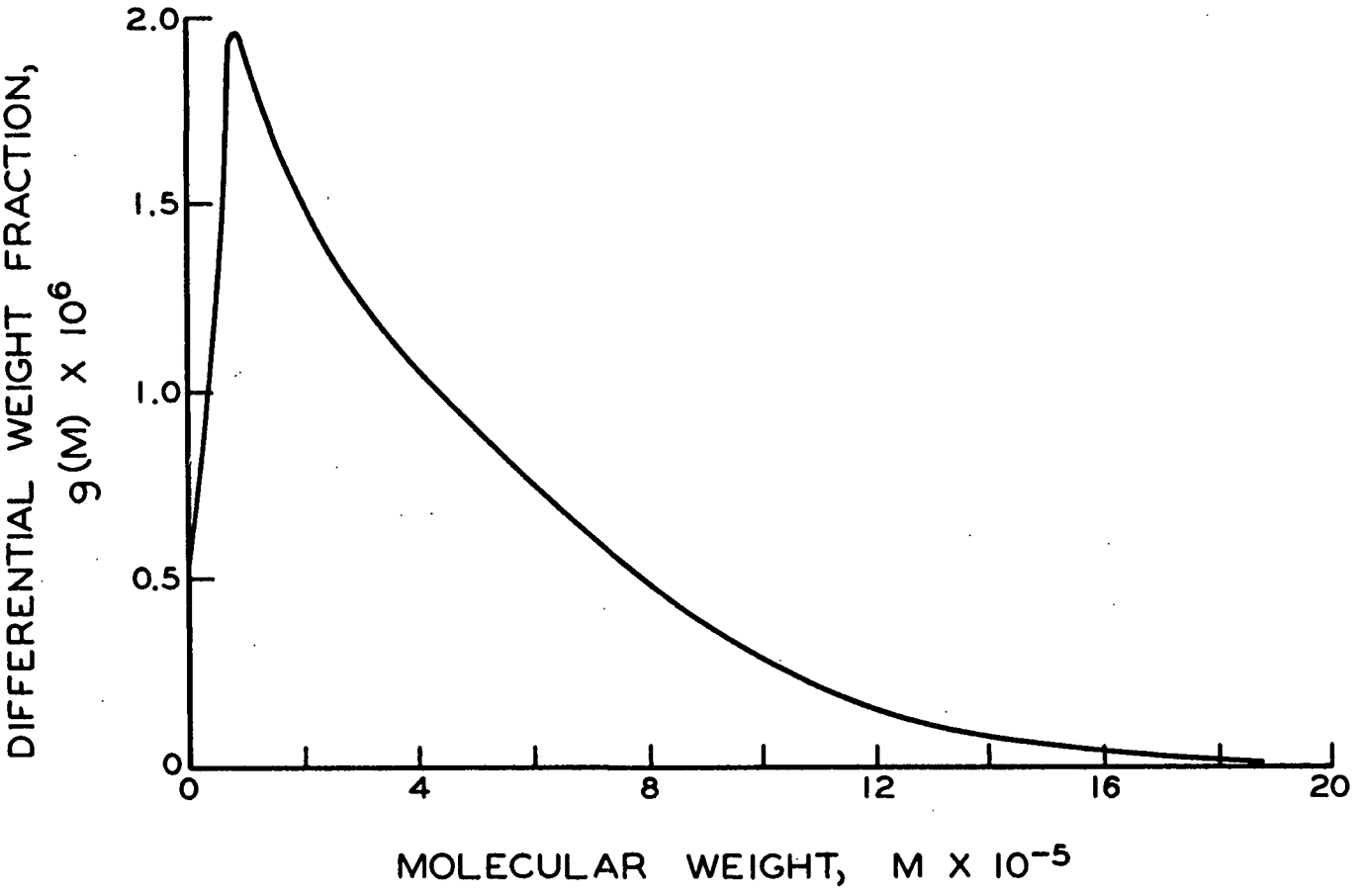

Figure 1. Molecular Weight Distribution of Polymer B6

Viscosity is a second consideration involved in the choice of solvents because of its effect on the hydrodynamic aspects of column thermal diffusion. The viscosity of polymer solutions increases with concentration most rapidly in thermodynamically good solvents, and therefore the good solvent chosen for the present study should have a higher viscosity than the poor solvent so as to avoid any reversal of the solution viscosity vs. solvent relation for different concentrations. Toluene and methyl ethyl ketone (MEK) have been found to satisfy the above requirements as shown in Table II.

TABLE II

SOLVENT CHARACTERISTICS

Solvent	Thermodynamic Solvent Power	Second Virial Coeff., atm. $I.^2/g.^2$ (33)	Viscosity, cp. at 30°C.
Toluene	Strong	1.46	0.52
MEK	Weak	0.12	0.38

Reagent-grade toluene (Baker's) was used after redistilling. Reagent-grade MEK (Matheson, Coleman, and Bell) was dried over anhydrous calcium sulfate and redistilled prior to use.

THERMAL DIFFUSION COLUMN

CONSTRUCTION

The thermal diffusion column employed throughout the experimental work was of the metallic concentric cylinder type and was purchased from the M. Fink Company, Brecksville, Ohio. The important dimensions were: (a) length of column holding test liquid, six feet, (b) width of annular space (distance of separation between tubes), 0.0300 inch, and (c) mean diameter of annulus, 0.6345 inch. Metal surfaces in liquid contact were of type 304 stainless steel. Gaskets and gland packing were of teflon. The volume capacity of the column (the annular volume) was 70.4 ml. Thirty sample ports connecting with the annulus and evenly spaced along the entire length of the column permitted adequate flexibility of sampling schedules. The inner of the two concentric tubes enclosing the working space served as the cold wall of the thermal diffusion column and was connected to hot and cold water taps through a Powers Fotoguard mixing valve which provided constant temperature cooling water at two to three gallons per minute. The column was equipped with three iron-constantan thermocouples silver soldered directly to the outer wall at top,

center, and bottom positions along the column. A triple strand nichrome heating wire was embedded in a ceramic cement and spiral-wound around the outer tube. As received from the manufacturer, the column was wrapped with a double layer of heavy asbestos tape, but initial experiments indicated a large 35% heat loss as well as a certain nonuniformity of hot wall temperature, and therefore the column construction was modified. The asbestos insulation was removed and five Cenco heating tapes, each six feet by one-half inch, were carefully wrapped around the column, edge to edge, directly on top of the ceramic cement; then the column was encased with a one-inch layer of magnesia pipe insulation which reduced the heat loss to about 5%. The electrical input to each of the five heating tapes and the nichrome heating element was controlled independently by means of six Variac variable transformers. A cross section of the column including sample port construction is shown in Fig. 2.

THERMOCOUPLE CALIBRATION

The permanently fixed thermocouples were calibrated in situ by pumping water from a thermostated bath through short sections of the column annulus by way of the sample ports on either side of each thermocouple. The calibration points obtained in the 20 to 80°C. range fell on well-defined straight lines in close agreement with literature values for iron-constantan. The thermocouple circuit used is shown in Fig. 3.

ANNULAR SPACING

The distance between the hot and cold wall is the most important geometrical factor in thermal diffusion column theory, and therefore this dimension was accurately determined. The inner tube of the column projected beyond the column proper and its outer diameter was therefore readily determined by micrometer to

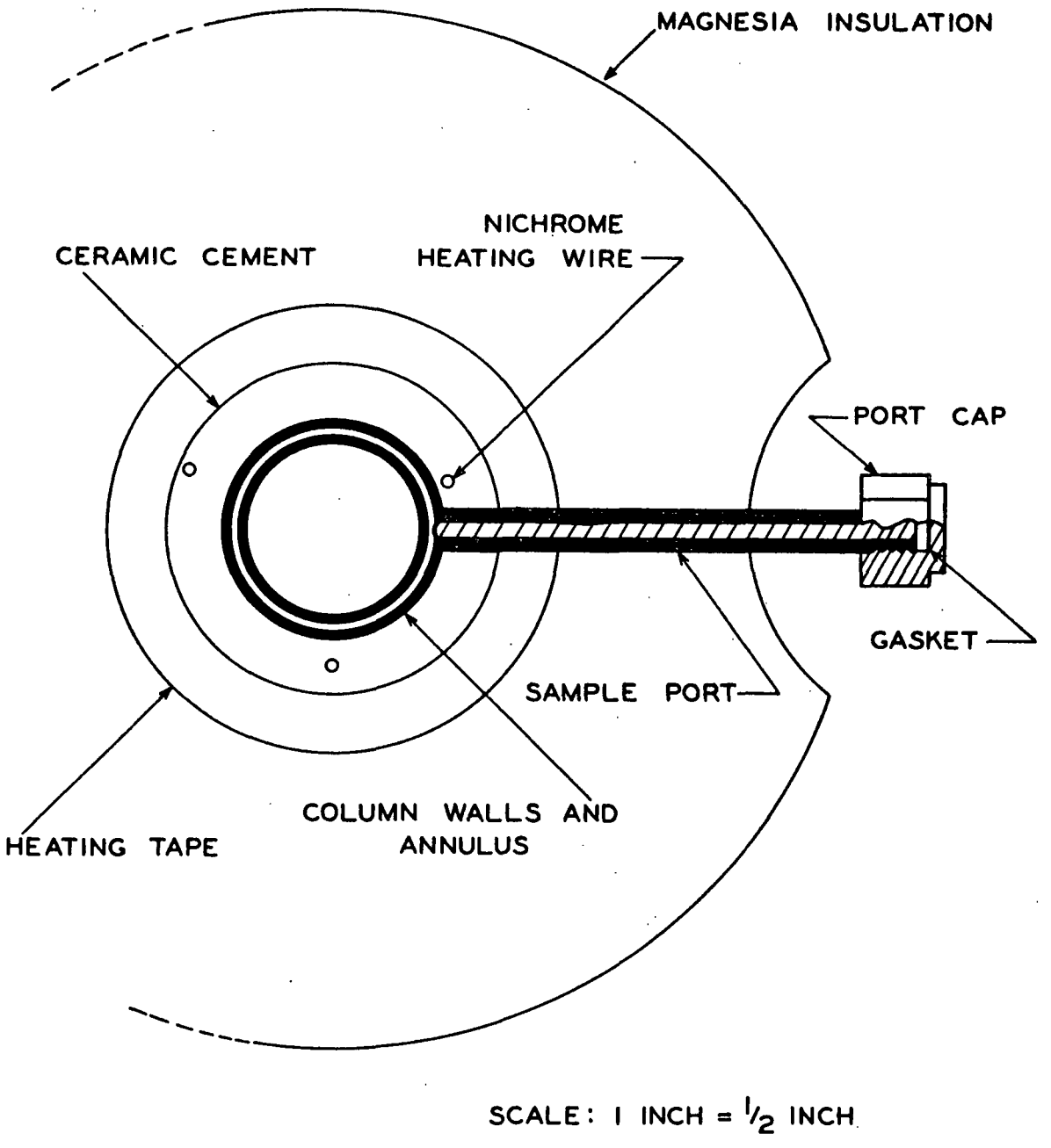

Figure 2. Column Cross Section

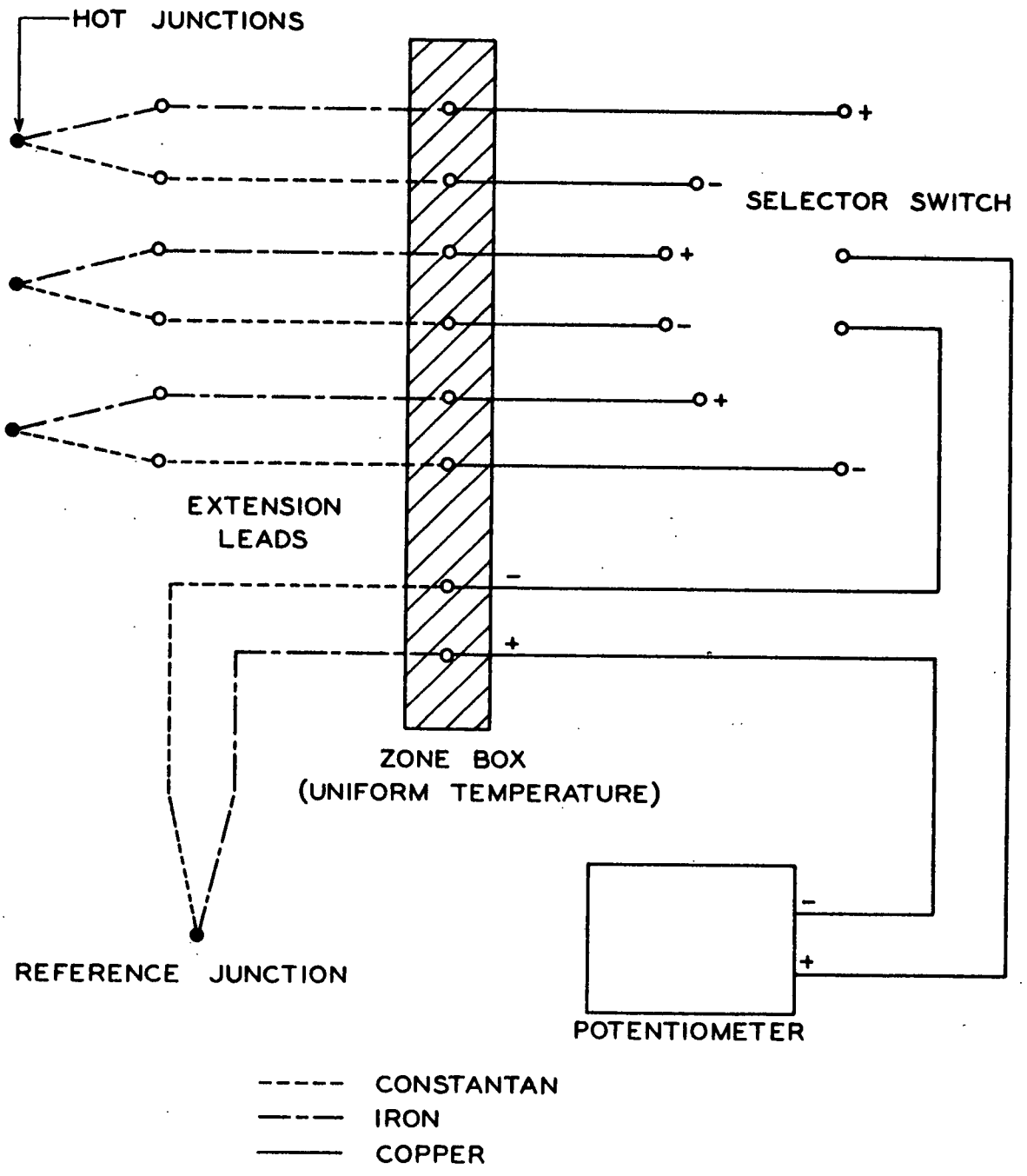

Figure 3. Thermocouple Circuit

be 0.6045 inch; this represents the inner diameter of the annulus. The total volume of the annulus was then determined by filling the column with n-hexane and weighing the drained liquid. The column was drained once in six stages and once in three stages, and the two total volumes (differing by about 0.4%) were extrapolated to zero number of draining stages (zero hold-up) to give a column volume of 70.37 cc. and a calculated annular spacing of 0.02992-inch which was in excellent agreement with the specified 0.0300 inch.

The spacing as found above is an average value. To measure the uniformity of spacing along the length of the column, ten sample volumes of n-hexane were drained from groups of three ports at a time. The data obtained indicated that the average spacing may vary at most by 0.6% along the length of the column.

Neither of the above measurements can evaluate the centering of the two tubes. Asymmetry of this sort would create disturbing cross-convection currents due to varying temperature gradients at a given level. The column as received was equipped with three sets of small spacers in the annulus at one and one-half foot intervals; it was assumed that these served adequately to maintain a precise centering of the tubes.

TEMPERATURE UNIFORMITY

Preliminary data showed that the hot wall temperatures indicated by the end thermocouples were several degrees below that recorded by the thermocouple located midway down the column. This relation held true whether the nichrome wire or the five heating tapes were employed as the heat source. To investigate the problem further, a small thermocouple probe was inserted successively up each sample port during operation of the column in an effort to measure the fine-scale variation of hot wall temperature along the entire column length. It was found that as the

probe was slowly advanced up a port, the indicated temperature would rise to a maximum, maintain that maximum for a considerable distance, and then fall rapidly as the probe entered the annulus. Thus, the hot wall temperature at a given port position corresponded to the maximum indicated probe temperature. The resulting data are presented in Fig. 4. The data were reproducible and therefore the small-scale temperature variations were physically real. The low temperatures recorded by the end thermocouples are seen to be due to column end effects. It is suspected that the small temperature variations were due to the wide spiral geometry of the nichrome wires (which advanced about an inch up the column per turn) and to the varying distance of the three strands of nichrome wire from the surface of the hot wall (as indicated in Fig. 2). There can be seen a suggestion of periodicity in the data which would support such a view. The permanent center thermocouple indicates a higher temperature than the probe data at the same position because the two points of measurement are actually separated by half the annulus circumference from each other. The wide heating tapes should not produce this hot wall temperature variation, but experimental difficulties such as heating of the sample ports by direct contact with the tapes precluded the obtaining of probe temperature data to demonstrate this hypothesis. It was concluded that the column should be operated using the heating tapes as the main power input source with the nichrome element being used only to the extent necessary. About 65% of the heat input required to maintain a 50°C. temperature difference across toluene solutions could be provided by the heating tapes each producing 110 watts maximum power.

The temperature rise of the cooling water in passing through the column was never more than 1.7°C. This factor cannot influence the temperature gradient in the column because there must be a corresponding gradient in temperature along the hot wall to maintain the steady-state heat conduction across the annulus.

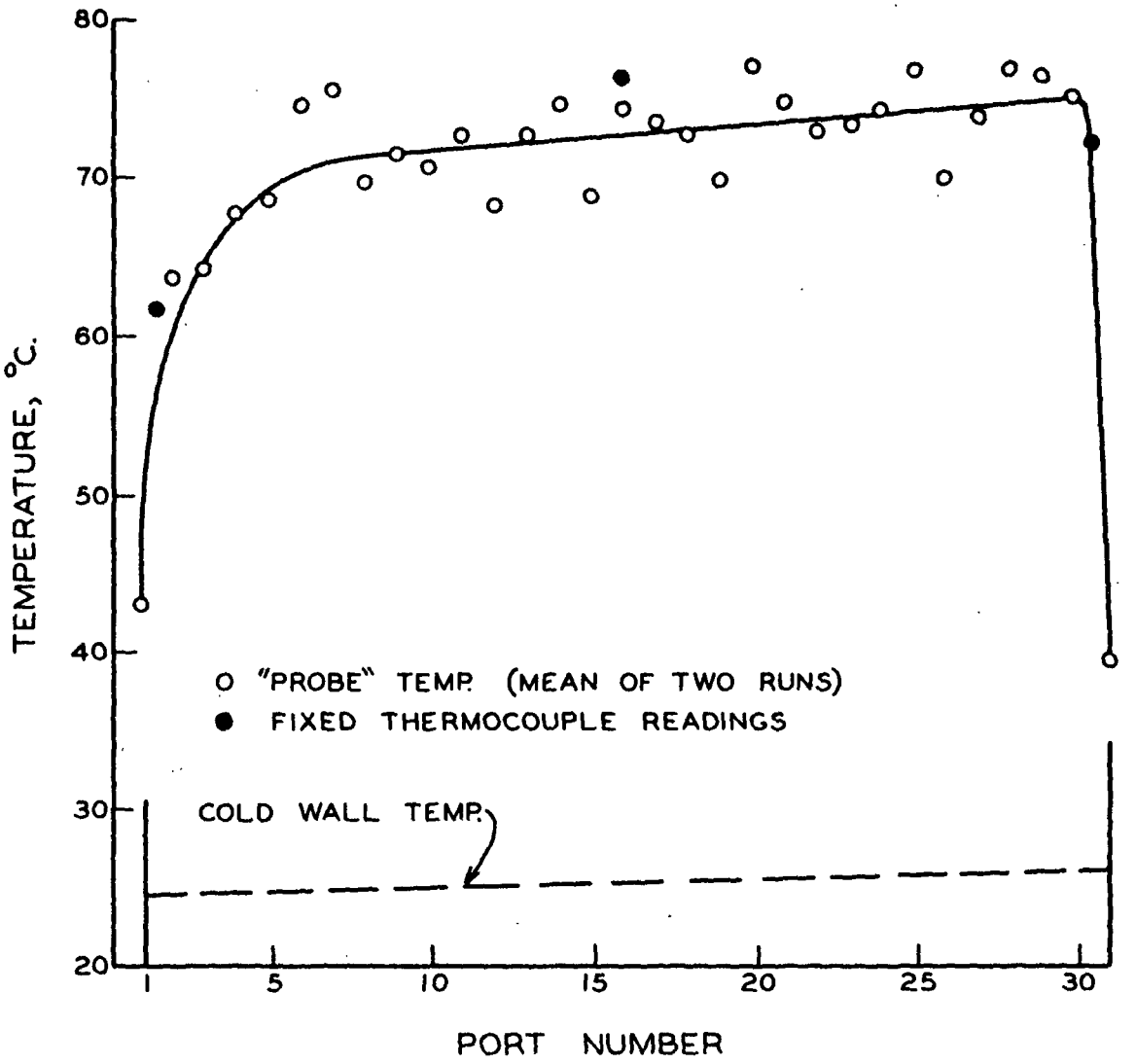

Figure 4. Wall Temperature Using Original Heating Equipment

The temperature difference across the annulus for each run was determined in the following manner. The cold wall temperature was taken to be the average of the inlet and outlet cooling water temperatures. (The temperature drop across the inner wall was estimated to be only 1°C.) The mean hot wall temperature was calculated from the temperature indicated by the fixed middle thermocouple corrected for the positive bias due to the uneven heat effect of the nichrome heating element shown in Fig. 4 and discussed above. This bias was assumed proportional to the power input from the nichrome element. The difference between the hot and cold wall means was then taken to be the effective operating temperature difference.

PROCEDURES AND TECHNIQUES

COLUMN OPERATION

LOADING

The column loading procedure described below was designed to eliminate entrapped air in the annulus which is always a problem when filling long narrow spaces. With reference to Fig. 5 the procedure was:

(1) Lower end of feed line into test solution, draw solution into feed line and reservoir by applying vacuum at 5, then pinch off feed line at 1;

(2) Attach feed line to opened bottom sample port and apply vacuum to column (pinchcock 2 and 4 open, 3 closed);

(3) Close pinchcock 2 and open 1 to allow solution to fill column and enter overflow bulb;

(4) Close 1 and relieve any remaining vacuum by opening 3;

(5) Close 4, remove feed line from lower port, and close off lower port with sample port cap;

(6) Remove line to overflow bulb from top port.

The flexible connecting links a, b, and c were of tygon when toluene solutions were used and of rubber for methyl ethyl ketone solutions.

RUNNING

The column was run with the top sample port open to allow for thermal expansion of the solution during heating. The cooling water was allowed to flow through the column at maximum rate while the electrical input to the heating tapes and nichrome heating element was adjusted to give the desired temperature difference across the annulus. Heating tape power input was divided equally between all

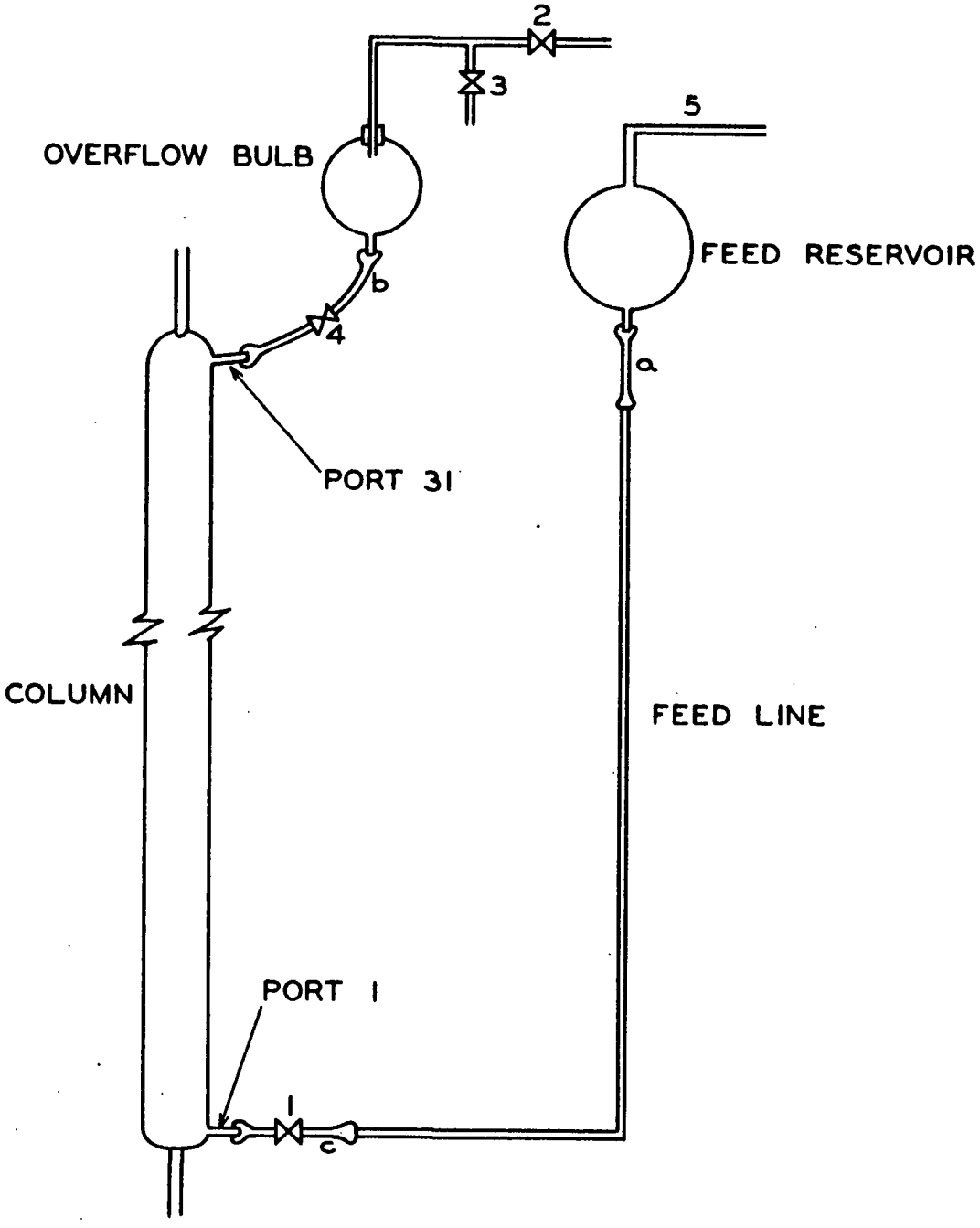

Figure 5. Column Loading Procedure

five tapes. All heating elements reached operating temperature within about fifteen minutes.

Preliminary experiments using polymer B6 in 0.5% toluene solution with a 50°C. temperature difference demonstrated that the steady-state concentration gradient in the column is largely established after one hour of operation and that no detectable changes occur after three hours. The time required to reach steady state is in order-of-magnitude agreement with approximate calculations based on unsteady state column theory (1). All runs were of at least nine hours duration to insure the attainment of steady state under various operating conditions.

SAMPLING

At the conclusion of a run, the heat inputs and cooling water were abruptly turned off and the top sample port was closed. The column was then sampled, starting from the top. If the first sample was to consist of the solution contained between sample port 31 (top port) and n_1, then port cap n_1 was removed, a short rubber sampling tube was attached to the opened port and lead into a receiving vessel, and port 31 was then opened to permit the solution to flow into the receiving vessel. The port caps were then replaced and the process repeated to obtain the solution contained between ports n_1 and n_2, and so forth until the entire column had been sampled. Low pressure air was admitted to the upper of each pair of open ports during draining of each section to enhance completeness of sampling. In this manner 95 to 98% of the total solution volume was sampled in about five minutes. Usually eight samples were taken for each run.

The column was then washed by running several hours with pure solvent, flushed with solvent and then acetone, and finally dried by applying vacuum.

SAMPLE ANALYSIS

CONCENTRATION

All sample concentrations were determined on a weight percentage basis by evaporation of solution and weighing of the dried polymer. Drying was accomplished at 120°C. and 29 in. Hg vacuum in preheated, tared aluminum dishes. The polymer samples weighed fifteen to sixty milligrams giving films about twenty microns thick. Under these conditions the polymer was completely dried from toluene in twenty hours and from methyl ethyl ketone (MEK) in ninety minutes. All weighings were performed on an ordinary laboratory analytical balance to tenths of a milligram.

INTRINSIC VISCOSITY

Because of its ease and rapidity of determination, intrinsic viscosity was chosen as the means of characterizing the molecular weight of fractions obtained from the numerous thermal diffusion runs. All intrinsic viscosity data were obtained at 25.00°C. using Cannon-Fenske viscometers.

The relation between intrinsic viscosity and molecular weight is satisfactorily given by

$$[\eta] = K\overline{M}_v^a \qquad (31)$$

where $[\eta]$ is the intrinsic viscosity, $\overline{M}_v$ the viscosity average molecular weight, and K and a are constants for a particular polymer-solvent system. Values for K and a reported in the literature vary somewhat, and therefore these constants were determined for use in the present work in the following unique manner which required no fractionation work. First, all literature values of K, a for fractionated

polystyrene in many different solvents and mixed solvents covering the entire range of solvent power (including theta solvents) were plotted as their logarithms and found to fall nicely on a straight line as shown in Fig. 6. Thus, for polystyrene we find the relation

$$K = ka^m \tag{32}$$

where k and m are constants for a given polymer. As far as is known, this relation has not previously been observed although Bawn (34) notes briefly a linear K,a relation for limited data.*

The viscosity average molecular weight for a given polymer specimen is related to the molecular weight distribution, g(M), and the value of the constant a by

$$\bar{M}_v = [\int M^a g(M) dM]^{1/a} \tag{33}$$

Because the function g(M) is accurately known for polystyrene B6, the constants K,a can be calculated from Equations (31)-(33) for any solvent in which the intrinsic viscosity of polymer B6 has been measured. The results of such an approach are presented in Table III, where data from the excellent work of Outer, Carr, and Zimm (36) are presented for comparison. One determination of $[\eta]$ for polymer B6 in toluene was made and agreed exactly with the value obtained by McCormick (28) on the same sample, and two determinations in MEK both gave the value reported in Table III.

*The units of K are the same as those of $[\eta]$ which is usually expressed in terms of dl./g.; if different units are chosen such as 100 g./g. (corresponding to concentrations measured as percentage by weight), then Equation (32) will not hold because the K's for each data point must then be multiplied by the appropriate solvent density, which bears no relation to the polymer dissolving power of the solvent. Hence, the existence of relation (32) indicates that $[\eta]$ is most fundamentally expressed in units of volume per unit weight. Molecular theories of the intrinsic viscosity (32) are in accord with this finding.

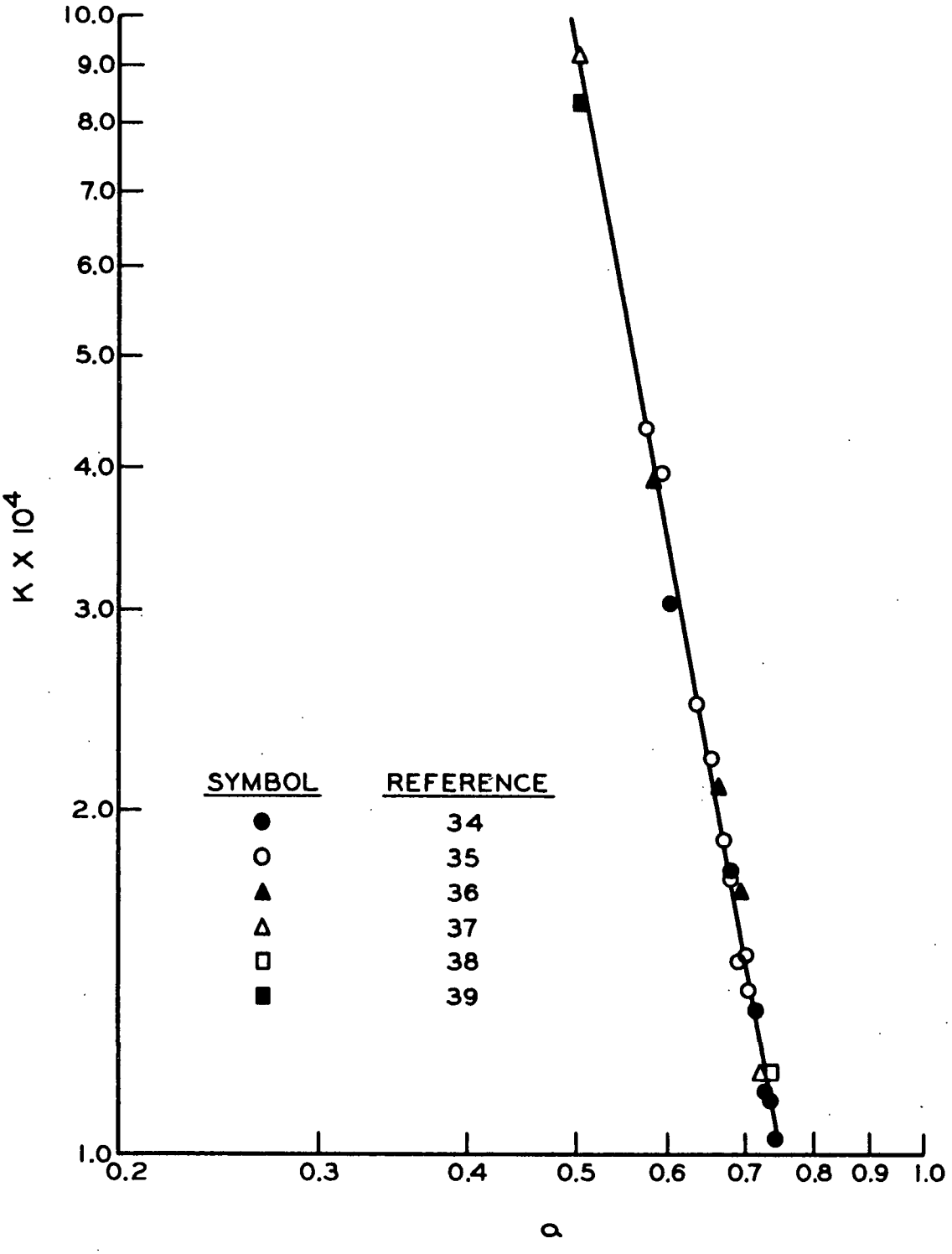

Figure 6. Polystyrene Literature Data

$$[\eta] = \underline{K}M^{\underline{a}}$$

TABLE III

INTRINSIC VISCOSITY CONSTANTS FOR POLYSTYRENE

Solvent	Source of Data	Polymer B6, $[\eta]$, dl/g.	$K \times 10^4$	a
Toluene	McCormick (28)	1.233	--	--
	This work	1.233	1.40	0.704
	Outer, et al. (36)	1.239[a]	1.7	0.69
MEK	This work	0.665	4.32	0.571
	Outer, et al.	0.674[a]	3.9	0.58

[a]Calculated from K,a of these authors

The values of K and a calculated from the measured intrinsic viscosities of polymer B6 were used in the present study for conversion of $[\eta]$ to molecular weight.

Toluene Solutions

The intrinsic viscosity of thermal diffusion fractions of toluene solutions were determined by a one-point method. Huggins' equation describing the viscosity behavior of many polymer-solvent systems is

$$\frac{\eta_{sp}}{c} = [\eta] + k' [\eta]^2 c \qquad (34)$$

where $\eta_{sp} = (\eta/\eta_o)-1$ = the specific viscosity,

η, η_o = viscosity of solution and solvent respectively,

$[\eta]$ = intrinsic viscosity,

c = concentration, and

k' = Huggins' constant.

For the polystyrene-toluene system, the best literature data give $k' = 0.38$ (34, 40, 41). Using the known value of k' one can then calculate $[\eta]$ from the measured value of η_{sp} at one concentration.

The adequacy of the literature value for $\underline{k}'$ was confirmed experimentally. Data on polymer B6 for five concentrations between 0.1 and 0.8 g./dl. gave $[\eta]$ = 1.233 dl./g. and $\underline{k}'$ = 0.362; with the value $\underline{k}'$ = 0.38, one-point determinations of intrinsic viscosity calculated from each of the five data points gave an average of $[\eta]$ = 1.229. Thus, the literature value for $\underline{k}'$ was sufficiently accurate for the present work.

The one-point intrinsic viscosity method was therefore adopted for analysis of toluene fractions. The column samples were diluted with solvent or concentrated by evaporation to give solutions of 0.2 to 0.5% concentration by weight for the viscosity determinations.

Methyl Ethyl Ketone Solutions

Literature data concerning the Huggins' constant for methyl ethyl ketone (MEK) show considerable variability, and therefore intrinsic viscosities of MEK solutions were not determined by the one-point method used for toluene solutions but by the usual procedure of extrapolating several experimental values of $\eta_{sp}/\underline{c}$ to zero concentration. Each thermal diffusion fraction was successively diluted or concentrated to permit determination of specific viscosity at three concentrations. The concentration of the final viscosity sample was then measured and the preceding concentrations, including that of the sample as it was removed from the column, were calculated from the known dilution ratios.

THERMAL DIFFUSION DATA ANALYSIS

POLYMER-SOLVENT SEPARATION

A solution of a polydisperse polymer may be considered as a two-component system in spite of the large number of different molecular weight species composing

the solute. In a thermal diffusion experiment we can then refer to the gross separation of polymer from solvent ("separation" effect) without regard to the separations occurring within the polymeric part of the system ("fractionation" effect). To compare the results of thermal diffusion under various operating conditions, a convenient measure of polymer-solvent separation has been devised:

$$PS \equiv \int_{z_o}^{1} (1-c/c_o)dz \qquad (35)$$

where $\underline{PS}$ = degree of polymer-solvent separation,

$\underline{z}$ = length co-ordinate along column in terms of fraction of total column length measured from bottom,

$\underline{c}$ = concentration at level $\underline{z}$ in the column,

$\underline{c_o}$ = starting concentration of solution, and

$\underline{z_o}$ = value of $\underline{z}$ where $\underline{c} = \underline{c_o}$.

$\underline{PS}$ is thus represented by the shaded area in Fig. 7 which is a typical plot of the concentration data from a thermal diffusion run. The scale of $\underline{PS}$ so defined ranges from zero to unity representing, respectively, no separation and total separation (all the polymer packed at the bottom of the column).

The concentration of a particular sample represents the average concentration over the length of column from which the sample was taken. In all runs except some at very low concentrations (see below: "Low Concentration Runs"), this average was assumed to represent the solution in the middle of the column length sampled.

POLYMER-POLYMER FRACTIONATION

The degree to which polymer molecules of differing molecular weight separate from one another will be referred to as polymer-polymer fractionation or $\underline{PP}$. A

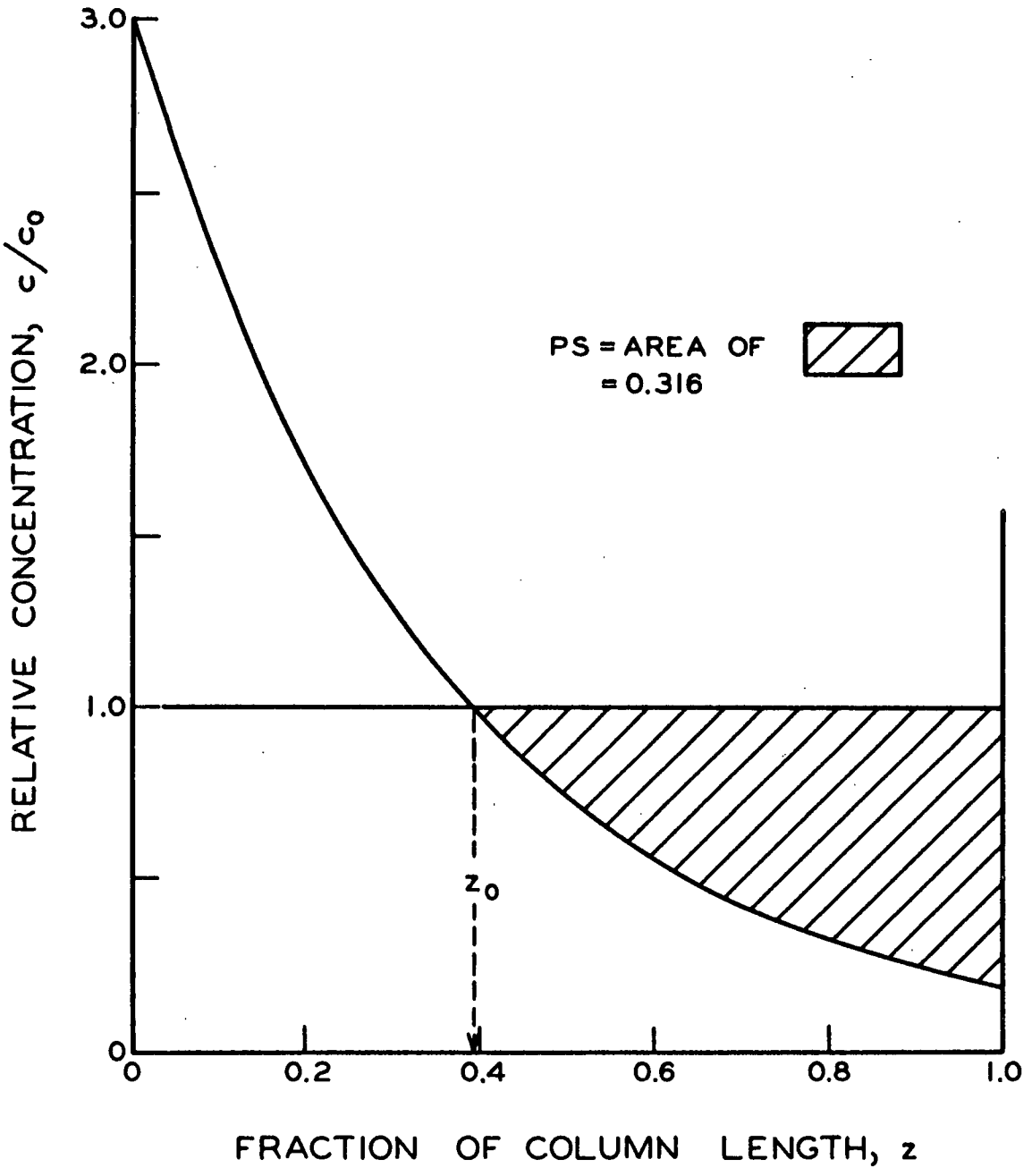

Figure 7. Calculation of Polymer-Solvent Separation, PS

measure of PP analogous to that of PS was devised to facilitate comparison of fractionation results from various thermal diffusion runs. The known molecular weight distribution, $g(M)$, of polymer B6 is the PP analogy to the starting concentration c_o in the measurement of PS, but experimentally it is more convenient to refer to the integral molecular weight distribution function, $G(M)$, given by

$$G(M) = \int_0^M g(M)dM \tag{36}$$

as customary; $G(M)$ represents that fraction of the total polymer having molecular weight M or less. If no fractionation effect occurs in a thermal diffusion run, then $G(M)$ will be a simple unit step function at the mean molecular weight of the sample. The degree of polymer-polymer fractionation produced in a given run may then be expressed in terms of the deviation of the experimentally determined $G(M)$ from the step function relative to that maximum deviation attainable corresponding to the true $G(M)$ for the polymer. Such a definition places PP on a zero-to-one scale as for PS discussed above. Because relative trends were of primary importance in the present work, any specific definition of the deviation of $G(M)$ from a step function was permissible, and the following was adopted for convenience:

$$\left.\begin{aligned} R &= \sum_{n=1}^{9} f(n) \left| M(G=0.1n) - M(G=0.5) \right| \\ f(n) &= 5 - \left|5-n\right| \\ &= 1,2,3,4,5,4,3,2,1 \text{ for } n = 1,\ldots,9 \\ PP &= R/R_o \end{aligned}\right\} \tag{37}$$

where $M(G=x)$ = molecular weight corresponding to a value x of $G(M)$, and

R_o = value of R for the known true $G(M)$.

The $f(n)$ are weighting factors which de-emphasize the importance of data at the "tails" of the molecular weight distribution. The comparison step function was

arbitrarily placed at the modal molecular weight. A schematic depiction of the calculation of R is presented in Fig. 8.

G(M) for a particular thermal diffusion run was calculated from the concentration and intrinsic viscosity data for that run by

$$G(M_i) = \int_{z_i}^{1} (c/c_o)dz \qquad (38)$$

where z_i was the level at which the molecular weight (calculated from intrinsic viscosity) was found to be M_i, and $z = 1$ was the top of the column.

EXTINCTION COEFFICIENT

The extinction coefficient γ, discussed previously in the "Theoretical Background" section, is essentially a measure of the degree of polymer-solvent separation but is more directly related to the transport coefficients D and D' than is PS as defined above. Experimentally, it was found that γ varied with z except for runs at low concentration where the relation between $\ln(c/c_o)$ and z approached linearity. However, at concentrations where $\ln(c/c_o)$ versus z is nonlinear, an "equivalent" γ may be determined; this is the negative of the slope of an ideal exponential c versus z relation which would give the same PS as actually measured. By combining the definitions of γ and PS with a material balance, it is found that

$$PS = [1-\exp(-\gamma')]^{-1} - (1/\gamma')\left\{1 + \ln[\gamma'/(1-\exp(-\gamma'))]\right\} \qquad (39)$$

where γ' is the value of γ equivalent to PS. Extrapolation of γ' calculated from Equation (39) to infinite dilution should yield an extinction coefficient amenable to interpretation according to the theoretical equations derived earlier. A plot of the above relation is presented in Fig. 9 along with experimental data from

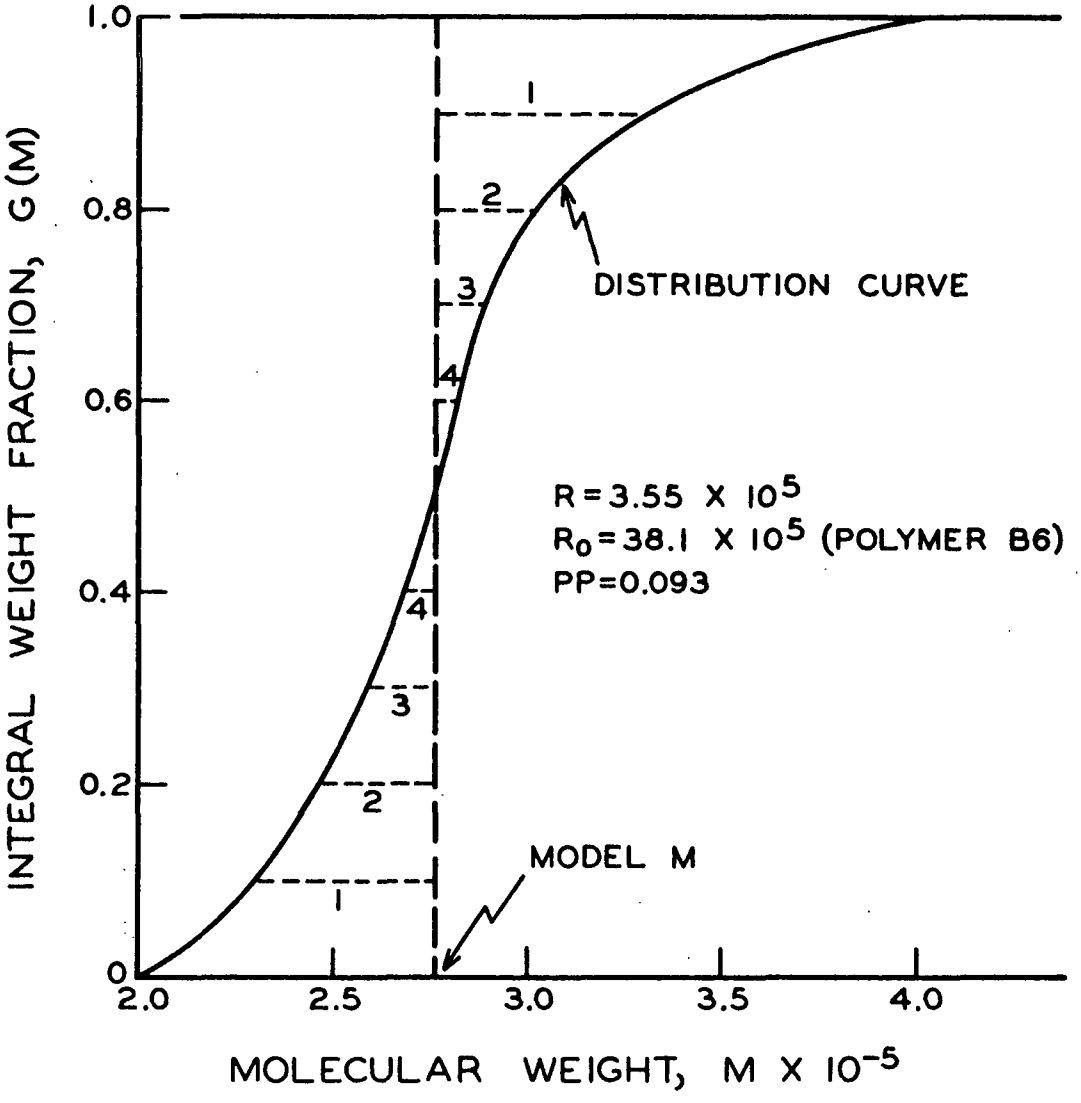

Figure 8. Calculation of Polymer-Polymer Separation, PP

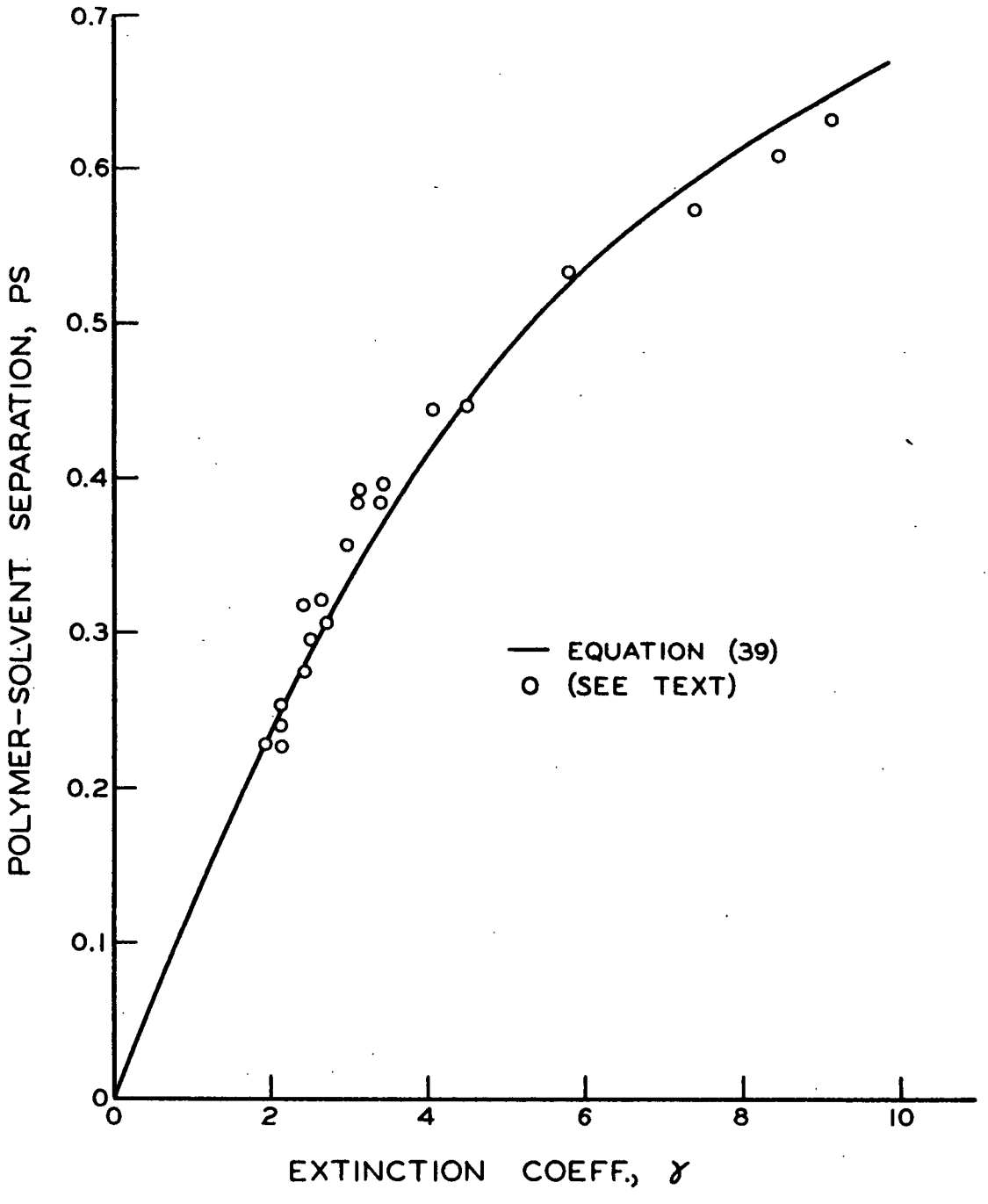

Figure 9. Calculated Relation Between PS and γ

several thermal diffusion runs which demonstrate the interesting sidelight that γ' is very nearly the slope of $\ln(\underline{c}/\underline{c}_o)$ vs. $\underline{z}$ measured at $\underline{c}/\underline{c}_o = 1$.

LOW CONCENTRATION RUNS

For thermal diffusion runs of low initial concentration, the average weight of the polymer fractions becomes small. To provide larger samples, duplicate runs may be performed or fewer samples may be taken from one run. If the latter course is chosen, then a measured sample concentration represents the average over a longer length of column, and consequently the mean concentration corresponds less precisely to the center of the sampled length than if a greater number of samples were taken. However, at low concentrations the extinction coefficient γ becomes more nearly independent of $\underline{z}$ and therefore a logarithmic interpolation may be performed to locate the level in the column corresponding to the measured sample concentration. Thus, if $\underline{z}_{il}$ is the bottom of this region, then the appropriate mean $\underline{\bar{z}}_i$ corresponding to the measured $\underline{c}$ is given by

$$\bar{z}_i = (1/\gamma)\ln[\gamma(z_{il} - z_{io})/(\exp(-\gamma z_{io})-\exp(-\gamma z_{il}))] \qquad (40)$$

The γ is first estimated by mid-point plotting of the concentration; improved positions of the data points are then calculated leading to a better estimate of γ, and so forth. Rarely more than two trials were needed.

RESULTS

OUTLINE OF EXPERIMENTAL PROGRAM

As stated earlier, the purpose of the present study was to elucidate the mechanism of polymer thermal diffusion in a Clusius-Dickel column in hopes of evaluating the applicability of the process to polymer fractionation or distribution characterization. Certainly the most important factor to be considered was the molecular weight of the polymer because differences in the thermal diffusion behavior of chemically identical polymer specimens must ultimately relate to molecular size. The molecular weight factor may be studied in two ways: (a) implicitly, through an examination of the factors affecting the thermal diffusion fractionation of a single broad distribution polymer, and (b) explicitly, by studying the factors relating to the polymer-solvent separation of several narrow distribution, nearly monodisperse polymers, both separated and mixed. The important experimental factors not related to the nature of the polymer species itself or to the column geometry may be divided into two categories:

(a) Those relating to the solution under study, such as
    (1) Solvent used, and
    (2) Concentration of polymer in solution; and
(b) Those relating to the temperature conditions employed, such as
    (1) Temperature gradient, and
    (2) Mean temperature.

The experimental program, therefore, consisted of a rather complete examination of the effects of solvent, concentration, temperature gradient, and mean temperature on the PS and PP separations for a polydisperse polystyrene followed by a more restricted study of these effects on the PS separation of some "monodisperse"

polystyrenes. Finally, the results obtained were interpreted in terms of a mathematical description of column operation.

EFFECT OF EXPERIMENTAL FACTORS ON THERMAL DIFFUSION OF A POLYDISPERSE POLYMER

Polystyrene B6 was chosen as the object of study in the investigation of experimental factors affecting thermal diffusion separations because of its broad molecular weight distribution which included species from ten thousand to two million molecular weight. The experimental results are divided into two sections concerning PS and PP separation.

POLYMER-SOLVENT SEPARATION

The PS separation was determined from measurement of the steady state concentration at several positions along the column as described earlier. The concentration data from a few typical runs are presented in Fig. 10. The curves depicted are representative of all the data obtained in two respects: (a) the polymer migrated toward the bottom of the column indicating a positive thermal diffusion coefficient for polystyrene (diffusive flux in the direction of heat flow); and (b) the concentration decreased rapidly with distance from the column bottom suggesting an exponential relation. The reproducibility of the concentration pattern established in the column at steady state is seen to be quite satisfactory. Measurements of PS for two replicate pairs of runs (numbers 9, 10 and 44, 45) differed by about 1%.

Because only one thermal diffusion column was used throughout the entire thesis, the temperature gradients employed were proportional to the temperature difference across the annulus for all runs. The terms "temperature gradient" and "temperature difference" are therefore used interchangeably in the following

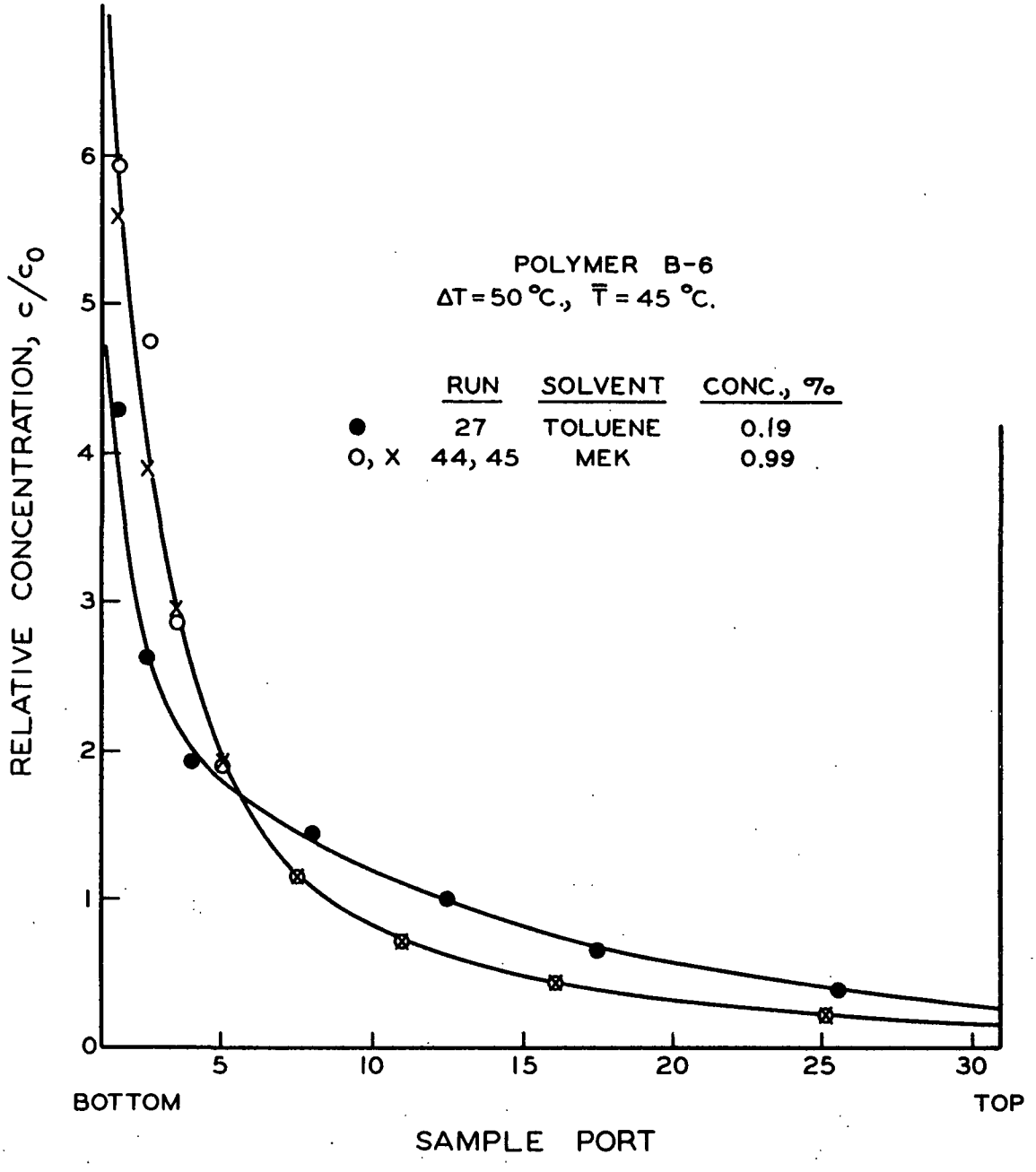

Figure 10. Typical Column Concentration Data

discussions. Most of the runs were made at ΔT = 50°C. which corresponded to a gradient of 656°C./cm.

The variation of PS with temperature difference, mean temperature, and concentration of polystyrene polymer B6 in toluene is shown in Fig. 11. The curves are drawn to give zero PS at zero temperature difference as must physically be true. At all conditions of mean temperature or initial concentration, PS became independent of temperature difference at sufficiently large ΔT. This is merely a reflection of the fact that the temperature gradient is the driving force for both the thermal diffusion and the convection flows which occur in mutually perpendicular directions. A proportional increase in both fluxes will not change the flow path of a solute molecule.

There was a small increase of PS with decreased mean temperature as indicated by the two low temperature data points in Fig. 11. For polyvinyl acetate Langhammer and Forster found the separation factor (related to PS) to be independent of the mean temperature and to increase steadily with increased temperature gradient (11); these data were not obtained under steady-state conditions and may differ from the present findings for this reason. The temperature dependence of PS suggests that the thermal diffusion coefficient D' for polystyrene decreases with temperature. The mean solution viscosity decreased by almost 30% as the mean temperature was reduced from 45 to 20°C. which would cause a large increase in PS if there were no change in D'. Because the increase in PS is found to be small, D' must have a positive temperature dependence so that at lower mean temperatures the decreased velocity of the convective flows is accompanied by a decreased horizontal thermal diffusive flow. There have been no conclusive data published in the literature on the temperature dependence of the thermal diffusion coefficient. Theoretical treatments concerning the thermal diffusion constant α [see

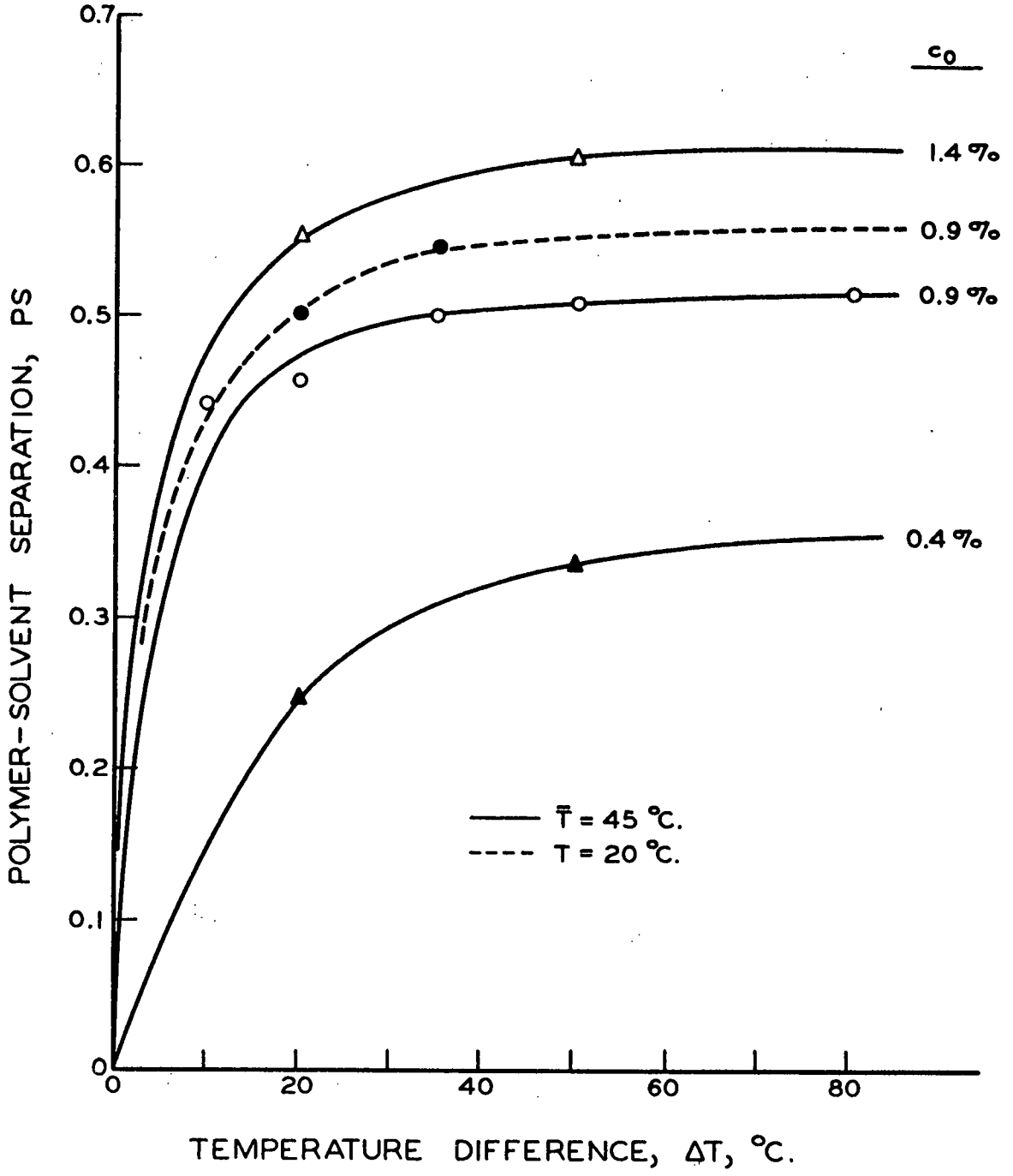

Figure 11. PS Data for Polystyrene B6 in Toluene

Equation (1)] indicate both positive (12) and negative (17) temperature coefficients for D' when the known temperature dependence of the ordinary diffusion coefficient is taken into account.

The polymer-solvent separation was found to increase with initial concentration as shown in Fig. 11. The increase of PS with concentration was characteristic of both solvent systems as Fig. 12 indicates. This behavior implies that the rate of horizontal mass transport by thermal diffusion is less concentration dependent than is the velocity of the vertical convection flows. The viscosity of polymer solutions is a very strong function of concentration even in dilute solutions, and therefore an increase in initial concentration would be expected to decrease greatly the convective velocities thus producing an increased PS. Langhammer (42) found a similar concentration dependence of his "separation factor."

It should be noted that the rate of PS increase with concentration decreases at higher concentrations, whereas it is well known that polymer solution viscosity increases more rapidly at higher than at lower concentrations; the apparent conflict is resolved when the equivalent extinction coefficient γ' [Equation (39) and Fig. 9] is substituted for PS. γ' is more fundamentally related to solution viscosity and does indeed increase more rapidly at higher concentrations as will be seen later (Fig. 20).

At the same concentration, PS for toluene solutions was greater than that for MEK solutions as shown in Fig. 12. It can be shown by simple calculation that the fluid properties determining the hydrodynamic flow are solely responsible for the relation of PS in MEK to that in toluene. The density, viscosity, and thermal expansion coefficient of MEK are such that the convective velocity is much greater at a given concentration in MEK than in toluene. The higher convective velocity

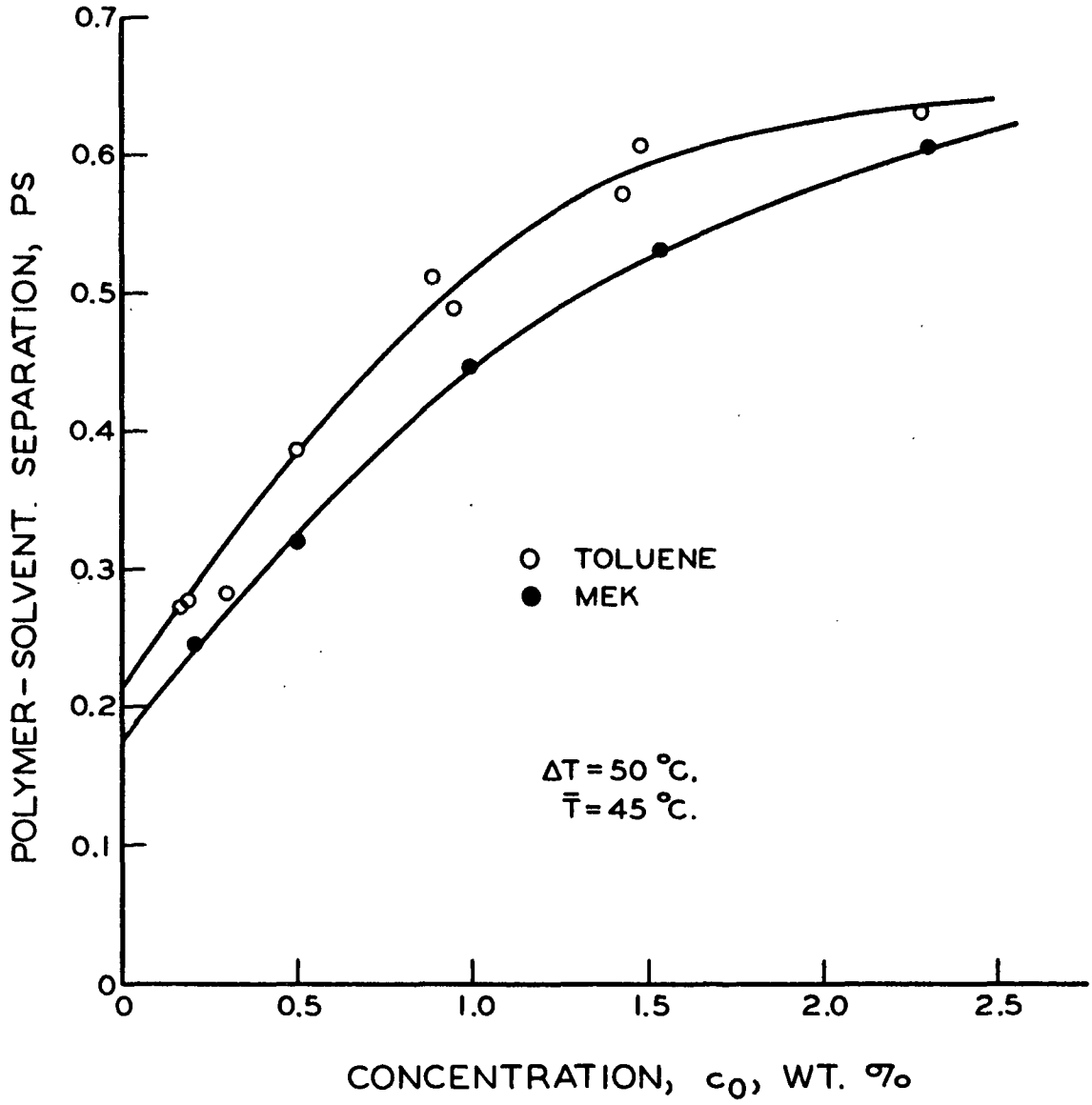

Figure 12. Effect of Solvent and Concentration on PS for Polymer B6

leads to a decreased PS because the solute molecules are carried further up the column in the warm flow stream before reversing their course upon entering the cool stream. Under identical hydrodynamic conditions, the PS would be much greater in MEK solutions than that in toluene solutions, and thus it appears that the thermal diffusion coefficient D' must be greater in the thermodynamically poor solvent, MEK. According to Ham's theory (17), D' is essentially determined by the solvent alone and is independent of the polymer; all data in the present study is for one polymer type and therefore Ham's contention cannot be directly verified, but his equations do indicate that a higher D' should be expected in MEK.

The relation of PS to the operating temperature gradient for MEK solutions is presented in Fig. 13. The trend is similar to that found for toluene solutions (see Fig. 11) and the same interpretations follow. A major difference, however, is the increase in PS at the highest temperature gradient. It is not clear why this increase occurred although the nearness of the hot wall temperature for the highest data points (76°C.) to the boiling point of MEK (80°C.) was probably a contributing factor. The highest hot wall temperature used in the toluene runs was twenty-five degrees below the toluene boiling point.

POLYMER-POLYMER FRACTIONATION

The degree of polymer fractionation, PP, was determined from measurement of intrinsic viscosity of column samples obtained at steady state as described earlier. The data indicate that the fractionation is not directly dependent on differences of thermal diffusion coefficient but is a secondary effect involving ordinary diffusion between the walls of the column. Hence, the form of the radial concentration gradient is an important factor in the fractionation process. Full interpretation of the PP results is therefore deferred until the results of the theoretical calculation have been presented.

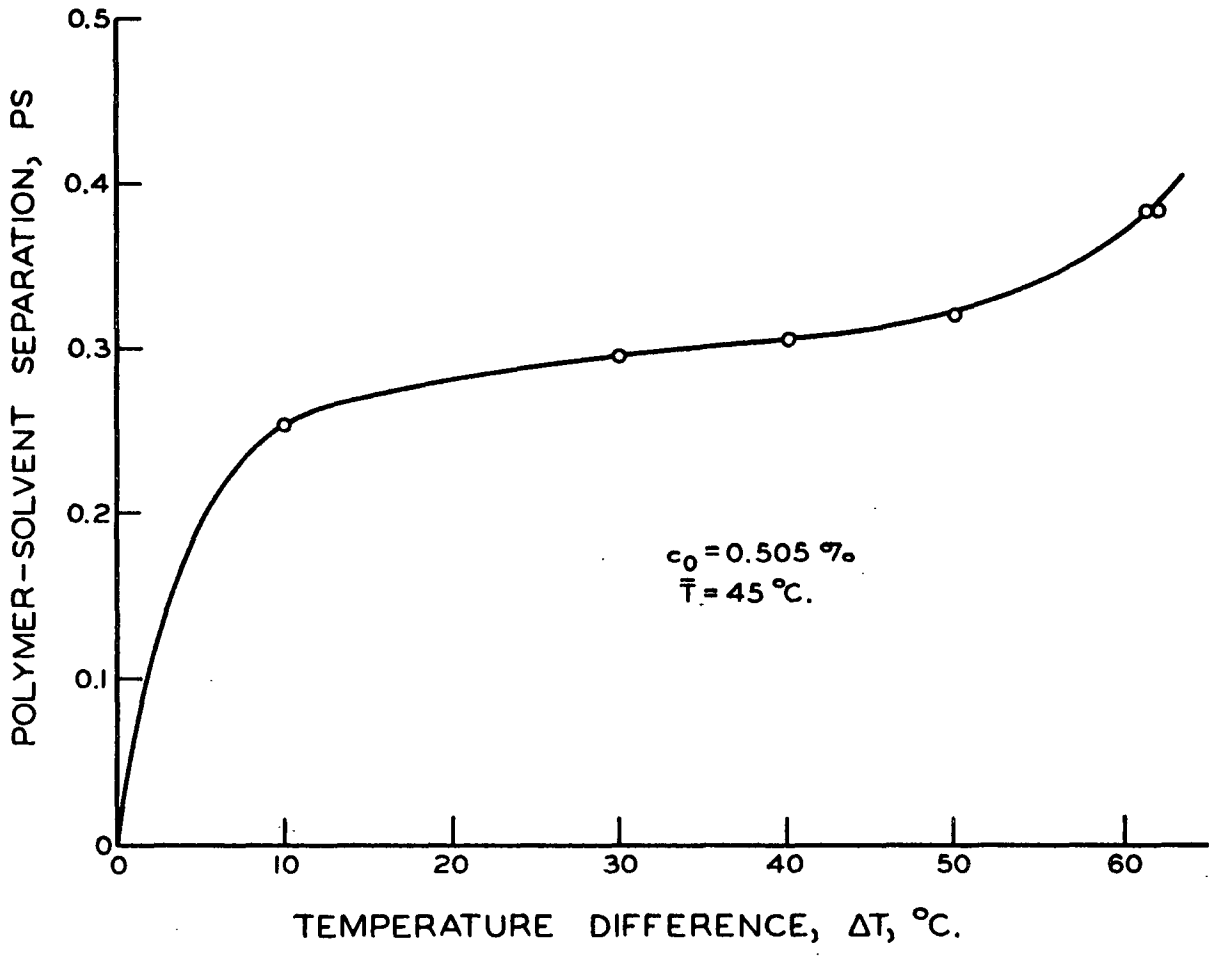

Figure 13. Effect of Temperature Gradient on PS Polymer B6 in MEK

In all runs for which the degree of polymer-polymer fractionation was measured, the highest molecular weight fractions were found at the bottom of the column. This result is in accord with the original work of Debye and Bueche (7) and with all other reports in the literature with one exception (43). One might tend to postulate on this basis that the thermal diffusion coefficient D' increases with molecular weight, but this is not necessarily so as will be demonstrated later.

The fractionation effect is seen to increase markedly with increased temperature gradient (Fig. 14) in spite of the levelling off of PS at temperature differences above 50°C. (Fig. 11 and 13). The better fractionation obtained in MEK solutions is to be expected because MEK is a more thermodynamically ideal solvent for polystyrene than is toluene. Some of the integral weight fraction molecular weight distribution curves from which the PP data for Fig. 14 were computed are presented in Fig. 15 and 16. The data points for some of the runs are omitted for clarity. The complete data for all runs can be found in Appendix IV. Increased temperature gradients produced broader molecular weight distribution curves for both toluene and MEK solutions, but at best the data included only the middle third of the true distribution (Fig. 1).

Because the mean temperature was found to have only a small effect on the PS separations, the influence of this factor on PP fractionation was not studied in detail. One pair of runs (Numbers 49 and 50) in MEK did serve to indicate the trend of PP with changes in mean temperature. The PP fractionation was found to increase by 40% for a decrease in mean temperature from 45 to 28°C. In future work, advantage might be taken of the low freezing point of organic solvents to produce a greater fractionation effect at low temperature.

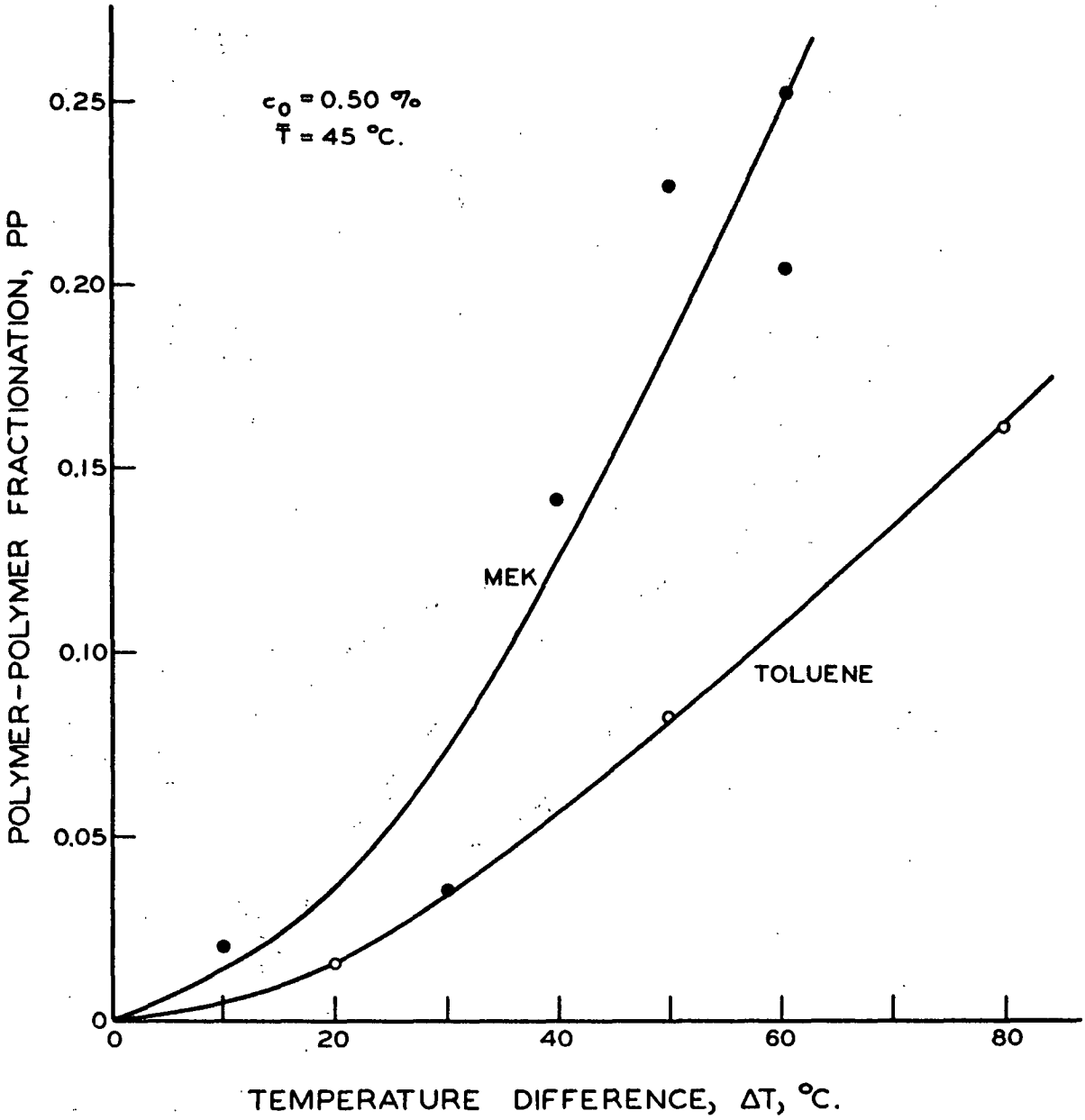

Figure 14. Effect of Temperature Gradient on PP Polymer B6

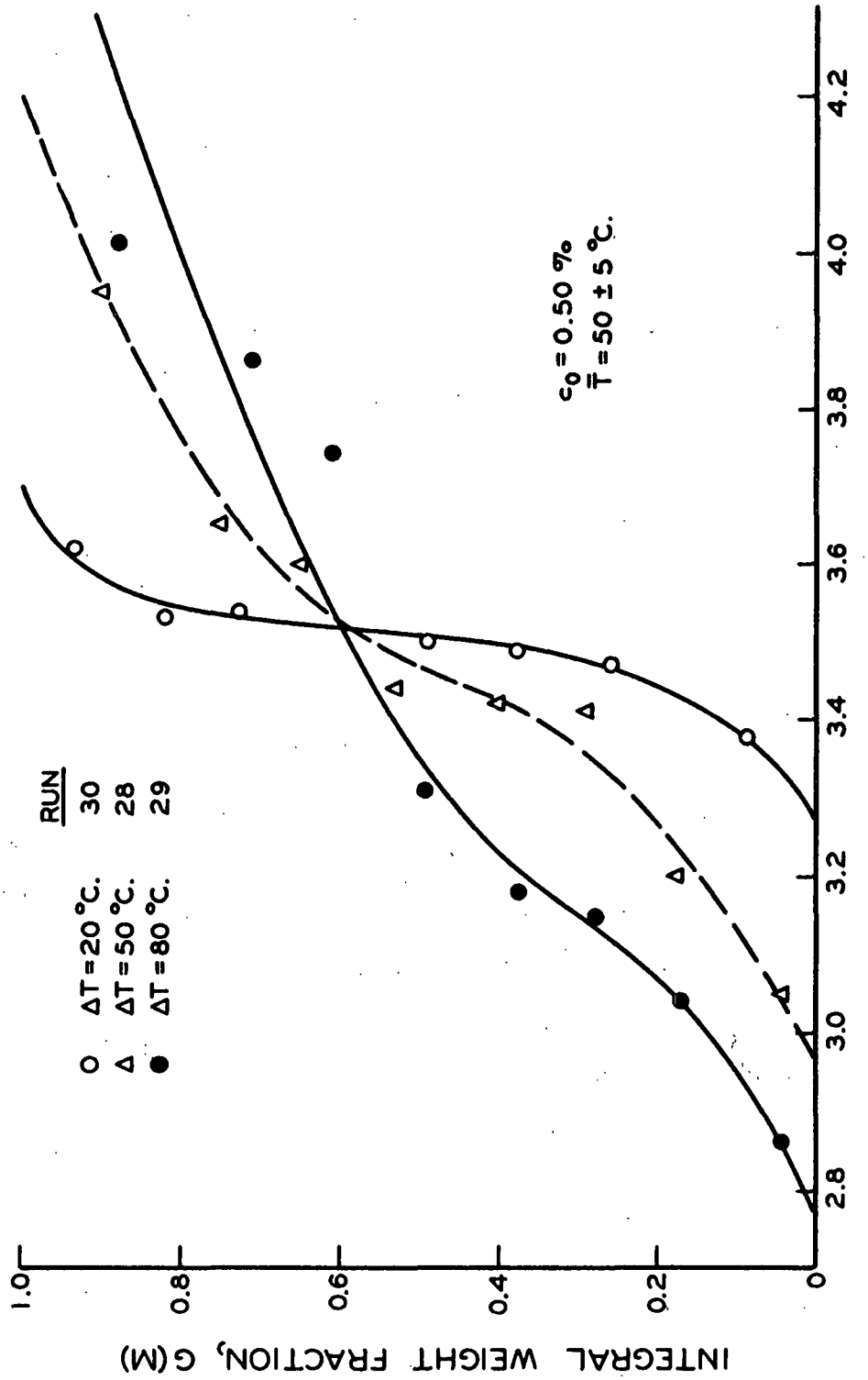

Figure 15. Effect of $\Delta\underline{T}$ on Molecular Weight Distribution Polymer B6 in Toluene

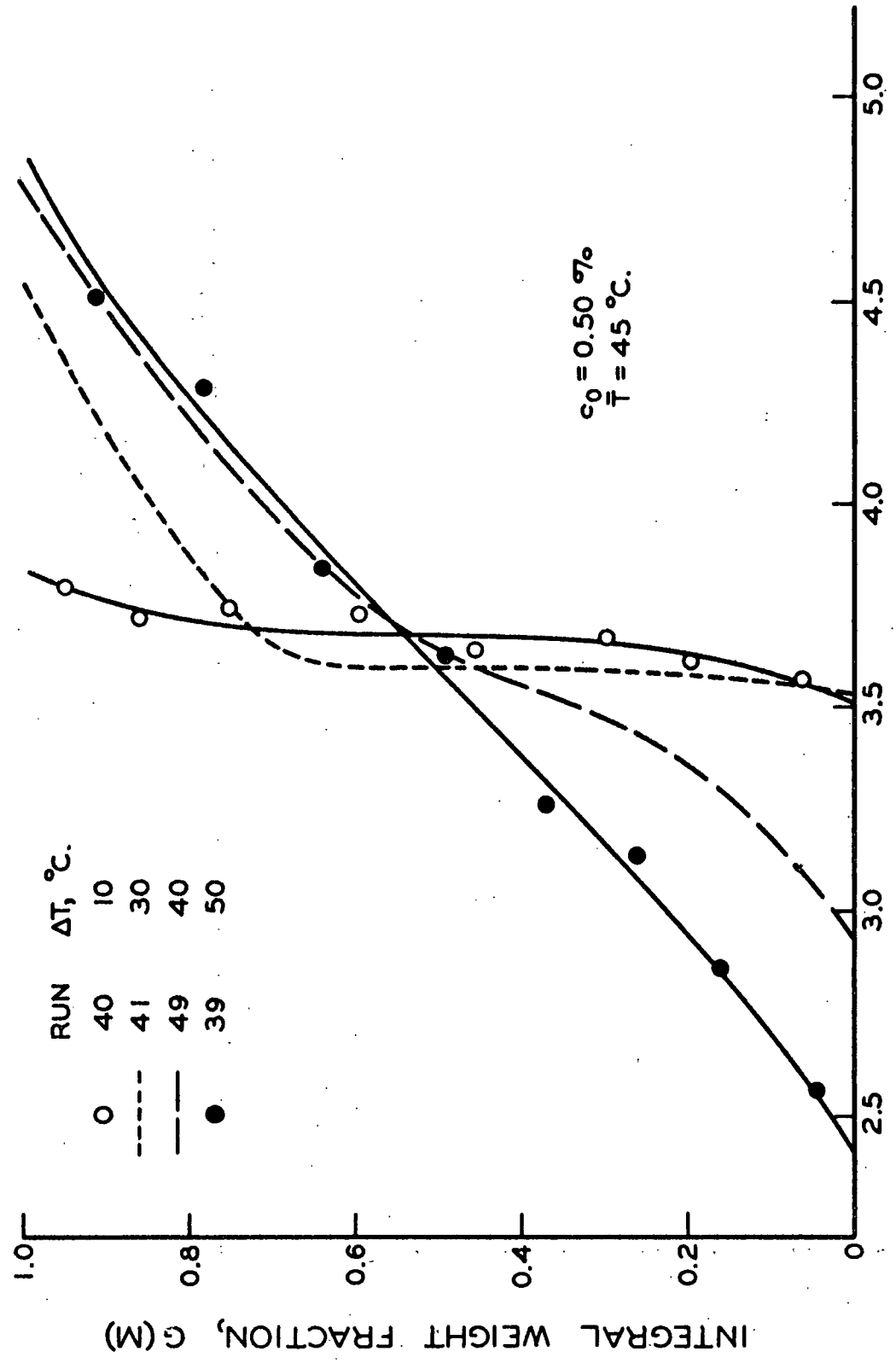

Figure 16. Effect of ΔT on Molecular Weight Distribution Polymer B6 in MEK

The effect of concentration on PP was quite surprising (Fig. 17). It was expected that greater fractionation would result from operation at lower concentrations because of the decreased intermolecular interactions at high dilutions and the resulting greater individuality of the polymer molecules. Such has been the experience with most methods of polymer fractionation, but in the present study an increased starting concentration produced an increased degree of fractionation as shown in Fig. 17. The effect was particularly strong for toluene solutions. Clearly, a more detailed understanding of the fractionation process in thermal diffusion than has been presented thus far is required for the interpretation of such results. The basis for a fuller understanding of the process resulted from the experiments described below. Some of the molecular weight distribution curves from which the PP data for Fig. 17 were computed are presented in Fig. 18 and 19.

DIRECT STUDY OF THERMAL DIFFUSION MOLECULAR WEIGHT EFFECT

OUTLINE OF STUDY

The narrow distribution polystyrenes S102 and S111 described earlier (weight average molecular weight 82,000 and 239,000, respectively) provided a direct means of examining the effect of molecular weight on the thermal diffusion of polymers in a Clusius-Dickel column. The distributions of these polymers are so narrow that little or no fractionation can occur, and therefore differences in PS separation for these two polymers under various sets of operating conditions can be attributed ultimately to the difference in molecular size of the two solutes. The differences in PS for the "monodisperse" polymers should then shed light on the effect of operating variables on the PP of a polydisperse polymer. A factorial experiment utilizing the narrow distribution polymers was performed in order to demonstrate explicitly the molecular weight--operating variable interactions. In addition, PS data

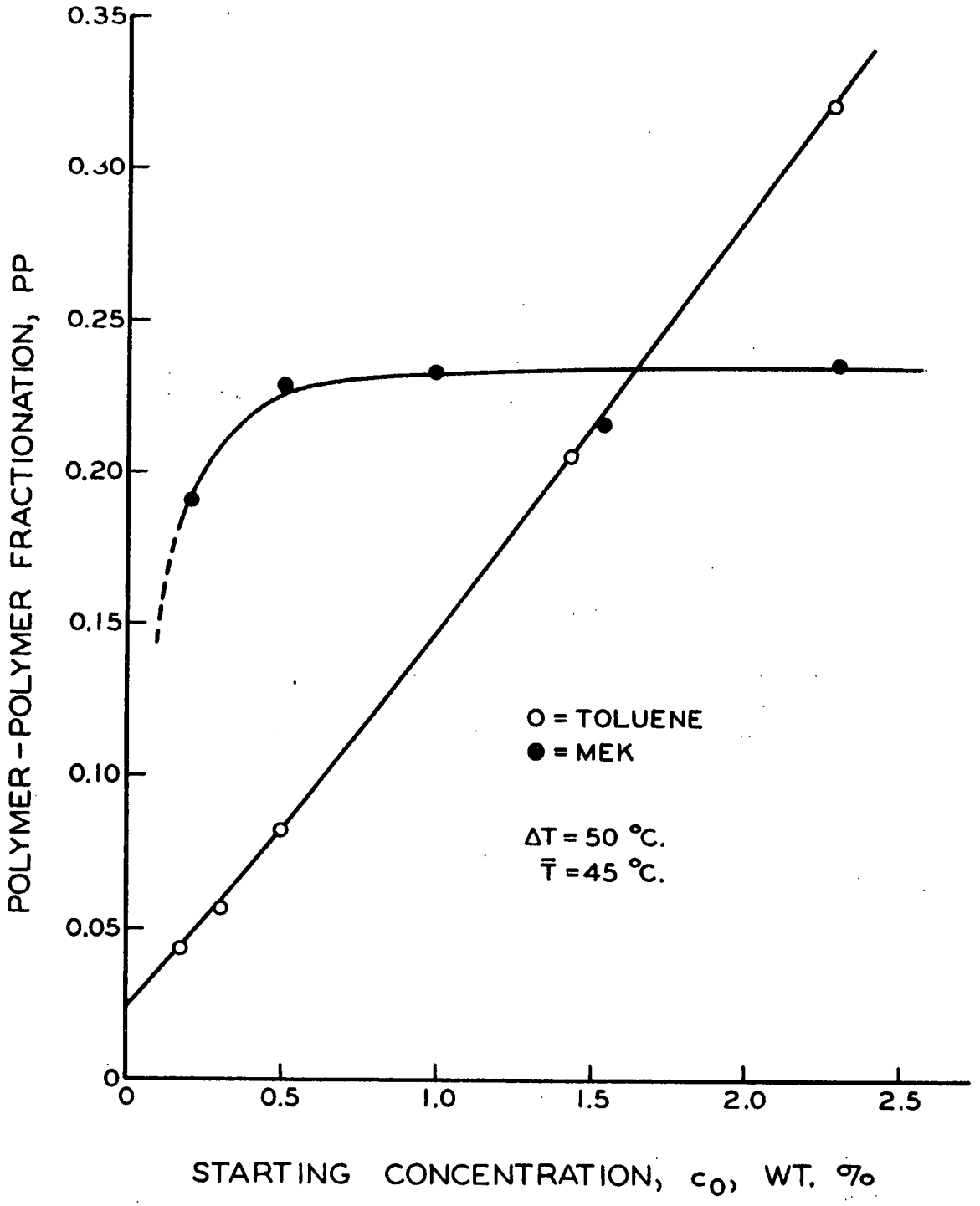

Figure 17. Effect of Concentration on PP Polymer B6

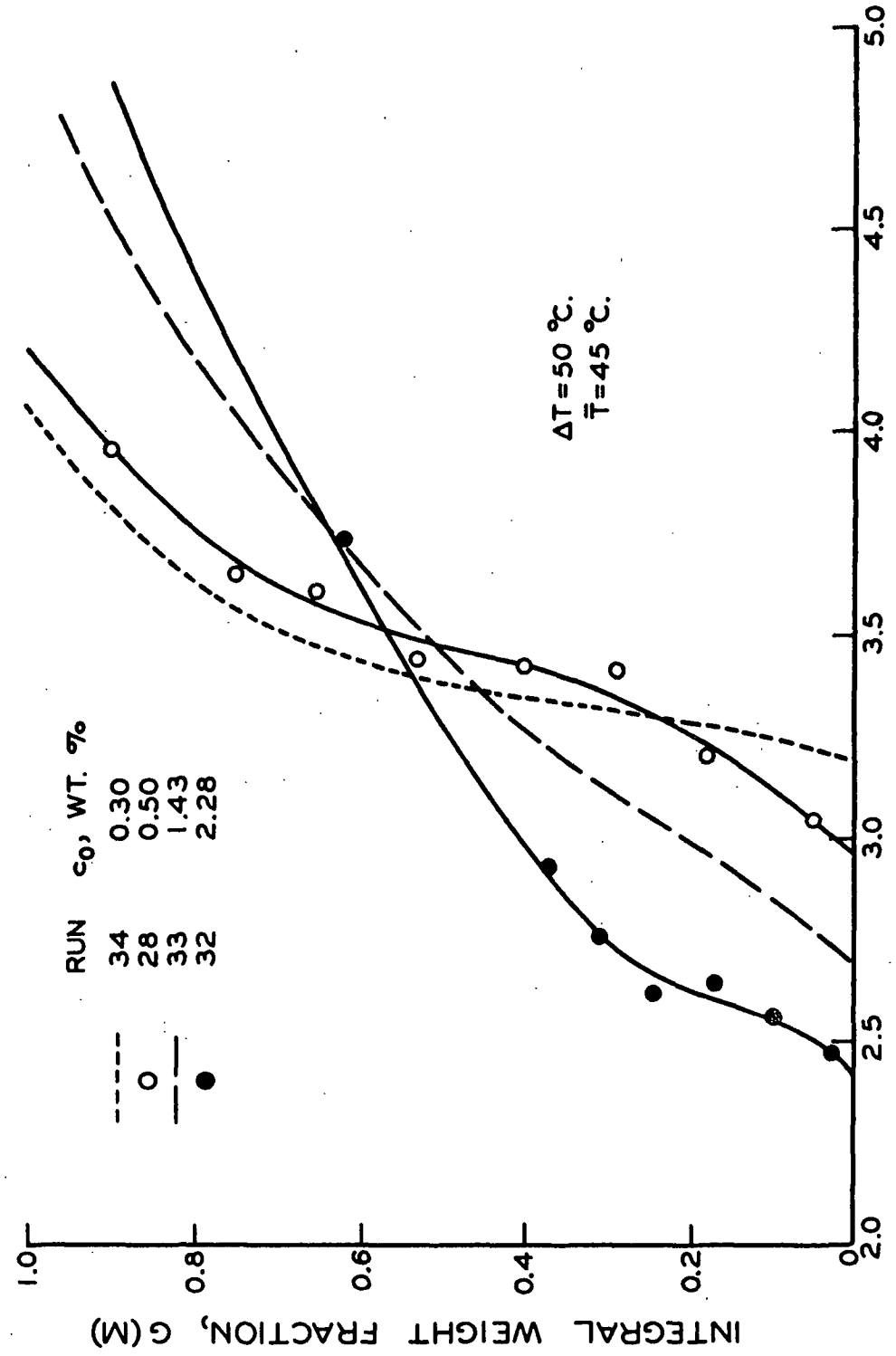

Figure 18. Effect of Concentration on Molecular Weight Distribution, Polymer B6 in Toluene

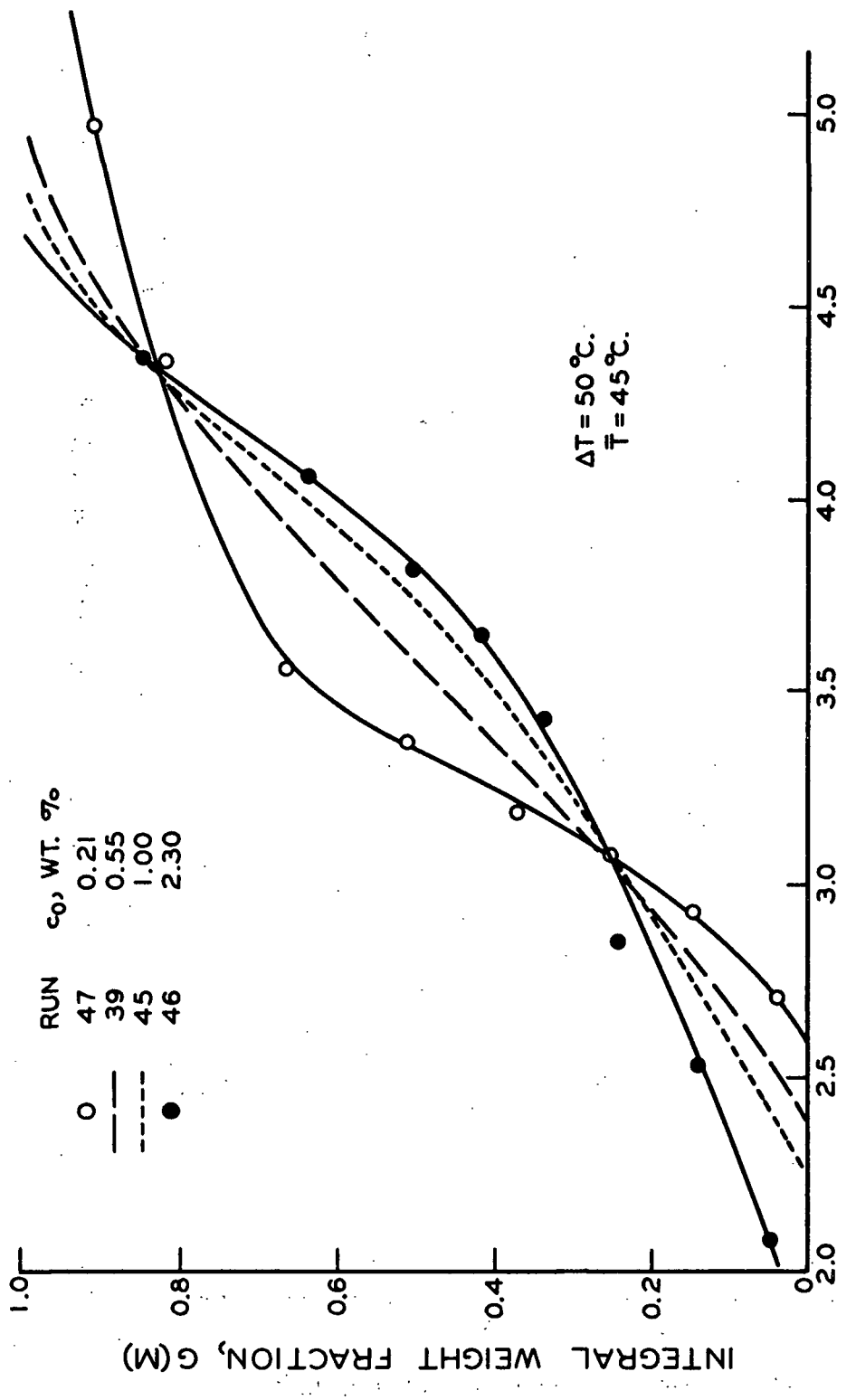

Figure 19. Effect of Concentration on Molecular Weight Distribution, Polymer B6 in MEK

extrapolated to infinite dilution should permit a calculation of the thermal diffusion coefficient and its molecular weight dependence from the column operating equations presented earlier. The results of these two approaches in obtaining explicitly the molecular weight effects are presented below.

FACTORIAL EXPERIMENT

A full four-factor two-level factorial experiment was completed using the two narrow distribution polymers. The factors and levels chosen are given in Table IV.

TABLE IV

COMPONENTS OF FACTORIAL EXPERIMENT

Factor	Designation	Low Level (-)	High Level (+)
Molecular wt.	A	82,000	239,000
Solvent	B	MEK	Toluene
Concentration, wt. %	C	0.4	1.0
Temperature diff., °C.	D	30	50

The mean temperature was maintained at 45°C. for all sixteen runs and was therefore not a factor in the experiment. The mean temperature was omitted from consideration because it had been shown earlier to have but a small effect on PS. The results are presented in Table V where:

(a) "Treatment Combination" describes the experimental conditions by indicating the high level factors involved in each run;

(b) PS is the measured degree of polymer-solvent separation as defined earlier;

(c) $R_1 = (PS)(\beta\rho/\eta_o) \times 10^2$ where β, ρ, and η_o are the thermal expansivity, density, and viscosity of the solvent at the mean temperature; and

(d) $R_2 = (PS)(\beta\rho/\eta) \times 10^2$ where η is the initial viscosity of the solution at the mean temperature of the run.

The mean velocity of the free convection currents is proportional to the factor $(\beta\rho/\eta)$, and the solvent-solute separation is inversely proportional to the convection velocity (1, 7). Therefore, the response R_1 should eliminate from PS the differences caused by physical differences of the solvent. The response R_2 should eliminate further the differences of solution viscosity between runs. R_2 then reflects differences in polymer-solvent separation which are due solely to differences in the molecular transport properties. The calculations are only approximate because no consideration has been given to the longitudinal viscosity gradient present in each run and because of other factors such as the different viscosity temperature dependencies of the solvents employed. Also, the assumptions inherent in the statistical testing of the three responses, PS, R_1, and R_2, cannot all be satisfied simultaneously. However, large effects and trends should be apparent.

The values of PS presented in Table V have been corrected for small deviations of starting concentration from the desired levels (see Appendix IV). The mean absolute correction was 0.002.

The fourth-order interaction and all smaller effects were pooled to give an error testing term to determine the significance of the various effects. In Table VI the effects significant at the 99% confidence level are denoted by three asterisks, those at 95% by two asterisks, and those at 90% by one. Significance tests enclosed by parentheses indicate that the corresponding effect was negative.

The B, C, and D main effects for the PS response had been manifested earlier in the data for Polymer B6 (see Fig. 11-13). The experimental levels of D, the temperature difference, were chosen to include the range in which PS for Polymer

TABLE V

RESULTS OF FACTORIAL EXPERIMENT

Run No.	Treatment Combination	PS	$\underline{R}_1$	$\underline{R}_2$
63	(1)	0.211	5.36	4.90
51	a	0.237	6.02	4.94
53	b	0.249	4.49	3.92
67	ab	0.290	5.23	3.95
52	c	0.260	6.60	5.29
62	ac	0.329	8.35	5.17
66	bc	0.308	5.55	3.99
54	abc	0.390	7.02	3.63
58	d	0.214	5.44	4.97
61	ad	0.243	6.17	5.06
64	bd	0.247	4.45	3.88
55	abd	0.292	5.26	3.97
60	cd	0.257	6.53	5.24
57	acd	0.412	10.46	6.47
56	bcd	0.310	5.59	4.01
65	abcd	0.415	7.49	3.88

TABLE VI

FACTORIAL EXPERIMENT--SIGNIFICANT EFFECTS AND INTERACTIONS

Effect	PS Response Mean Effect	Significance of Effects PS Response	R_1 Response	R_2 Response
A	0.069	***	***	--
B	0.042	***	(***)	(***)
C	0.087	***	***	*
D	0.014	*	--	--
AC	0.034	***	**	--
AD	0.014	*	--	--
BC	--	--	--	(**)
CD	0.012	*	--	--
ACD	0.013	*	--	--

B6 changed very little while the PP changed rapidly. The large dependence of the fractionation effect on temperature gradient should then appear as an AD interaction in the factorial experiment. The D effect for the PS response is seen to be small, but so is the AD interaction. It should be observed that the molecular weight of Polymers S102 and S111 lie in the lower one-third of the molecular weight distribution of Polymer B6. Discrepancies between the fractionation data for Polymer B6 and the factorial experiment data for the narrow distribution polymers might therefore be attributable to the presence of large quantities of higher molecular weight species in Polymer B6. Thus, the smallness of the AD interaction may indicate that fractionation of Polymer B6 occurs mainly among the larger molecules.

The large A effect for the PS response does not necessarily indicate a positive molecular weight dependence of the thermal diffusion coefficient; increased

solution viscosity accompanies an increase in molecular weight which in turn must increase PS through a reduction of the convection velocity. The large AC effect merely reflects the fact that the highest solution viscosities occur under combined conditions of high molecular weight and high concentration.

When the polymer-solvent separations are considered in terms of the R_1 response, which eliminates differences in physical properties of the solvent, the B effect reverses sign. This implies that the thermal diffusion flux of polymer in MEK is greater than in toluene at the same concentration, but that the greater free convection velocities attained with MEK cause the PS to be less in this solvent. (See discussion of Fig. 12).

The effects calculated from the R_2 responses should be approximately proportional to those which would result from a hypothetical experiment where the hydrodynamical aspects of all runs were identical. The main result of "correcting" the PS data in this manner is seen to be the elimination of the molecular weight effect entirely: the A effect for the R_2 response is zero. It is therefore inferred that the column thermal diffusion process does not distinguish differences in molecular weight in the range represented by Polymers S102 and S111. The existence of a significant concentration effect for the R_2 responses would indicate that an increase in concentration increases the magnitude of the thermal diffusion coefficient relative to the ordinary diffusion coefficient. Such a relation would agree with the theory of polymer thermal diffusion developed by Ham (17). However, because of the approximate nature of the R_2 responses, it is questionable whether the C and BC effects for the R_2 responses are real.

MOLECULAR WEIGHT EFFECT INDEPENDENT OF HYDRODYNAMIC VARIABLES

Mixture Experiment

In view of the uncertainty of conclusions drawn from the factorial experiment R_2 data, a more direct confirmation of the absence of a real molecular weight effect for Polymers S102 and S111 was desired. A simple method of checking the conclusion was to subject a mixture of the two polymers to thermal diffusion and measure the proportion of each polymer at several levels in the column. If indeed there were no molecular weight effect in the range under investigation then there would be no relative separation of the two polymers because at any point in the column the hydrodynamics are identical for each molecular species.

A 1% solution of equal weight proportions of Polymers S102 and S111 was subjected to thermal diffusion under the temperature conditions for Runs 56 and 65 (which involved 1% solutions of the polymers separately). The relative proportion of the two polymers present in any sample could be calculated from the intrinsic viscosity of the sample and the known intrinsic viscosities of the starting polymers. (The intrinsic viscosity of a multicomponent solute is the simple weighted average of the intrinsic viscosities of the solute constituents because of the additivity of specific viscosities at low concentrations.) The data from the mixed polymer run presented in Table VII demonstrates that no appreciable fractionation of the two polymers occurred. The small difference between the intrinsic viscosity of the column samples and the calculated viscosity of the mixture was probably due to a small error in the solution makeup or to a consistent bias in the viscosity measurements for the runs. In any event, these data are in accord with the data of the factorial experiment.

TABLE VII

RESULTS OF MIXED POLYMER RUN

RUN 69

Wt. fraction of Polymer S102 in mixture = 0.50

Wt. fraction of Polymer S111 in mixture = 0.50

A. Intrinsic Viscosity

S102	0.340	100 g./g.
S111	0.670	100 g./g.
Mixture	0.505	100 g./g. (calculated)

B. Sample Intrinsic Viscosity

Sample Range, Ports Number	$[\eta]'$, 100 g./g.
1 (Column Bottom)	0.504
2	0.499
3-4	0.500
5-7	0.500
8-10	0.495
11-14	0.500
15-19	0.495
20-30 (Top)	0.496

C. PS Separation

Run 56 (S102 alone)	0.316
Run 65 (S111 alone)	0.417
Run 69 (Mixture)	0.366

Data at Infinite Dilution

Another means of obtaining the explicit effect of polymer molecular weight on the column thermal diffusion separation process is to compare data for the different polymers at infinite dilution where the hydrodynamics of the column operation for given temperature conditions are determined only by the physical properties of the pure solvent. The measured equivalent extinction coefficient, γ', for Polymers S102, S111, and B6 in toluene are extrapolated to zero concentration in Fig. 20. Once again it is seen that in the range of molecular weight up to a few hundred thousand there is very little intrinsic effect of molecular weight on the degree of polymer-solvent separation. The small molecular weight dependence of γ' at infinite dilution is consistent with the small fractionation effect found in toluene solutions at low concentrations (Fig. 14). Langhammer's data for some vinyl polymers at low concentrations also indicate a small inherent molecular weight effect (10).

THEORETICAL CALCULATION

Equations (17) and (30) describing the processes occurring in a long narrow thermal diffusion column under conditions of infinite dilution of solute may now be employed to calculate the thermal diffusion coefficients of Polymers S102, S111, and B6 corresponding to the data extrapolated to zero concentration presented above. The result for Polymer B6 will be some mean value of all the molecular species present in this polydisperse sample.

FLOW PROBLEM

The solution of the flow problem consisted of obtaining a velocity profile of the free convection currents--that is, obtaining v_z of Equation (17) as a function of r. The experimental conditions for which the solution was obtained

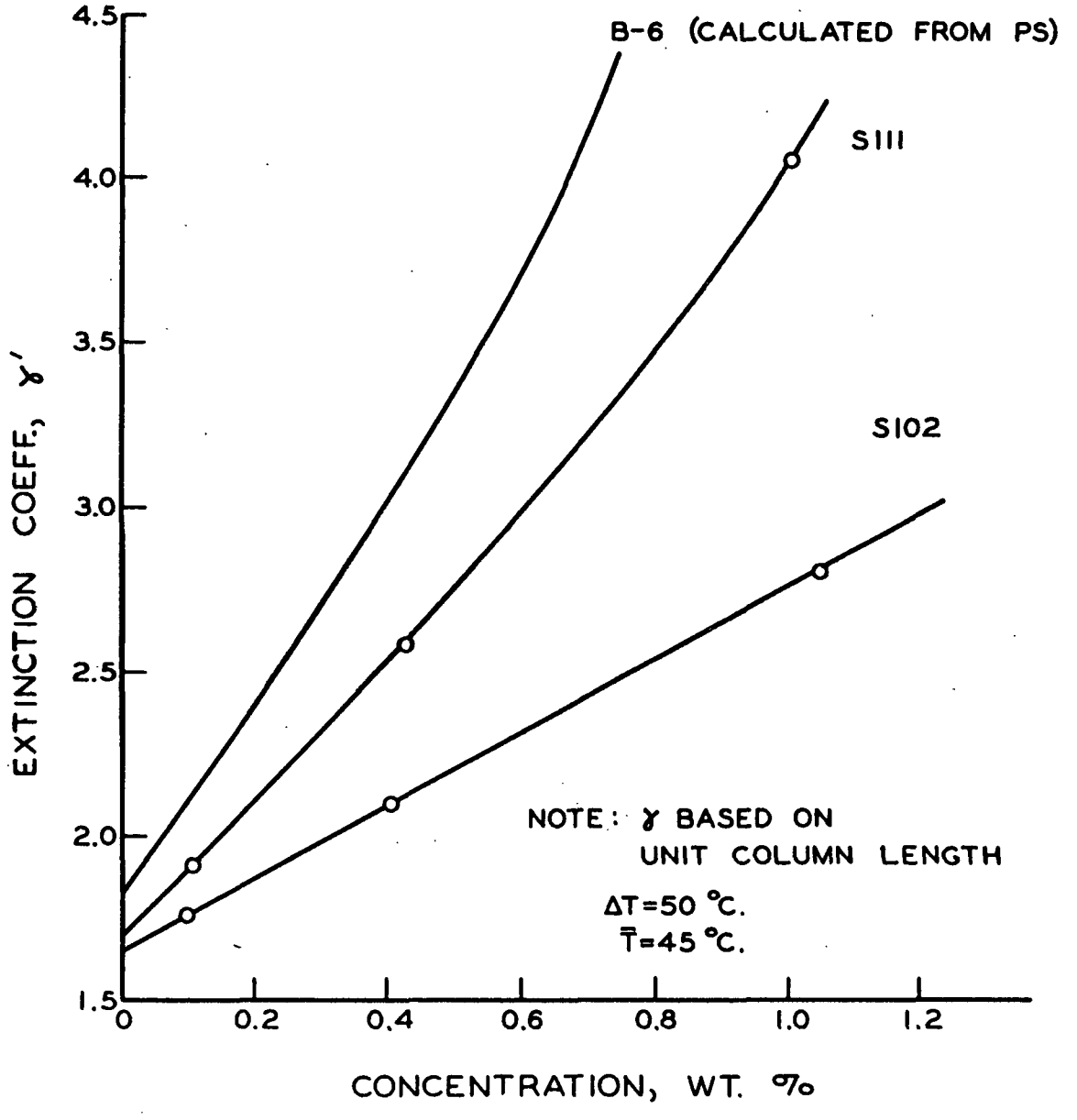

Figure 20. Concentration Dependence of Extinction Coefficient Polystyrene in Toluene

were: (a) toluene solvent, (b) 50°C. temperature difference, and (c) 45°C. mean temperature. The temperature dependence of viscosity and density of toluene were taken from the International Critical Tables. Equation (17) may be integrated explicitly but the resulting expression for v_z would be very complex; instead the equation was solved by numerical methods to yield v_z in tabular form. Equation (17) was integrated directly once to give a first-order differential equation. The constant of integration and the quantity dp/dz were then adjusted so that the boundary and integral conditions were simultaneously satisfied as calculated by means of the Newton-Cotes six-point method. The details of the computation are given in Appendix V. One hundred and forty-four equally spaced values of v_z were calculated. The resulting velocity profile is shown in Fig. 21. The deviation from symmetry of the v_z function caused by the temperature dependence of the viscosity is seen to be small for toluene; if the calculation had been performed for a rectangular geometry (rather than cylindrical), the asymmetry of the velocity profile would be somewhat greater.

DIFFUSION PROBLEM

For a given solution to the hydrodynamic problem, the steady-state concentration as a function of both horizontal and vertical position in the column is given by Equation (30) with auxiliary conditions (26) and (27). P expresses the concentration as a function of the radial co-ordinate r and is independent of the vertical co-ordinate z, and γ is related to the rate of diminution of concentration with z and is independent of r. If P is a solution of Equation (30) then any multiple of P is also a solution; the absolute value of P corresponding to a given level in the column would be proportional to the mean solute concentration at that level. However, for the purpose of computing D' from experimental values of γ, the magnitude of P may be assumed arbitrary. Because P and its derivative are interrelated

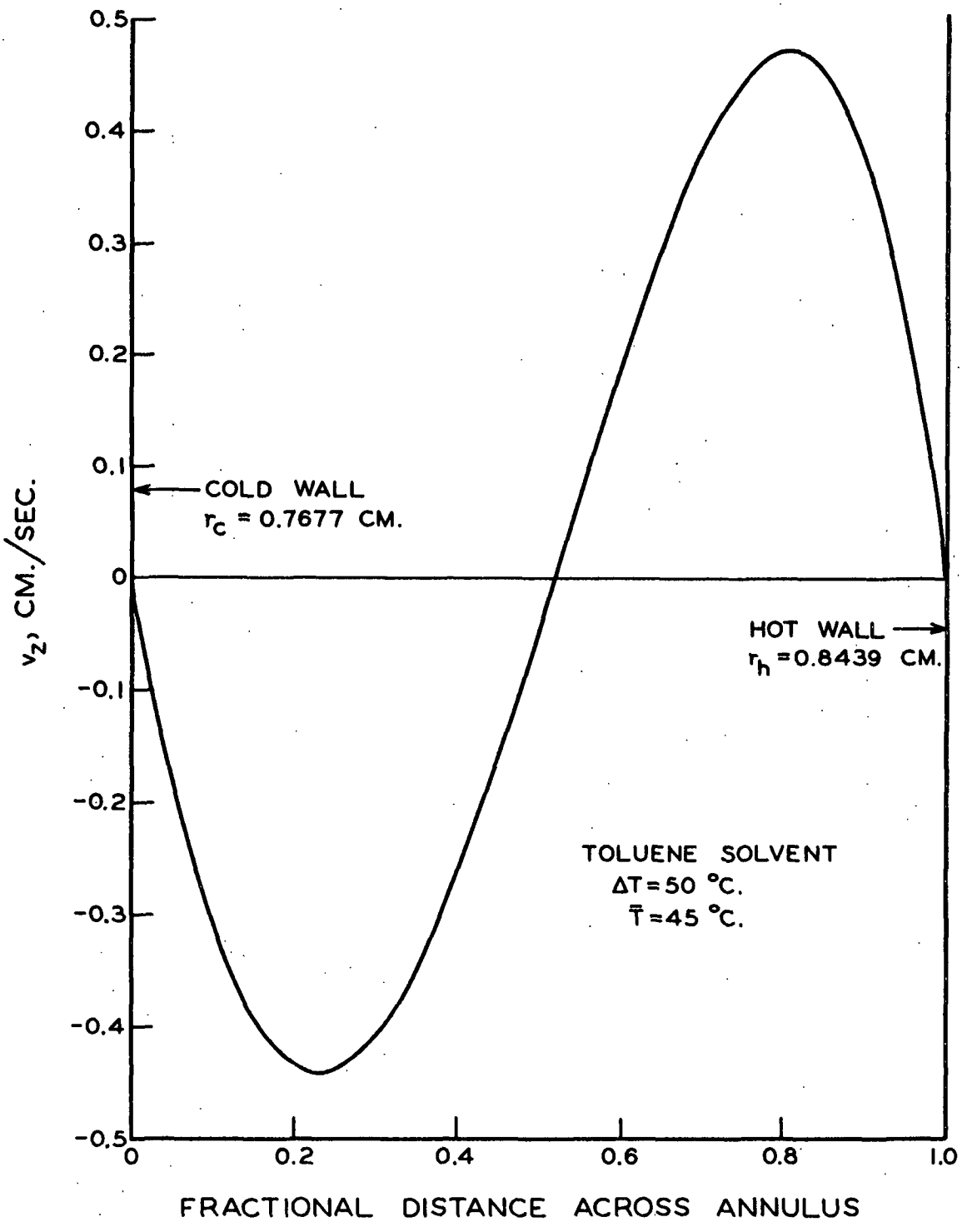

Figure 21. Velocity Profile of Convection Streams

at the walls of the column by Equation (26), a solution of Equation (30) which satisfies condition (26) at both boundaries must necessarily satisfy the flow condition of Equation (27). Therefore, the diffusion problem reduces to a boundary value problem with only one adjustable parameter. In the present case, all quantities except $\underline{D}'$ are known. The thermal diffusion coefficient of the polymer yielding a given value of γ at infinite dilution is therefore that value of $\underline{D}'$ which satisfies the differential Equation (30) with the proper boundary conditions (26). The function $\underline{P}$ is of course an important by-product of the trial and error calculation of $\underline{D}'$. The degree to which Equation (27) is satisfied when the boundary condition (26) is fulfilled is a measure of the adequacy of the assumptions made in arriving at Equation (30) including the effect of omitting the $\underline{D}'$ temperature dependence term.

Equation (30) was first expressed as two simultaneous first-order differential equations and then solved numerically by the Runge-Kutta method for simultaneous differential equations. The tabulated values of $\underline{v}_z$ from the solution of the flow problem were used in the computation. The details of the calculation are given in Appendix V.

The $\underline{P}$ function for Polymer S111 presented in Fig. 22 is similar in shape to those obtained for the other polymers. The concentration is highest at the cold wall (toward which the polymer migrates by thermal diffusion). The concentration gradient at the cold wall must be large in order that back-diffusion may balance the thermal diffusion flux to give no net transport through the wall. The concentration gradient at the cold wall must be greater for larger polymer molecules because the ordinary diffusion coefficient decreases with molecular weight. In several trial runs with Polymer S114 (molecular weight of three and one-half million), the large cold wall $\underline{dP/dr}$ and concomitant high concentration at the

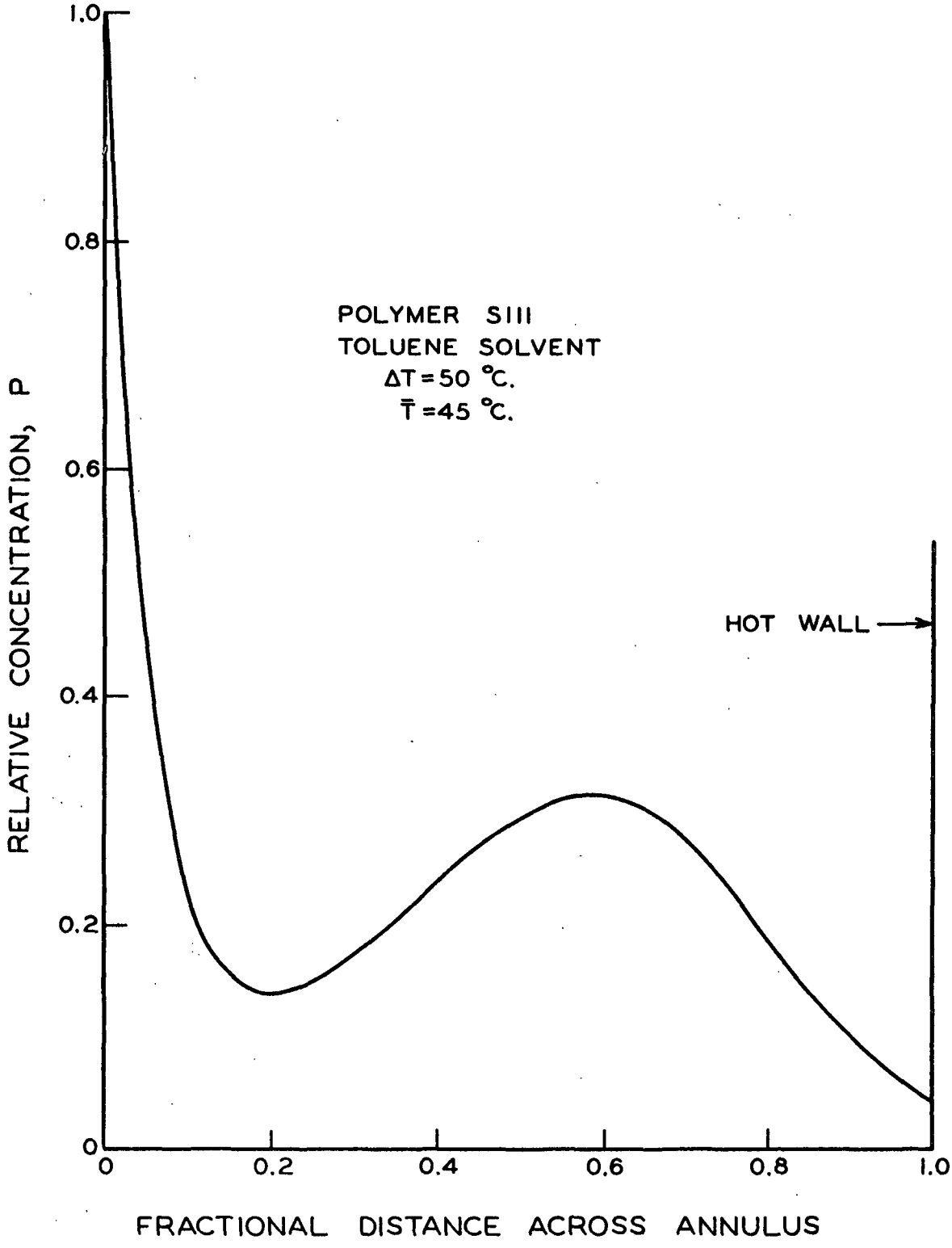

Figure 22. Radial Concentration Function in Column

wall was very much in evidence; although 95% of the solution volume was sampled from the column only 60% of the polymer could be recovered. Very high molecular weight polymers can therefore give rise to serious experimental difficulties in thermal diffusion work.

The over-all shape of the $\underline{P}$ function reflects the downward transport of low concentration solution by the cold convection stream and the upward transport of higher concentration solution by the warm stream. In the absence of any convective flows, $\underline{P}$ would be a smoothly decreasing function of $\underline{T}$ or $\underline{r}$ (as can be deduced from the integrated form of Equation (15), but the convective flows distort the function in the manner shown.

RESULTS OF CALCULATION

The results of the calculation of $\underline{D}'$ for Polymers S102, S111, and B6 are presented in Table VIII. The data are for toluene solutions and a mean temperature of 45°C.

TABLE VIII

ANALYSIS OF DATA AT INFINITE DILUTION

Polymer	Mol. Wt., Wt. av.	Extinction Coeff. γ, cm.$^{-1}$	$\underline{D} \times 10^7$, sq.cm./sec.	$\underline{D}' \times 10^7$, sq.cm./sec.-deg.
S102	82,000	0.00902	7.5	1.072
S111	239,000	0.00930	3.91	0.954
B6	425,000	0.00985	2.81	0.900

The value of the integral expressed by Equation (27) for each of the above three solutions to the diffusion problem was less than 1% of the partial integral taken across either half of the annulus. The simplifications involved in obtaining Equation (30) therefore do not seriously affect the results obtained.

To provide a more complete picture of the manner in which $\underline{D}$ and $\underline{D}'$ determine γ, the computations were extended to wider ranges of the variables. The results are plotted in Fig. 23. For these calculations both transport coefficients were assumed independent of temperature. As an example of the effect of the temperature independence assumption, the $\underline{D}'$ for Polymer S111 would have been calculated as 0.898×10^{-7} had a constant $\underline{D}$ of 3.91×10^{-7} been used. The large temperature dependence of the ordinary diffusion coefficient has only a mild effect on the calculated results.

The significance of the above calculations is discussed in the next section.

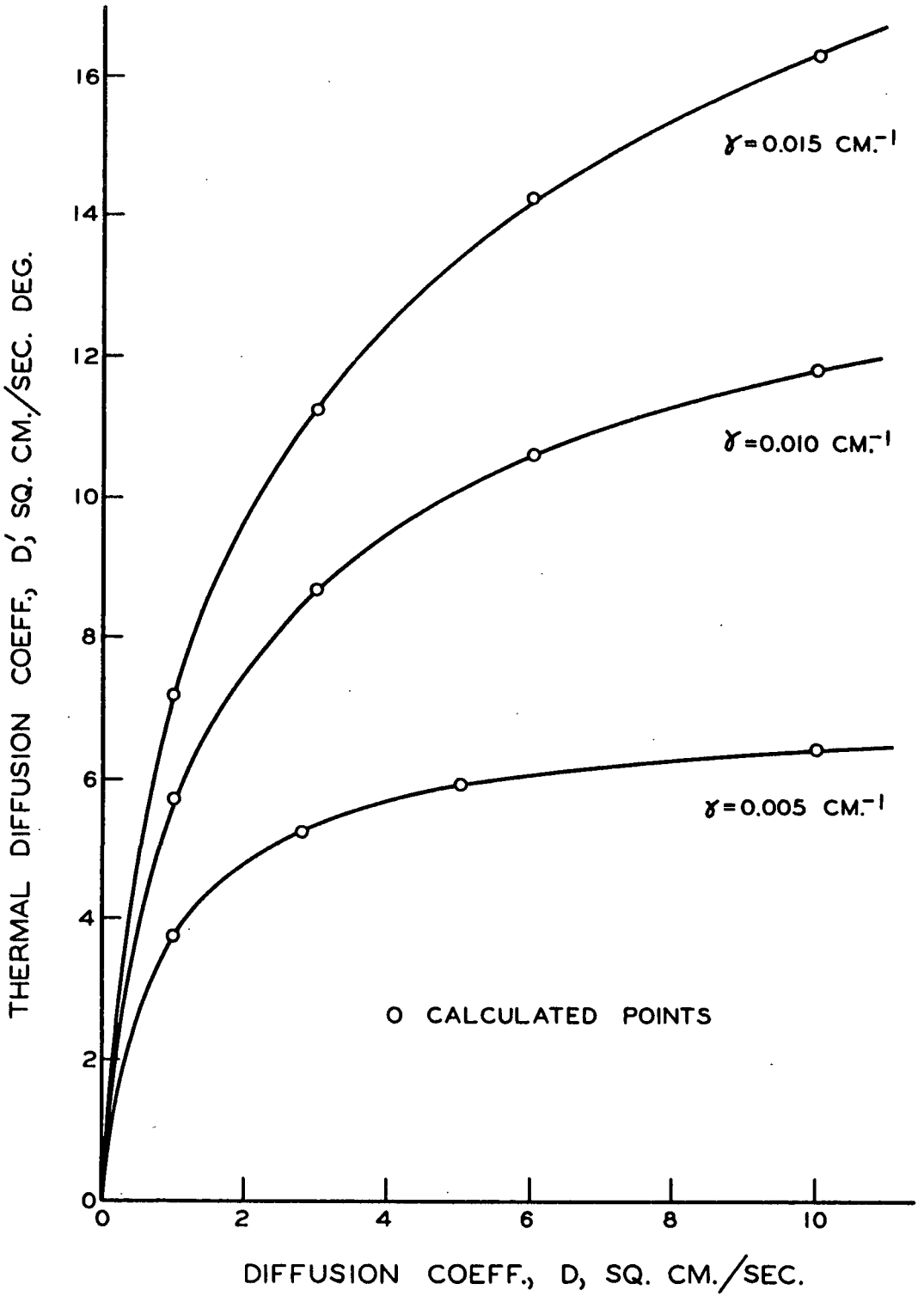

Figure 23. Column Operating Characteristics

DISCUSSION OF THE FRACTIONATION EFFECT

MECHANISMS OF FRACTIONATION

Let us examine carefully the data entered in Table VIII. The experimental values of the extinction coefficient γ depended very slightly on molecular weight, being somewhat greater for the larger molecules, but the diffusion coefficient D varied significantly over the range studied. Therefore, D did not have a strong influence in determining γ. The relative constancy of D' (compared with D) suggests that D' determines the order of magnitude of γ. However, if D' alone determined γ then the largest γ would correspond to the largest D', but the data contradict this. Therefore, the ordinary diffusion coefficient D must assume an important secondary role in determining the relative values of γ for different molecular weights. Thus, in the range of molecular weights studied it appears that D' mainly determines the extent of polymer-solvent separation (PS) while differences in D govern the extent of the polymer-polymer fractionation effect (PP). According to the recent theory of Ham (17) the thermal diffusion coefficient is not a strong function of molecular weight for sufficiently large molecules, and therefore any fractionation effect in a thermal diffusion column should be due primarily to differences in the ordinary diffusion coefficient; the larger molecules would have a greater rate of transport toward the cold wall because of their smaller tendency to diffuse back toward the lower concentrations near the hot wall. The results presented in Table VIII are therefore in qualitative agreement with Ham's theory.

Accepting the hypothesis that the fractionation effect is largely associated with differences in the ordinary diffusion coefficient, we can now develop a more detailed view of the fractionation mechanism. Assume for the moment that D and D'

are both independent of temperature and concentration and that only $\underline{D}$ is dependent on molecular weight. Imagine a differential volume element across which exists a temperature gradient $\underline{dT}/\underline{dr} = \theta$ and a constant concentration gradient $-\partial\underline{c}/\partial\underline{r}$ (Fig. 24).

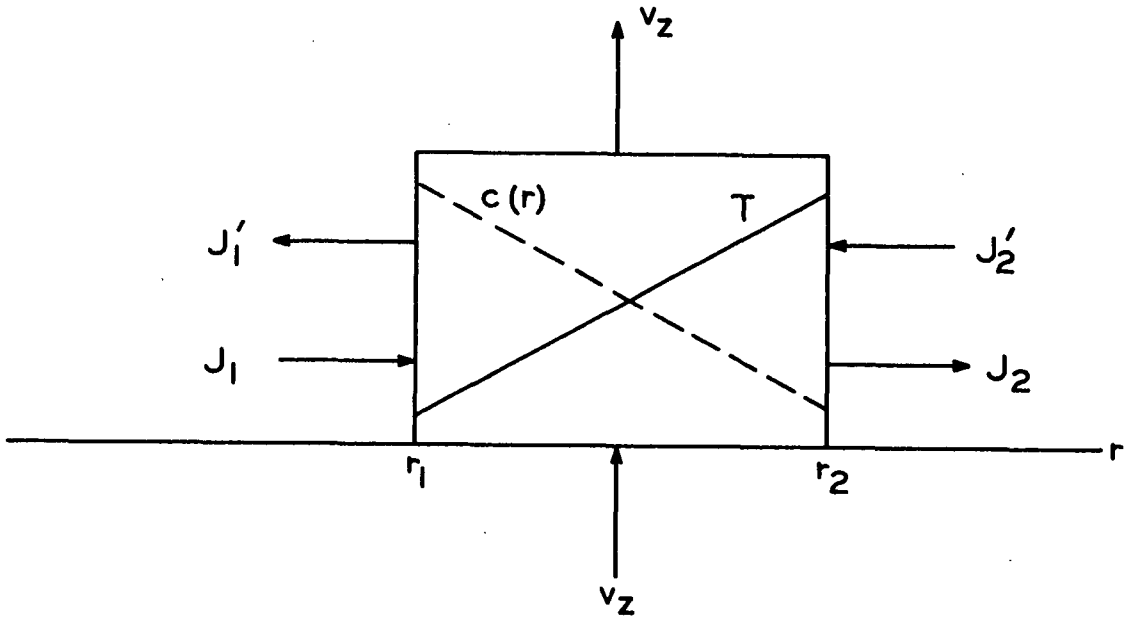

Figure 24. Volume Element Material Balance

The convective flow is represented by $\underline{v_z}$, the flux of material due to thermal diffusion by $\underline{J}'$, and that due to ordinary diffusion by $\underline{J}$. The horizontal fluxes are assumed separable in concept although in reality there is only a resultant net flux. The subscripts refer to the left and right boundaries of the volume element. Assume the solute consists of two species, $\underline{i}$ and $\underline{j}$, species $\underline{i}$ possessing the larger $\underline{D}$. The transports into and out of the volume element by $\underline{v_z}$ and $\underline{J}'$ do not discriminate the two species present, but the $\underline{J}$ transport is different for $\underline{i}$ and $\underline{j}$ because $\underline{D_i} > \underline{D_j}$. Hence, it is apparent that $\underline{J_{1,i}} > \underline{J_{1,j}}$ and $\underline{J_{2,i}} > \underline{J_{2,j}}$ where the double subscript identifies both position and species. However, such a condition does not necessarily imply that a fractionation effect occurs in the volume element. Indeed, in the present case, because the concentration gradient is

linear, $J_{1,i} = J_{2,i}$ and $J_{1,j} = J_{2,j}$, and the relative quantity of species i and j is therefore the same at r_1 and r_2. This is equivalent to the obvious statement that in regions where $c(r)$ (or P) is linear with r the middle term of Equation (20) vanishes if D is concentration independent. Thus, fractionation will occur to the greatest extent where dP/dr varies greatly with r--that is, where d^2P/dr^2 is greatest. The various concentration dependencies of polymer solutions will modify the above treatment, but the general correlation of the large second derivative of P with regions producing a strong fractionation effect should be valid.

Examination of Fig. 22 reveals that d^2P/dr^2 is greatest in the region extending from the cold wall to the first zero value of dP/dr. The value of the second derivative is several times greater in this region than anywhere else across the annulus. The major portion of the fractionation process should therefore occur near the cold wall.

A second item of interest in Fig. 22 is the region between zero values of dP/dr where the concentration gradient and the temperature gradient have the same sign. Any fractionation occurring in this region must be detrimental to the overall fractionation effect for the following reason. Across the entire annulus the net diffusive flux for all polymer molecules is directed toward the cold wall; in the regions near the walls fractionation occurs because molecules with high diffusion coefficients have smaller net velocities toward the cold wall, but in the central region the reversal of sign of dc/dr causes molecules with largest D to have the greatest net velocity toward the cold wall. Hence, a counter-fractionation occurs in the central region.

A third observation concerning the fractionation effect should be discussed before an attempt to interpret the experimental data is made. At steady state

conditions the total polymer concentration of any volume element is maintained constant by an exact balance of the three material fluxes through the element due to thermal diffusion, ordinary diffusion, and convection. It is to be expected that any change of conditions which increases the ratio of the ordinary diffusion flux to the thermal diffusion flux will tend to increase the fractionation effect.

TEMPERATURE GRADIENT EFFECT

As was shown in Fig. 14, the degree of polymer-polymer fractionation (PP) increased markedly with temperature. If differences in the thermal diffusion coefficient were the main source of the fractionation effect, then changes in the temperature gradient should not affect PP to any great extent. This follows from either the Furry-Jones (1, 26, 27) or Debye (7) treatment of column operation where it is shown that the separation factor (PS in the present terminology) of individual solute species is independent of temperature gradient because the velocity of both the convective flow and the thermal diffusion flux are proportional to the temperature gradient. If, however, PP is governed by differences in the ordinary diffusion coefficient of the solute species, then the observed effect is readily explainable in the following manner.

An increased temperature gradient must cause an increase in the concentration gradient at the cold wall so that Equation (22) is satisfied. Physically this means that the greater thermal diffusion flux caused by increased temperature gradient must be accompanied by an increased backward diffusion at the wall because there can be no net flow of material through the wall. An increased temperature gradient does not significantly affect the symmetry of the velocity profile; therefore, the location of the first minimum in the radial concentration function

(Fig. 22) will not be greatly altered. It follows that $\partial^2 c/\partial r^2$ must increase in the region near the cold wall (extending to where $\partial c/\partial r = 0$). As was shown above, the fractionation effect is probably strongly associated with the magnitude of $\partial^2 c/\partial r^2$ near the cold wall, and therefore the PP increases with increased temperature gradient.

CONCENTRATION EFFECT

The increase of PP with increased concentration of toluene solutions (Fig. 17) can also be explained in terms of the detailed mechanism of the fractionation process presented above.

The viscosity of polymer solutions increases rapidly with concentration, and therefore the velocity of the convection currents in a thermal diffusion experiment are smaller for higher initial concentrations. The maintenance of a steady state concentration for any volume element then becomes more of a balance between thermal diffusion and ordinary diffusion because of the decreased importance of convective transport. Hence, the fractionation effect is increased because the ratio of ordinary diffusion flux to thermal diffusion flux is increased.

A decrease in the convective flow implies a decrease in the deviation of the radial concentration function (Fig. 22) from the smooth logarithmic relation which exists in the absence of any convection. As the convectionless state is approached, the counter-fractionation zone described above must vanish. Thus, a further increase in PP will result from the reduction of the detrimental fractionation process occurring in the central regions of the annulus.

An increased initial concentration will contribute to the increase in PP in the same manner as an increased temperature gradient. According to Equation (22),

a higher concentration will cause $\partial c/\partial r$ at the walls to become larger which in turn leads to greater fractionation as discussed above with regard to the influence of temperature gradient.

Increased concentration can adversely affect PP in at least two ways. First, the relative differences in the diffusion coefficients of various size polymer molecules are reduced because of the strong concentration dependence of D for polymers. Second, increased concentration greatly magnifies the variation of solution viscosity across the annulus which in turn distorts the convection velocity profile in such a manner that the cold stream is broadened and the position of maximum downward velocity is shifted away from the cold wall (27). The position where $\partial c/\partial r = 0$ will also be shifted away from the cold wall so that $\partial^2 c/\partial r^2$ must be reduced in this region resulting in a reduced fractionation effect. Apparently, in the MEK system (Fig. 17) the concentration factors which tend to decrease PP approximately balance those which tend to increase PP so that PP for polystyrene in MEK is largely concentration independent.

The influence of a reduction in mean temperature in increasing PP is probably associated with the increased solution viscosity and resultant diminution of convection velocities in parallel with the effects noted above for increased concentration.

MOLECULAR WEIGHT EFFECT

The data have suggested that fractionation occurs among the higher molecular weight species present in Polymer B6 but not among the lower: (a) The interaction of molecular weight with temperature gradient in the factorial experiment was small even though the temperature gradient strongly influenced PP for the polydisperse Polymer B6; (b) The molecular weight effect in the factorial experiment was small

when differences in solution physical properties were eliminated; (c) No fractionation occurred when a mixture of Polymers S102 and S111 was subjected to thermal diffusion. If there is no intrinsic molecular weight effect on thermal diffusion for the smaller polystyrene molecules (those included in the range covered by Polymers S102 and S111 and the lower half of the Polymer B6 distribution), then differences in PS for the three polymers should be attributable to differences in solution viscosity over the entire range studied. The data of Fig. 20 have been replotted in Fig. 25 using the relative viscosity of the initial solutions rather than the concentrations. (The relative viscosities were calculated from data obtained in the determination of the intrinsic viscosity of the polymers.) It is apparent that the equivalent extinction coefficient is independent of molecular weight for the range of molecular weight involved. The measured differences in PS at a given concentration are due entirely to the hydrodynamical differences attributable to the viscosity effect.

According to Ham's theory, polymer thermal diffusion coefficients are not a strong function of molecular weight (17). For polystyrene, D' should increase with molecular weights less than 300,000 and then should be relatively constant (15). If such a behavior of D' is superimposed upon the theoretical relations presented in Fig. 23, the experimental results become quite plausible. For polystyrene, molecules larger than 300,000 molecular weight have diffusion coefficients of less than 2.5×10^{-7} sq. cm./sec. In this region it is seen that small changes of D for constant D' result in large differences of γ. In the region of higher D the γ curves diverge and also become more nearly parallel to the D axis; differences in D or D' for smaller molecules therefore should not produce large differences in γ. The experimental results, the theoretical calculations, and Ham's theory are therefore in mutual agreement.

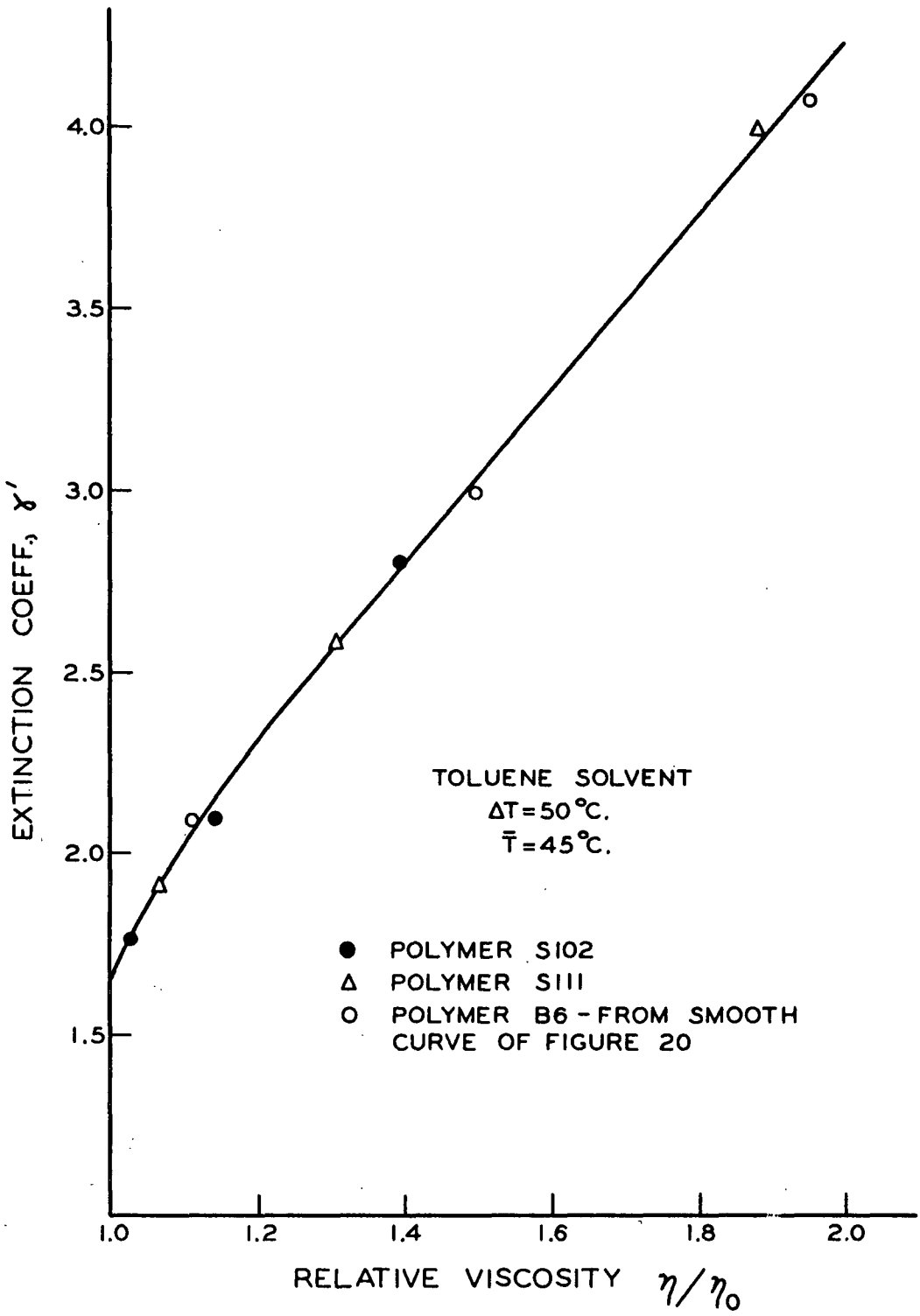

Figure 25. Effect of Solution Viscosity on Extinction Coefficient

Drickamer's theory of polymer thermal diffusion (12) predicts that the thermal diffusion constant, α, [see Equation (1)] should be directly proportional to molecular weight. For the polystyrene-toluene system, D is proportional to $M^{-0.56}$ and therefore D' should be proportional to $M^{0.44}$ which is a much stronger relation than predicted by Ham's theory. The experimental results cannot be interpreted in terms of Drickamer's theory as well as in terms of Ham's theory. It should be noted that the experimental data presented by Drickamer do not fully support his theory: the values of α at infinite dilution are more nearly proportional to $M^{1/2}$ than to M particularly if the α-concentration data are fitted empirically rather than theoretically to provide an extrapolation to zero concentration. If α is proportional to $M^{1/2}$, then D' would be relatively independent of molecular weight.

The calculated thermal diffusion coefficients presented in Table VIII are of the same order of magnitude as the few data available in the literature (14-16). A detailed comparison is not possible because of varying conditions of temperature and concentration. All literature values of D', given directly or calculated from values of α, fall in the range from 0.4×10^{-7} to 4.0×10^{-7} sq. cm./sec. deg. for the polystyrene-toluene system except for a few data of Whitmore (13). The small decrease of D' with molecular weight indicated in Table VIII may or may not be real. Errors in the extrapolated values of the extinction coefficient and in the measured width of the annulus would strongly affect the calculated D'. Nonuniformity of the temperature gradient in the column and consistent error in the temperature difference could also have an effect. Some literature data (13, 14) indicate a small inverse dependence of D' on molecular weight in accord with the present results. However, regardless of the accuracy of the calculations, it is clear that the data indicate that D' is not strongly dependent on molecular weight.

SUMMARY AND CONCLUSIONS

The objective of the present work has been to elucidate the mechanism of polymer thermal diffusion in a Clusius-Dickel separation column. The approach to the problem consisted of determining systematically the effects of important experimental factors on the separations obtainable and interpreting these effects in light of a mathematical description of column operation and recent theories of polymer thermal diffusion.

The thermal diffusion column employed was of the concentric cylinder type with an annular space of 0.0300-inch equipped with thirty sample ports. The column was electrically heated externally and water cooled internally to produce a radial temperature gradient.

The test polymers for the entire study were several polystyrene samples of varying known molecular weight and polydispersity. The experimental factors investigated were temperature gradient, mean temperature, solvent type, and concentration. The solvents employed were toluene and methyl ethyl ketone (MEK) which represented thermodynamically good and poor solvents, respectively, for the polymer in question.

The molecular separations occurring in the column due to thermal diffusion were divided conceptually into two classes: (a) the gross separation of polymer from solvent, designated by "PS", and (b) the separation of different size polymer molecules from each other, which is the fractionation effect or "PP". PS was determined by measuring the steady-state concentration gradient established in the column as a result of thermal diffusion and PP was related to the gradient of intrinsic viscosity in the column. Under all conditions the polymer was found to migrate in the direction of heat flow.

Considerable data concerning the thermal diffusion of the most polydisperse polymer sample showed that PS increased with temperature gradient and initial concentration and decreased with mean temperature in both solvents. These effects were readily interpreted in terms of known operating characteristics of thermal diffusion columns. PS was greater in toluene than in MEK, but this was shown to be due to the greater viscosity of the toluene solutions rather than to a larger thermal diffusion effect in the good solvent. For the very wide distribution polymer, PP was found to increase with temperature gradient and decrease with mean temperature. PP was largely independent of concentration in MEK but increased markedly with concentration in toluene solutions. The interpretation of these effects was derived from a theoretical computation of the influence of both ordinary and thermal diffusion on the column behavior in conjunction with a calculation of the horizontal concentration gradients existing in the column at steady state.

A factorial experiment involving two narrow distribution polymers indicated that molecular weight may have no intrinsic effect on polymer thermal diffusion for molecular weights below a few hundred thousand. The apparent effect of molecular weight in this range in causing an increased PS, was explained entirely by the dependence of solution viscosity on molecular weight of the solute. An auxiliary experiment involving the thermal diffusion of a known mixture of two nearly monodisperse polymers confirmed this finding.

The differential equations describing the thermal diffusion column operation were simplified to the special case of infinite dilution in a long narrow column. The reduced equations permitted a calculation of: (a) the dependence of PS on the molecular transport coefficients, (b) the variation of concentration across the annulus, and (c) the thermal diffusion coefficients of the polymers studied.

The results of (a), above, indicated that if the thermal diffusion coefficient is not a strong function of molecular weight, then the fractionation process should be more efficient for the larger molecules, as was found to be the case. The theoretical calculation and the experimental data also showed that the solute molecules with largest thermal diffusion coefficients do not necessarily show the greatest tendency to separate from the solvent. The results of (b) showed that the greatest portion of the fractionation process must take place as the polymer molecules approach the cold wall, and that some detrimental counter-fractionation occurs near the middle of the annulus. The effects of concentration on the degree of fractionation were inferred from the theoretical calculations at infinite dilution by considering the manner in which the horizontal concentration gradients must be affected by the changes of initial concentration. The results of (c), above, indicated that the thermal diffusion coefficient of polystyrene in toluene is not a strong function of molecular weight in agreement with the recent theory of Ham.

With regard to the usefulness of column thermal diffusion for molecular weight characterization of linear homologous high polymers, the following conclusions may be made:

(1) The degree of fractionation obtained is <u>not</u> necessarily greatest for infinitely dilute solutions as one might at first expect, and therefore an analytical correction of data at infinite dilution cannot provide an accurate description of true molecular weight distributions;

(2) For a given temperature gradient, the changes in experimental conditions which produce an increase in the degree of fractionation are precisely those changes which diminish the velocity of the convection currents--hence, the maximum degree of fractionation should be obtained in a convectionless cell (with its concomitant disadvantage of small apparatus dimensions or long equilibrium times);

(3) The fractionation effect appears to be greatest for the larger molecules present in a specimen.

SUGGESTIONS FOR FUTURE WORK

The data obtained indicate that polydisperse linear homologous high polymers are not effectively fractionated by the column thermal diffusion process. However, many of the high molecular weight substances encountered in the pulp and paper industry are not of this type--for example, tall oil of the kraft process, dissolved lignin, and hemicellulosic extracts. These are more heterogeneous materials than those studied in the present thesis and might be more responsive to thermal diffusion fractionation because the varied constituents may exhibit large differences in thermal diffusion coefficient. Maximum fractionation of these substances would be obtained using a mean temperature midway between the solvent boiling and freezing points where the greatest temperature gradient is attainable.

The data indicate that the fractionation effect is greatest under conditions of high temperature gradient and small convection velocity. In the extreme, these conditions correspond to the convectionless cell-type thermal diffusion experiment. This suggests that a thermal diffusion moving boundary technique similar to that developed in sedimentation velocity work might be valuable in analyzing heterogeneous solutions such as those mentioned above. The techniques would be quite similar--the temperature gradient replacing the gravitational field as the driving force--but complexities of equipment and theory resulting from the rotational motion necessary in ultracentrifugation would be eliminated.

ACKNOWLEDGMENTS

The author wishes to acknowledge the encouragement and assistance given him by his Advisory Committee, Dr. S. F. Kurath, Dr. R. W. Nelson, and Mr. H. A. Swenson. Particular thanks are due Dr. Nelson for his generous assistance in the development of a mathematical description of the column operation and his guidance in the solution of the resulting equations.

NOMENCLATURE

a = constant in molecular weight--intrinsic viscosity relation

c = concentration, wt. % or g./dl.

D = diffusion coefficient, sq. cm./sec.

D' = thermal diffusion coefficient, sq. cm./sec.-deg.

G = integral distribution function

g = differential distribution function, or gravitational constant

J = generalized flux of mass or energy

K = constant in molecular weight--intrinsic viscosity relation

k = optical constant of the ultracentrifuge, or a constant relating to K and a

k' = Huggins' constant relating to polymer solution viscosity

k_s = constant relating to concentration dependence of sedimentation coefficient

L = generalized phenomenological coefficient

M = molecular weight

m = a constant relating to K and a

MEK = methyl ethyl ketone

N = mole fraction

P = radial concentration function in column theory

PP = degree of polymer-polymer fractionation

PS = degree of polymer-solvent separation

Q = longitudinal concentration function in column theory

Q^* = net heat of transport

R = polydispersity parameter used in calculating PP

r = radial dimension in column geometry

S = sedimentation coefficient as measured, uncorrected

S^o = sedimentation coefficient, corrected

s = sedimentation coefficient

$\underline{T}$ = absolute temperature, °K.

$\overline{\underline{T}}$ = average of hot and cold wall temperature, °C.

$\underline{t}$ = time

$\underline{v}$ = velocity, cm./sec.

$\underline{X}$ = generalized driving force

$\underline{z}$ = longitudinal dimension in column geometry

GREEK LETTERS

α = thermal diffusion constant equal to $\underline{D'T}/\underline{D}$

β = volume expansivity

γ = extinction coefficient, $cm.^{-1}$ or per unit column length

γ' = equivalent extinction coefficient, calculated from $\underline{PS}$

η = solution viscosity

η_o = solvent viscosity

$[\eta]$ = intrinsic viscosity, dl./g.

$[\eta]'$ = intrinsic viscosity, 100 g./g.

θ = temperature gradient, °C./cm.

μ = chemical potential

ρ = density, g./cc.

ϕ = ultracentrifuge schlieren blade angle

ω = ultracentrifuge rotational velocity

LITERATURE CITED

1. Onsager, L., Phys. Rev. 37:405; 38:2265(1931); Jost, W. Diffusion in solids, liquids, gases. Chap. XII. New York, Academic Press, 1952. 558 p.
2. Fox, M. C., Chem. & Met. Eng. 52:102(Dec., 1945).
3. Jones, A. L., Ind. Eng. Chem. 47:212(1955).
4. Jones, A. L., Petrol. Refiner 36, no. 7:153(1957).
5. Mair, B. J., and Rossini, F. D., Ind. Eng. Chem. 47:1062(1955).
6. Jones, A. L., and Foreman, R. W., Ind. Eng. Chem. 44:2249(1952).
7. Debye, P., and Bueche, A. M. Thermal diffusion of polymer solutions. In H. A. Robinson's High polymer physics. p. 497. New York, Remsen, 1948.
8. Kossler, I., and Krejsa, J., J. Polymer Sci. 29:69(1958).
9. Kossler, I., and Stolka, M., J. Polymer Sci. 44:213(1960).
10. Langhammer, G., Svensk. Kem. Tidskr. 69:328(1957).
11. Langhammer, G., and Forster, H., Z. physik. Chem. (Frankfurt) 15:212(1958).
12. Emery, A. H., and Drickamer, H. G., J. Phys. Chem. 23:2252(1955).
13. Whitmore, F. C., J. Appl. Phys. 31:1858(1960).
14. Hoffman, J. D., and Zimm, B. H., J. Polymer Sci. 15:405(1955).
15. Herren, C. L., and Ham, J. S., J. Chem. Phys. 35:1479(1961).
16. Meyerhoff, V. G., Lutje, H., and Rauch, B., Makromol. Chem. 14-16:489(1961).
17. Ham, J. S., J. Appl. Phys. 31:1853(1960).
18. Tyrrell, H. J. V., Trans. Faraday Soc. 56:770(1960).
19. Denbigh, K. G., A.I.Ch.E. Journal 5:20(1959).
20. Dougherty, E. L., and Drickamer, H. G., J. Chem. Phys. 23:295(1955).
21. Dougherty, E. L., and Drickamer, H. G., J. Phys. Chem. 59:443(1955).
22. Prager, S., and Eyring, H., J. Chem. Phys. 21:1347(1953).
23. Denbigh, K. G., Trans. Faraday Soc. 48:1(1952).
24. Oriani, R. A., J. Chem. Phys. 34:1773(1961).

25. Trevoy, D. J., and Drickamer, H. G., J. Chem. Phys. 17:1120(1949).

26. Jones, R. C., and Furry, W. H., Rev. Mod. Phys. 18:151(1946).

27. Emery, A. H., Jr., Ind. Eng. Chem. 51:651(1959).

28. McCormick, H. J., J. Polymer Sci. 36:341(1959).

29. Baldwin, R. L., J. Phys. Chem. 63:1570(1959).

30. Baldwin, R. L., J. Am. Chem. Soc. 76:402(1954).

31. Williams, J. W., and Saunders, W. M., J. Phys. Chem. 58:854(1954).

32. Flory, P. J. Principles of polymer chemistry. Ithaca, Cornell Univ. Press, 1953. 672 p.

33. Schultz, G. V., Angew. Chem. 64:553(1952).

34. Bawn, C. E. H., Freeman, R. F. J., and Kamaliddin, A. R., Trans. Faraday Soc. 46:1107(1950).

35. Bawn, C. E. H., Grimley, T. B., and Wajid, M. A., Trans. Faraday Soc. 46:1112(1950).

36. Outer, P., Carr, C. J., and Zimm, B. H., J. Chem. Phys. 18:830(1950).

37. Bianchi, U., and Magnasco, V., J. Polymer Chem. 41:177(1959).

38. Weissberg, S. G., Simha, R., and Rothman, S., J. Research Natl. Bur. Standards 47:298(1951).

39. Krigbaum, W. R., Mandelkern, L., and Flory, P. J., J. Polymer Sci. 9:381(1952).

40. Fox, T. G., and Flory, P. J., J. Am. Chem. Soc. 73:1915(1951).

41. Goldberg, A. I., Hohenstein, W. P., and Mark, H., J. Polymer Sci. 2:503(1947).

42. Langhammer, G., Kolloid Z. 146:44(1956).

43. Langhammer, G., Makromol. Chem. 21:74(1956).

44. Baldwin, R. L., and Williams, J. W., J. Am. Chem. Soc. 72:4325(1950).

45. McCormick, H. J., J. Polymer Sci. 36:341(1959).

46. Schachman, H. K. Ultracentrifugation in biochemistry. New York, Academic Press, 1959. 272 p.

47. Baldwin, R. L., J. Phys. Chem. 63:1570(1959).

48. Baldwin, R. L., J. Am. Chem. Soc. 76:402(1954).

49. Schick, A. F., and Singer, S. J., J. Phys. Chem. 54:1028(1950).

50. Newman, S., and Eirich, F., J. Colloid Sci. 5:541(1950).

51. Meyerhoff, G. In H. A. Stuart's Physics of high polymers. Vol. II. The macromolecule in solution. Berlin, Springer-Verlag, 1953. 782 p.

52. Scholtan, W., Makromol. Chem. 7:209(1951).

53. McCormick, H. W., The Dow Chemical Company. Personal communication, 1960.

54. Schick, A. F., and Singer, S. J., J. Phys. Chem. 54:1028(1950).

55. Nachtigall, V. K., and Meyerhoff, G., Makromol. Chem. 33:85(1959).

56. Meyerhoff, G., Z. physik. Chem. (Frankfurt) 4:335(1955).

57. Meyerhoff, G., Makromol. Chem. 37:97(1960).

58. Flory, P. J. Principles of polymer chemistry. Chap. XIV. Ithaca, Cornell Univ. Press, 1953. 672 p.

APPENDIX I

DEMONSTRATION THAT LONGITUDINAL DIFFUSION IS NEGLIGIBLE

In the present analysis of polymer thermal diffusion in a Clusius-Dickel separation column, the mass flux due to ordinary diffusion along the length of the column has been omitted from consideration. This is easily justified in the following manner.

At any position along the radial co-ordinate, there is a net longitudinal mass transport due to convection and ordinary diffusion. Because of the non-linear concentration gradient along the column, there will be a net accumulation (or depletion) of solute in any elemental volume which must be compensated for at steady state by the horizontal diffusion process taking place. The concentration gradient along the column (z-direction) in the ideal case is given by

$$c = c_o \exp(-\gamma z) \tag{41}$$

with first and second derivatives

$$\partial c/\partial z = -\gamma c \tag{42}$$

$$\partial^2 c/\partial z^2 = \gamma^2 c \tag{43}$$

The z-direction solute flux due to convection is given by

$$J_v = cv \tag{44}$$

where v is the convective velocity. The accumulation of solute in the elemental volume due to convection is then

$$\text{Accum. due to v} = -\partial J_v/\partial z$$

or

$$\text{Accum. due to v} = -v\partial c/\partial z \tag{45}$$

$$= \gamma v c$$

The z-direction solute flux due to diffusion is given by

$$J_D = -D\ \partial c/\partial z \tag{46}$$

where D is the diffusion coefficient (assumed independent of concentration). The accumulation due to longitudinal diffusion is then

$$\text{Accum. due to D} = -\partial J_D/\partial z \tag{47}$$

$$= D\ \partial^2 c/\partial z^2$$

$$= \gamma^2 Dc \tag{48}$$

The ratio of (48) to (45) is $(\gamma D/v)$ which is of the order 10^{-9} for the present system.

APPENDIX II

SUGGESTED APPROACH TO POLYMER CHARACTERIZATION BY THERMAL DIFFUSION

For physical reasons, thermal diffusion cannot produce a complete fractionation of a polydisperse polymer, but an analytical correction of thermal diffusion data to yield a true molecular weight distribution for the polymer may be possible under certain conditions. If column data can be obtained at low concentration where the extinction coefficient γ is constant along the column and if the molecular weight dependence of γ is known, then the following approach may prove useful.

The unknown concentration of species $\underline{i}$ at level $\underline{z}$ in the column is given by

$$c_{i,z} = c_{i,o} \exp(-\gamma_i z) \tag{49}$$

where $\gamma_{\underline{i}}$ is the extinction coefficient for species $\underline{i}$ and $c_{\underline{i},o}$ is the concentration of $\underline{i}$ at $\underline{z} = 0$. The concentration of $\underline{i}$ in the original solution, $c_{\underline{i}}^{\,o}$ is given by

$$c_i^{\,o} = \int_o^1 c_{i,z}\,dz \tag{50}$$

Substituting Equation (49) in (50) and integrating we obtain

$$c_{i,o} = \gamma_i c_i^{\,o}/(1-\exp(-\gamma_i)) \tag{51}$$

Let $g_{\underline{i}}^{\,o}$ be the fraction of $\underline{i}$ in the starting polymer and $g_{\underline{i},\underline{z}}$ the fraction of $\underline{i}$ in the polymer at level $\underline{z}$. Then

$$g_i^{\,o} = c_i^{\,o}/c^o \tag{52}$$

where c^o is the total concentration of the original solution, and

$$g_{i,z} = c_{i,z}/c_z \tag{53}$$

where c_z is the measured concentration at z. Combining Equations (49) and (51)-(53) gives

$$g_{i,z} = [\gamma_i \exp(-\gamma_i z)/(1-\exp(-\gamma_i))](c^o/c_z)g_i^o \qquad (54)$$

Suppose that some parameter F which measures a mean molecular size for a given polymer specimen is determined for each of several samples from the column. Such a parameter could be the intrinsic viscosity. If the nature of the mean which F measures is known, then we can write

$$F_z = \Phi_{i=1}^{\infty} (g_{i,z}) \qquad (55)$$

where the functional relation Φ is known. Substituting Equation (54) into (55) gives a relation between the experimentally measurable F_z and the desired distribution g_i^o. If F_z is measured for n samples from the column, n values of g_i^o may be determined from the n resulting simultaneous equations.

If a heterogeneous solute is studied, F could be the specific refractive increment and Φ would then represent a simple weighted average.

APPENDIX III

CHARACTERIZATION OF POLYMER B6 BY ULTRACENTRIFUGATION

GENERAL OUTLINE

The complete molecular weight distribution of polydisperse Polystyrene B6 was determined by means of the velocity ultracentrifugation technique. Were it not for the effects of diffusion and concentration dependence of sedimentation coefficient, the refractive index gradient recorded by schlieren optics during a velocity run would give directly the distribution of sedimentation coefficient describing the polydispersity of the solute. All that need be done would be to transform the optical co-ordinates of the refractive index gradient into $\underline{s}$-$\underline{g}(\underline{s})$ co-ordinates where $\underline{g}(\underline{s})$ is the frequency function of $\underline{s}$, the sedimentation coefficient. In a real system with diffusion and concentration effects, the transformation gives an "apparent" distribution of sedimentation coefficient: $\underline{S}$-$\underline{g}^*(\underline{S})$. The spreading of the boundary between sedimenting solute and free solvent due to back-diffusion can be eliminated by extrapolating apparent distributions to infinite time because diffusion spreading is proportional to the square root of time whereas that due to polydispersity is directly proportional to time (44). The diffusion-free distribution, designated $\underline{S}$-$\underline{g}(\underline{S})$, can then be analytically corrected for concentration effects if $\underline{S}$ is known as a function of $\underline{S}^o$ (the sedimentation coefficient at infinite dilution) and $\underline{c}$, the concentration.

EXPERIMENTAL DETAILS

Concentration effects were minimized by using a theta solvent for polystyrene (cyclohexane at 35°C.) as suggested by McCormick (45) and centrifuging at a very low concentration (about 0.1 g./dl.). To minimize the contribution of diffusion to the boundary spreading, the maximum ultracentrifuge speed of 59,780 r.p.m. was used.

The wide molecular weight distribution of the polymer under study necessitated the use of a synthetic boundary cell so that a region of pure solvent would exist above the boundary. To maximize the duration of the run (and thus enhance the infinite time extrapolation) the cell centerpiece was nearly filled with solution so that the boundary was formed high in the cell.

The acceleration time required to attain maximum rotational velocity was a considerable fraction of the total duration of the run. Therefore, speed-time data were taken during acceleration to permit an exact calculation of the equivalent time of acceleration given by

$$t_e = (1/\omega_f^2) \int \omega^2 dt \qquad (56)$$

where ω_f is the final speed of rotation.

Because the original solution-solvent boundary position was an important factor in the calculation, a photograph was taken immediately after boundary formation before any noticeable spreading occurred.

CALCULATIONS

TRANSFORMATION OF CO-ORDINATES (46)

The spatial co-ordinate $\underline{x}$, measured from the center of rotation, and the refractive index gradient (proportional to the concentration gradient $\underline{dc}/\underline{dx}$) were transformed to $\underline{S}$-$\underline{g}^*(\underline{S})$ co-ordinates by

$$S = (1/\omega^2 t)\ln(x/x_o) \qquad (57)$$

and

$$g^*(S) = (dc/dx)\omega^2 t x^3/x_o^2 c_o \qquad (58)$$

where ω is the operating rotational velocity, $\underline{x}_o$ is the original boundary location, and $\underline{c}_o$ is the original solution concentration given at any time by

$$c_o = \int (x/x_o)^2 (dc/dx)dx \qquad (59)$$

The value of $\underline{t}$ in the above equations is the total time of rotation including the equivalent time of acceleration. In the present work $\underline{c}_o$ calculated from Equation (59) was time dependent (diminishing by 10% during the run) and therefore the $\underline{c}_o$ corresponding to the value of $\underline{t}$ was used in Equation (58).

EXTRAPOLATION TO INFINITE TIME

The extrapolation to infinite time was accomplished by Baldwin's method (47) which has a theoretical basis. The method consists of extrapolating $(\underline{S}-\bar{\underline{S}})^2$ to zero value of the time function $[\underline{t}\ \exp(\bar{\underline{S}}\omega^2\underline{t})]^{-1}$ for selected values of $\underline{g}^*(\underline{S})/\underline{g}^*(\underline{S})_{max}$ on each photograph during the run. It was found that an appropriate mean sedimentation coefficient to use in the calculation was

$$\bar{S} = \bar{S}_1 \cong \int Sg^*(S)dS \qquad (60)$$

The diffusion free curve of $(\underline{S}-\bar{\underline{S}}_1)^2$ vs. $\underline{g}(\underline{S})/\underline{g}(\underline{S})_{max}$ was then converted to the desired frequency distribution of $\underline{S}$ vs. $\underline{g}(\underline{S})$ by applying the extrapolated value of $\bar{\underline{S}}_1$ and the infinite time value of $\underline{g}(\underline{S})_{max}$ obtained from

$$g(S)_{max} = \left\{ \int [g(S)/g(S)_{max}]dS \right\}^{-1} \qquad (61)$$

CONCENTRATION CORRECTION

Procedure

Baldwin's method of correcting the $\underline{S}$-$\underline{g}(\underline{S})$ curve for concentration effects (48) was followed except that the tedious correction for the Johnston-Ogston

effect was omitted. This effect is usually small compared to the sharpening correction in polymer systems. The procedure is outlined as follows:

(1) Choose a time t corresponding to a photograph taken near the middle of the run.

(2) Calculate

$$dc/dS = g(S)c_o \exp(-2\omega^2 St) \tag{62}$$

where the concentrations are in the optical units of the centrifuge and c_o is given by Equation (59).

(3) Calculate the actual concentration C in the cell as a function of S by

$$C(S) = k \tan \phi \int_o^S (dc/dS)dS \tag{63}$$

where k is a constant for the system relating real concentration to the optical units, and ϕ is the schlieren blade angle. In the present case, k was obtained from the data of the run by

$$k = C_o/A_o \tan \phi \tag{64}$$

where C_o = the starting concentration of the solution, g./dl., and

A_o = area of the schlieren peak at zero time, square inches on the photographic plate.

The calculated value of k was 7.50 g./dl.-sq. cm.

(4) Knowing $C(S)$ and S, calculate S^o, the corrected sedimentation coefficient, from the known concentration dependence of S. The concentration relation was deduced from literature data as described below.

(5) From the calculated pairs of S, S^o find dS/dS^o as a function of S. This was done graphically in the present case. The slope ranged from 0.85 to 1.00.

(6) Correct the frequency function by

$$g(S^o) = g(S)\, dS/dS^o \tag{65}$$

The corrected distribution is then $g(S^o)$ vs. S^o.

Concentration Dependence of S

The concentration dependence of S for many substances, including linear high polymers, is described by

$$S = S^o/(1 + k_s c) \tag{66}$$

where k_s is independent of concentration but does depend on S^o. There is at present insufficient literature data available establishing an experimentally verified k_s - S^o relation for polystyrene-cyclohexane. However, an interesting correlation from which k_s may be computed can be derived from the literature data of several polymer systems.

In Fig. 26 are plotted the results of two independent investigations (49, 50) concerning the concentration dependence of S^o for the polystyrene-MEK system. (Concentration was in g./dl.). Two other widely different systems, for which there were sufficient data, gave similar results: polymethylmethacrylate in acetone [(51), p. 475, 479] and polyvinylpyrrolidone in salt water (52). The relation between k_s and $[\eta]$ for a given system is understandable if $[\eta]$ is interpreted as a measure of the effective size of the polymer in solution. The slope of the logarithmic k_s-$[\eta]$ relation for a given polymer should be independent of

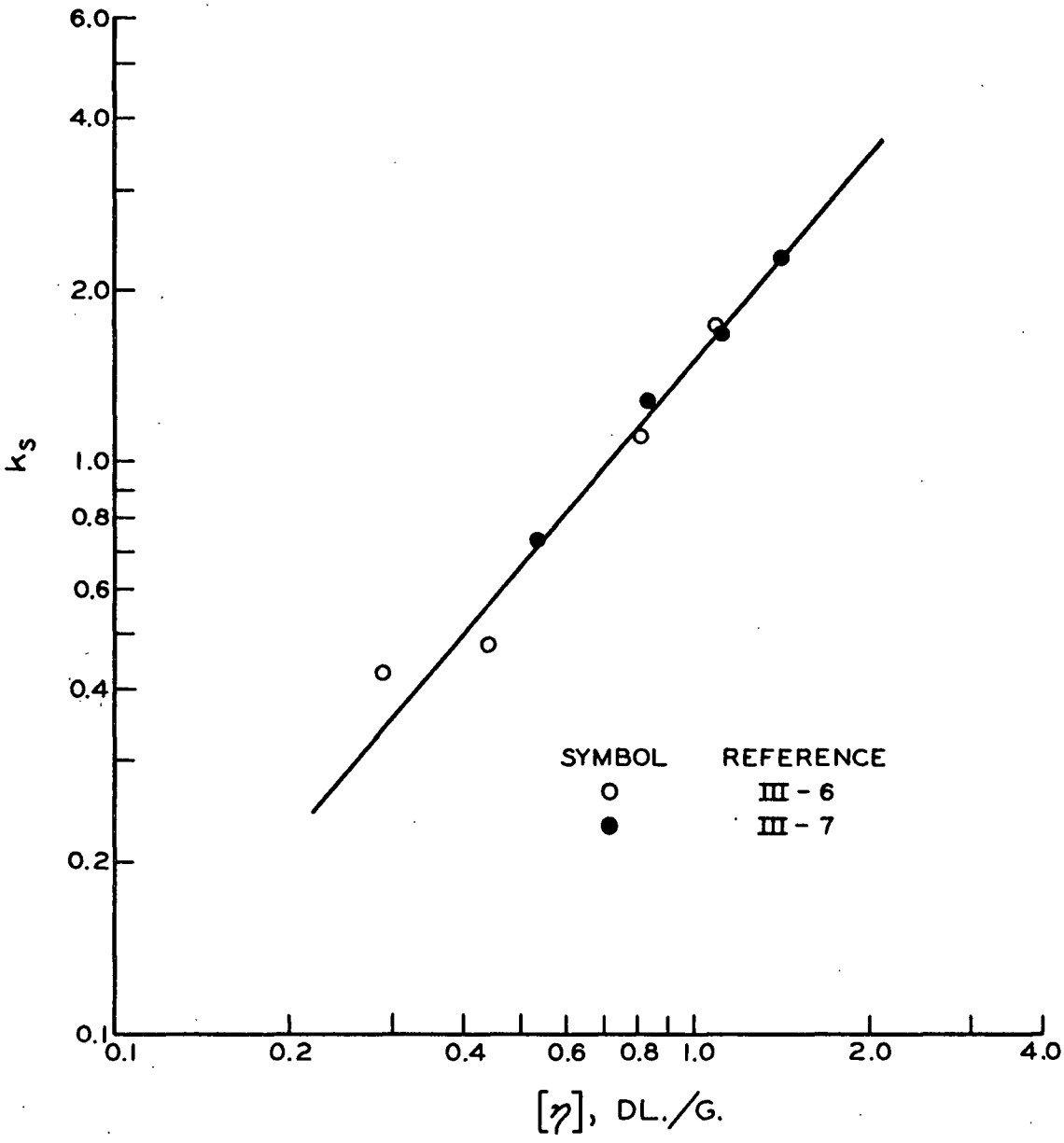

Figure 26. Correlation of Sedimentation Concentration Dependence With Intrinsic Viscosity-- Polystyrene in MEK

solvent because the influence of solvent on the effective molecular size is already included in the intrinsic viscosity. Differences in the k_s-$[\eta]$ relation for different solvents should then depend only on physical properties of the pure solvent. The solvent viscosity is probably the most important property involved. The slope of the relation given in Fig. 26 is 1.2, and therefore the quantity $k_s[\eta]^{-1.2}$ for polystyrene in various solvents should be a simple function of the solvent viscosity. For one of their polystyrene fractions Newman and Eirich (50) obtained both k_s and $[\eta]$ in the good solvents toluene and chloroform, and McCormick has reported these data (53) for one polystyrene fraction in cyclohexane. With these three single data points plus the well-established value of $k_s[\eta]^{-1.2}$ for MEK, we obtain a verification of the above reasoning as seen in Fig. 27. The resulting relation is

$$k_s = 9.93 \times 10^{-3} [\eta]^{1.2}/\eta_o^{0.9} \qquad (67)$$

where η_o is in poises and $[\eta]$ is in dl./g. Combining Equation (67) with the $[\eta]$ -s relation for polystyrene-cyclohexane found by McCormick (45) we obtain

$$k_s = 0.0250\ s^{1.26} \qquad (68)$$

Equation (66) with the above value of k_s is plotted in Fig. 28.

RESULTS

Some of the data pertaining to the ultracentrifuge run from which the molecular weight distribution of Polymer B6 was calculated are presented in Table IX. The initial concentration, at 35°C. was 0.107 g./dl.

The mean sedimentation coefficient which McCormick relates to weight molecular weight is the second moment of the distribution of sedimentation coefficient:

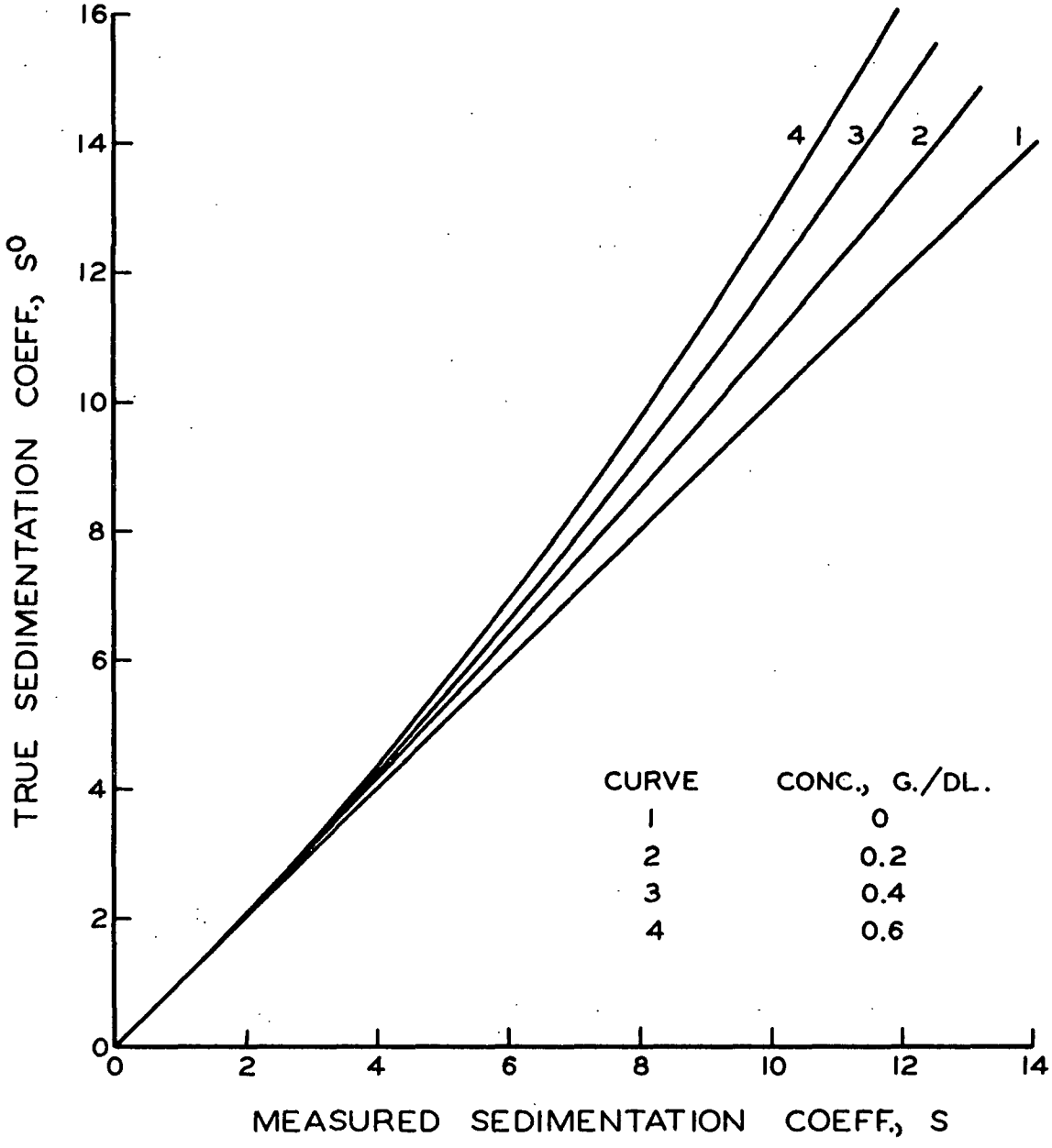

Figure 27. Effect of Solvent Viscosity on Friction Parameter for Polystyrene

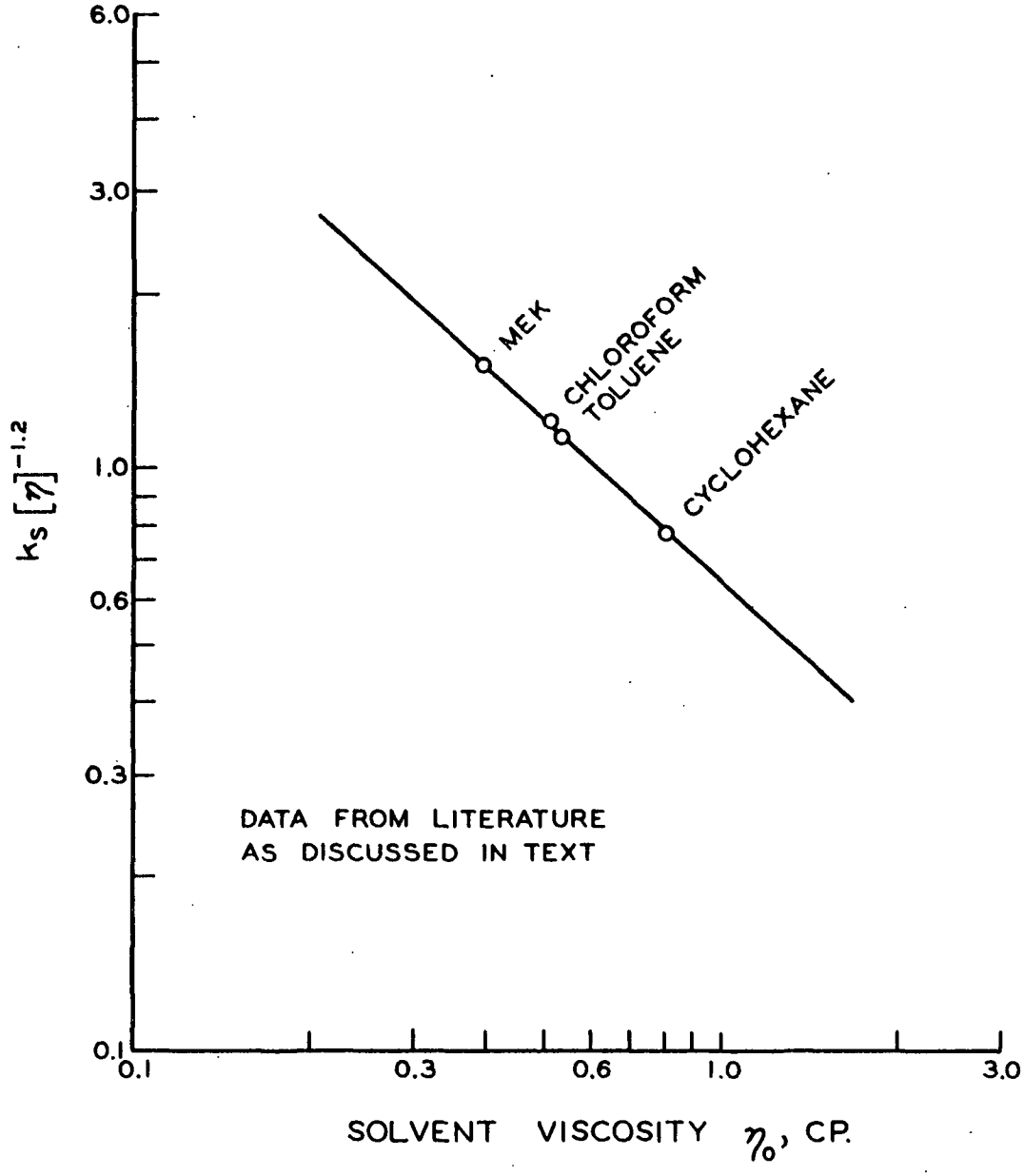

Figure 28. Calculated Concentration Dependence of Sedimentation Coefficient--Polystyrene in Cyclohexane

$$\bar{S}_2 = [\int S^2 g(S)dS]^{1/2} \qquad (69)$$

The change in both $\bar{S}_1$ and $\bar{S}_2$ upon application of the diffusion and concentration corrections is presented in Table X.

TABLE IX

ULTRACENTRIFUGE VELOCITY RUN DATA

Photograph Plate-Frame	Time from Start, min.	Equivalent[a] Time, min.	Schlieren Angle, ϕ	Area, $c_o \tan\phi$	$\bar{S}_1$
256-1	1.00	--	--	(Location of x_o)	
2	10.37	--	70	0.01400	--
3	14.37	10.31	70	0.01380	7.309
4	18.37	14.31	60	0.01313	7.467
5	21.13	19.08	60	0.01250	7.483

[a]The acceleration time of 9.50 minutes was equivalent to 5.44 minutes of operation at top speed.

TABLE X

MAGNITUDE OF DIFFUSION AND CONCENTRATION CORRECTIONS

Condition	Mean Sed. Coeff., Svedbergs $\bar{S}_1$	$\bar{S}_2$
At infinite time	7.73	8.29
Corrected for sharpening	7.92	8.56
McCormick's data	--	8.59

McCormick graphically extrapolated the infinite time curves for various starting concentrations to zero concentration, and therefore his value of $\bar{S}_2$ for Polymer B6 implicitly includes the Johnston-Ogston correction. If all the above data are correct, then it appears that the sharpening correction is about an order

of magnitude greater than the Johnston-Ogston correction. This is approximately the relation found for a dextran sample analyzed by Baldwin and Williams (48).

The computed distribution of sedimentation coefficient at various stages in the correcting process is presented in Fig. 29.

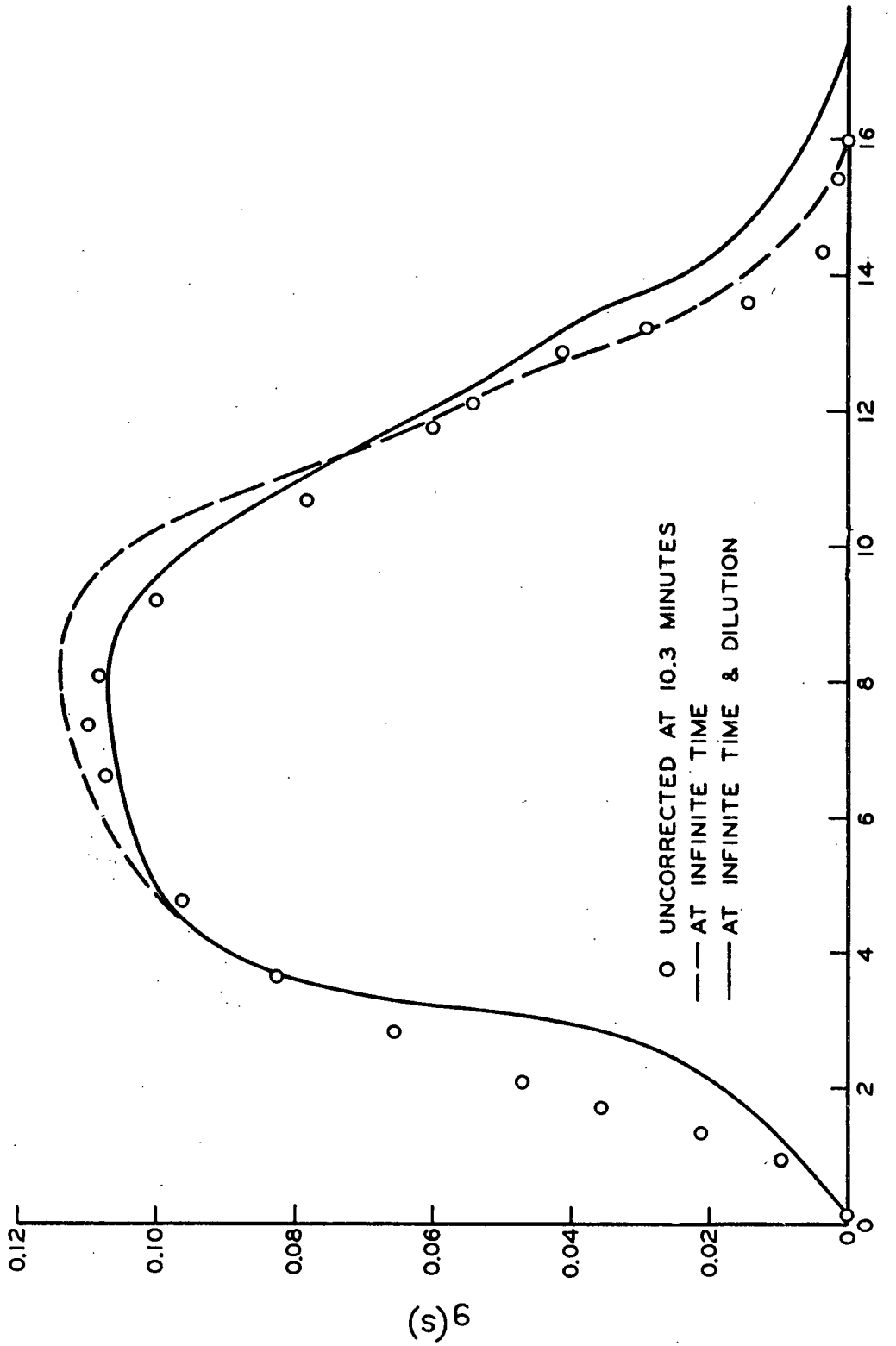

Figure 29. Sedimentation Corrections for Polymer B6

APPENDIX IV

DATA OF THE THERMAL DIFFUSION RUNS

DETERMINATION OF STEADY STATE

Six runs using Polymer B6 in toluene at 0.38% concentration by weight were performed in the determination of steady state (Table XI). The cold and hot wall temperatures were maintained at 20 and 70°C., respectively. The duration of the run was taken as the total length of time the heating elements were on. In this series of runs, each sample represented solution between two adjacent sample ports. Thus, the sample from Port n is the solution between Ports n and $n+1$. The concentrations are given as relative concentrations, c/c_o, where c_o is the starting concentration stated above, in order to facilitate comparison with other runs if desired.

TABLE XI

RUNS TO DETERMINE STEADY STATE

	Run Numbers					
Duration, hr.	13 / 1.0	11 / 2.0	12 / 4.0	7 / 12.7	9 / 22.3	10 / 35.5
Sample Port	Relative Concentrations c/c_o					
1	6.20	6.35	5.70	6.53	6.79	6.11
2	3.22	2.93	3.28	3.20	3.16	3.24
4	2.16	1.90	1.97	2.06	2.02	2.09
8	1.20	1.18	1.23	1.28	1.32	1.30
13	0.68	0.76	0.79	0.81	0.82	0.79
18	0.49	0.48	0.53	0.59	0.52	0.53
23	0.36	0.37	0.34	0.33	0.34	0.34
28	0.21	0.28	0.25	0.21	0.28	0.29

GENERAL SUMMARY OF THERMAL DIFFUSION RUNS

The operating conditions for all runs and the resulting separations obtained are presented in chronological order. The data are not grouped by operating condition to avoid repetition.

TABLE XII

SUMMARY OF THERMAL DIFFUSION DATA

Run No.	Polymer	Solvent	Concn., Wt.%	$\underline{T}$, °C.	$\overline{T}$, °C.	PS	PP
14	B6	Toluene	1.48	50	45	0.607	--
15	B6	Toluene	0.887	50	45	0.511	--
16	B6	Toluene	0.919	20	45	0.458	--
17	B6	Toluene	0.370	20	45	0.248	--
18	B6	Toluene	1.45	20	45	0.554	--
19	B6	Toluene	0.892	35	45	0.502	--
21	B6	Toluene	0.888	10	45	0.441	--
22	B6	Toluene	0.902	80	45	0.519	0.565
23	B6	Toluene	0.893	20	20	0.502	--
24	B6	Toluene	0.898	35	23	0.547	--
25	B6	Toluene	0.947	50	45	0.489	--
27	B6	Toluene	0.189	50	45	0.276	--
28	B6	Toluene	0.497	50	45	0.386	0.082
29	B6	Toluene	0.497	80	55	0.392	0.162
30	B6	Toluene	0.497	20	50	0.251	0.016
31	B6	Toluene	0.174	50	45	0.273	0.043
32	B6	Toluene	2.28	50	45	0.632	0.321
33	B6	Toluene	1.43	50	45	0.573	0.213
34	B6	Toluene	0.300	50	45	0.283	0.056
39	B6	MEK	0.503	50	47	0.320	0.228
40	B6	MEK	0.506	10	45	0.252	0.020
41	B6	MEK	0.503	30	45	0.296	0.035
42	B6	MEK	0.506	62	45	0.384	0.204
43	B6	MEK	1.54	50	45	0.531	0.216
45	B6	MEK	0.993	50	45	0.447	0.232
46	B6	MEK	2.30	50	45	0.608	0.236
47	B6	MEK	0.208	50	45	0.246	0.190
48	B6	MEK	0.506	61	44	0.383	0.252
49	B6	MEK	0.507	40	45	0.304	0.141
50	B6	MEK	0.515	40	28	0.357	0.199

TABLE XII (Continued)

Run No.	Polymer	Solvent	Concn., Wt.%	T, °C.	$\bar{T}$, °C.	PS	PP
51	S111	MEK	0.417	30	45	0.240	--
52	S102	MEK	1.003	30	45	0.260	--
53	S102	Toluene	0.417	30	45	0.251	--
54	S111	Toluene	1.037	30	45	0.396	--
55	S111	Toluene	0.424	50	45	0.297	--
56	S102	Toluene	1.052	50	45	0.316	--
57	S111	MEK	1.015	50	45	0.416	--
58	S102	MEK	0.408	50	45	0.228	--
60	S102	MEK	1.009	50	45	0.258	--
61	S111	MEK	0.404	50	45	0.244	--
62	S111	MEK	0.991	30	45	0.328	--
63	S102	MEK	0.410	30	45	0.212	--
64	S102	Toluene	0.411	50	45	0.248	--
65	S111	Toluene	1.011	50	45	0.417	--
66	S102	Toluene	0.979	30	45	0.306	--
67	S111	Toluene	0.412	30	45	0.292	--
69	S102 +S111	Toluene	1.018	50	45	0.366	0.00
70	S102	Toluene	0.104	50	45	0.210	--
71	S111	Toluene	0.107	50	45	0.226	--

DATA OF THERMAL DIFFUSION SAMPLES

In the following tables the data under the heading "Sample" are the numbers of the pairs of sample ports indicating the region of the column included by the sample. The ports were numbered from 1 at the bottom of the column to 31 at the top. Because all concentrations were measured as a percentage by weight, the intrinsic viscosities obtained were in units of 100 g./g. rather than the customary dl./g. The intrinsic viscosities reported below are given in the original units of 100 g./g., and are therefore denoted by $[\eta]'$. The simple conversion formula relating $[\eta]'$ and the normal $[\eta]$ is

$$[\eta]' = \rho[\eta] \qquad (70)$$

where ρ is the solvent density. At 25°C. the density of toluene and MEK are, respectively, 0.861 and 0.800 g./ml. The operating conditions for the runs listed in Table XIII have been given in Table XII.

TABLE XIII

RUNS DETERMINING PS ONLY

Relative Concentration c/c_o

Sample	Run 14	Run 15	Run 16	Run 17	Run 18
1-2	8.26	8.96	6.59	4.60	--
2-3	3.06	3.32	3.21	3.70	3.29
4-5	1.27	1.63	1.71	2.52	1.52
8-9	0.59	0.79	0.80	1.43	0.69
13-14	0.33	0.49	0.46	0.90	--
18-19	0.20	0.29	0.29	0.68	0.27
23-24	0.12	0.19	0.22	0.50	0.17
28-29	0.09	0.14	0.14	0.44	0.11

Sample	Run 19	Run 21	Run 23	Run 24
1-2	6.31	6.68	5.97	6.25
2-3	3.21	3.88	3.16	3.34
4-5	1.73	2.08	1.67	1.66
8-9	0.86	1.01	0.78	0.77
13-14	0.49	0.58	0.46	0.42
18-19	0.31	0.40	0.32	0.28
23-24	0.20	0.27	0.21	0.16
28-29	0.14	0.17	0.18	0.09

Run 25

Sample	c/c_o
1-2	6.33
2-3	3.46
3-4	2.68
4-5	1.73
5-6	1.46
7-8	0.994
11-13	0.574
17-31	0.230

Run 27

Sample	c/c_o
1-2	4.28
2-3	2.62
3-5	1.93
5-6	--
6-10	1.45
10-15	1.00
15-20	0.678
20-31	0.404

Run 51

Sample	c/c_o
1-2	2.82
2-3	2.30
3-5	2.03
5-8	1.70
8-12	1.28
12-17	0.961
17-22	0.664
22-31	0.413

Run 52

Sample	c/c_o
1-2	2.88
2-3	2.46
3-5	2.18
5-8	1.66
8-12	1.22
12-17	0.886
17-22	0.614
22-31	0.394

Run 53

Sample	c/c_o
1-2	2.64
2-3	2.16
3-5	1.98
5-8	1.67
8-12	1.24
12-17	0.915
17-22	0.625
22-31	0.405

Run 54

Sample	c/c_o
1-2	5.79
2-3	3.75
3-4	2.97
4-6	2.04
6-9	1.34
9-13	0.870
13-19	0.538
19-31	0.270

Run 55

Sample	c/c_o
1-2	3.86
2-3	2.63
3-5	2.14
5-8	1.74
8-12	1.21
12-17	0.870
17-22	0.555
22-31	0.324

Run 56

Sample	c/c_o
1-2	3.65
2-3	2.90
3-5	2.38
5-8	1.71
8-12	1.12
12-17	0.796
17-22	0.521
22-31	0.322

Run 57

Sample	c/c_o
1-2	8.02
2-3	3.00
3-4	1.70
4-6	1.42
6-9	1.08
9-13	0.754
13-19	0.530
19-31	0.274

Run 58

Sample	c/c_o
1-2	2.58
2-3	2.22
3-5	1.91
5-8	1.64
8-12	1.28
12-17	1.00
17-22	0.704
22-31	0.441

Run 60

Sample	c/c_o
1-2	3.52
2-3	2.47
3-5	2.12
5-8	1.64
8-12	1.27
12-17	0.910
17-22	0.610
22-31	0.387

Run 61

Sample	c/c_o
1-2	3.74
2-3	2.37
3-5	1.97
5-8	1.64
8-12	1.24
12-17	0.945
17-22	0.635
22-31	0.412

Run 62

Sample	c/c_o
1-2	4.66
2-3	2.95
3-4	2.54
4-6	1.99
6-9	1.43
9-13	0.987
13-19	0.664
19-31	0.345

Run 63

Sample	c/c_o
1-2	2.46
2-3	2.15
3-5	1.94
5-8	1.67
8-12	1.31
12-17	1.00
17-22	0.710
22-31	0.455

Run 64

Sample	c/c_o
1-2	2.79
2-3	2.28
3-5	1.92
5-8	1.66
8-12	1.26
12-17	0.952
17-22	0.645
22-31	0.405

Run 65

Sample	c/c_o
1-2	6.46
2-3	3.58
3-4	2.78
4-6	1.91
6-9	1.26
9-13	0.795
13-19	0.525
19-31	0.252

Run 66

Sample	c/c_o
1-2	3.32
2-3	2.82
3-5	2.34
5-8	1.66
8-12	1.20
12-17	0.823
17-22	0.550
22-31	0.338

Run 67

Sample	c/c_o
1-2	3.22
2-3	2.66
3-5	2.20
5-8	1.74
8-12	1.22
12-17	0.860
17-22	0.570
22-31	0.342

Run 70

Sample	c/c_o
1-3	2.29
3-6	1.78
6-11	1.44
11-20	0.976
20-31	0.510

Run 71

Sample	c/c_o
1-3	2.52
3-6	1.77
6-11	1.44
11-20	0.919
20-31	0.471

TABLE XIV

RUNS DETERMINING PS AND PP

Sample	Run 22 c/c_o	$[\eta]'$	Sample	Run 28 c/c_o	$[\eta]'$
1-2	6.98	2.05	1-2	5.80	1.06
2-3	4.77	1.12	2-3	3.85	1.00
4-5	1.91	0.990	3-4	2.87	0.995
8-9	0.938	0.915	4-6	1.97	0.957
13-14	0.450	0.863	6-9	1.64	0.957
18-19	0.264	0.800	9-12	0.956	0.956
23-24	0.176	0.645	12-18	0.648	0.916
28-29	0.146	0.731	18-31	0.290	0.886

Sample	Run 29 c/c_o	$[\eta]'$	Sample	Run 30 c/c_o	$[\eta]'$
1-2	7.40	1.08	1-2	4.45	1.00
2-3	4.04	1.05	2-3	3.50	0.980
3-4	2.87	1.03	3-4	2.88	0.983
4-6	1.90	0.939	4-6	2.10	--
6-9	1.31	0.912	6-9	1.53	0.976
9-12	0.893	0.908	9-12	1.07	0.974
12-18	0.615	0.884	12-18	0.728	0.971
18-31	0.267	0.850	18-31	0.515	0.954

Sample	Run 31 c/c_o	$[\eta]'$
1-2	4.38	1.03
2-3	2.49	0.950
3-5	1.99	--
5-7	1.87	0.941
7-10	1.46	0.942
10-14	1.10	0.916
14-20	0.728	0.924
20-31	0.395	0.889

Sample	Run 32 c/c_o	$[\eta]'$
1-2	9.	1.05
2-3	4.21	0.995
3-4	1.90	0.865
4-5	1.20	0.828
5-7	0.750	0.800
7-11	0.468	0.802
11-17	0.259	0.790
17-31	0.108	0.764

Sample	Run 33 c/c_o	$[\eta]'$
1-2	14.	1.07
2-3	3.64	0.932
3-4	2.30	0.941
4-5	1.35	0.875
5-8	0.876	0.886
8-12	0.520	0.869
12-18	0.313	0.865
18-31	0.141	0.816

Sample	Run 34 c/c_o	$[\eta]'$
1-2	5.05	1.04
2-3	3.35	1.01
3-5	2.55	0.978
5-7	2.26	--
7-10	1.73	0.935
10-14	1.11	0.940
14-19	0.741	0.944
19-31	0.380	--

Sample	Run 39 c/c_o	$[\eta]'$
1-2	4.95	0.593
2-3	3.61	0.575
3-5	2.38	0.540
5-8	1.66	0.522
8-11	1.16	0.491
11-15	0.865	0.480
15-20	0.604	0.455
20-31	0.324	0.428

Sample	Run 40 c/c_o	$[\eta]'$
1-2	3.04	0.533
2-3	2.68	0.528
3-5	2.30	0.531
5-8	1.72	0.530
8-11	1.36	0.522
11-15	1.03	0.525
15-20	0.720	0.520
20-31	0.449	0.518

Sample	Run 41 c/c_o	$[\eta]'$
1-2	4.34	0.569
2-3	2.90	0.546
3-5	2.16	0.521
5-8	1.72	0.519
8-11	1.24	0.518
11-15	0.957	0.517
15-20	0.649	0.517
20-31	0.364	0.514

Sample	Run 42 c/c_o	$[\eta]'$
1-2	4.53	0.579
2-3	3.65	--
3-5	2.34	0.555
5-8	1.45	0.530
8-11	1.04	0.516
11-15	0.721	0.474
15-20	0.479	0.452
20-31	0.281	0.444

Sample	Run 43 c/c_o	$[\eta]'$
1-2	5.45	0.568
2-3	3.40	0.545
3-4	2.40	0.532
4-5	2.34	--
5-8	1.05	0.492
8-12	0.615	0.468
12-18	0.370	0.440
18-31	0.175	0.415

Sample	Run 45 c/c_o	$[\eta]'$
1-2	5.59	0.584
2-3	3.87	0.563
3-4	2.96	0.557
4-6	1.94	0.528
6-9	1.14	0.487
9-13	0.708	0.472
13-19	0.451	0.452
19-31	0.222	0.407

Sample	Run 46 c/c_o	$[\eta]'$
1-2	5.65	0.581
2-3	3.28	0.555
3-4	2.36	0.537
4-5	1.56	0.523
5-7	0.899	0.506
7-11	0.503	0.454
11-17	0.297	0.424
17-31	0.139	0.378

Sample	Run 47 c/c_o	$[\eta]'$
1-2	4.39	0.624
2-3	2.91	0.579
3-6	1.99	0.515
6-9	1.49	0.500
9-13	1.16	0.484
13-17	0.924	0.474
17-22	0.665	0.463
22-31	0.400	0.440

Sample	Run 48 c/c_o	$[\eta]'$
1-2	5.15	0.590
2-3	3.70	0.580
3-5	2.40	0.548
5-8	1.50	0.516
8-11	1.08	0.493
11-15	0.736	0.458
15-20	0.490	0.436
20-31	0.265	0.410

Sample	Run 49 c/c_o	$[\eta]'$
1-2	4.71	0.590
2-3	3.24	0.566
3-5	2.29	0.538
5-8	1.60	0.521
8-11	1.14	0.511
11-15	0.880	0.504
15-20	0.594	0.494
20-31	0.272	0.471

Sample	Run 50 c/c_o	$[\eta]'$
1-2	5.17	0.595
2-3	3.62	0.570
3-5	2.29	0.538
5-8	1.48	0.509
8-11	1.05	0.494
11-15	0.776	0.482
15-20	0.525	0.472
20-31	0.244	0.456

Sample	Run 69 c/c_o	$[\eta]'$
1-2	4.73	0.504
2-3	3.28	0.499
3-5	2.57	0.500
5-8	1.61	0.500
8-11	1.09	0.495
11-15	0.801	0.500
15-20	0.517	0.495
20-31	0.296	0.496

APPENDIX V

DETAILS OF THEORETICAL CALCULATIONS

FLOW PROBLEM

The reduced flow equation was

$$(1/r)(d/dr)(\eta r dv_z/dr) = \rho g + dp/dz \tag{71}$$

with boundary and integral conditions given by

$$v_z = 0 \quad \text{when } r = r_c,\ r_h \tag{72}$$

$$\int_{r_c}^{r_h} \rho v_z r dr = 0 \tag{73}$$

The thermal conductivity of the solvent was assumed independent of temperature so that the temperature gradient was constant across the annulus. The absolute temperature at any $\underline{r}$ is then given by

$$T = \overline{T} + \theta(r-\overline{r}) \tag{74}$$

where $\overline{T}$ is the mean temperature at $\overline{r} = (\underline{r_c} + \underline{r_h})/2$. The density of toluene in the 20-70°C. range of interest is closely linear with temperature, so that

$$\rho = a_o - a_1 T \tag{75}$$

Substituting the equations for ρ and $\underline{T}$ in Equation (71) and integrating once gives

$$dv_z/dr = (b_1 r + (r/2)\, dp/dz - b_2 r^2 + C/r)/\eta \tag{76}$$

where

$\underline{b_1} = (\underline{a_o} - \underline{a_1}\overline{T} + \underline{a_1}\,\theta\overline{r})\underline{g}/2$

$\underline{b_2} = \underline{a_1}\,\theta\underline{g}/3$

$\underline{C}$ = constant of integration.

The viscosity of toluene was expressed as a function of temperature by

$$\eta = a_o \exp(a_3/T) \tag{77}$$

The above constants, obtained from the International Critical Tables, were

$\underline{a}_o$	= 1.1359	g./cc.
$\underline{a}_1$	= 9.225×10^{-4}	g./cc.-deg.
$\underline{a}_2$	= 1.628×10^{-4}	poise
$\underline{a}_3$	= 1050	deg.

The computation (performed on an IBM 1620 computer) consisted of numerically integrating Equation (76) for assumed values of the constants $\underline{dp/dz}$ and $\underline{C}$ with the initial condition $\underline{v}_z(\underline{r}_c) = 0$. The constants were adjusted until Equations (72) and (73) were simultaneously satisfied. Equation (76) was integrated by the Newton-Cotes six-point formula (NC-6) applied on a "sliding" basis--that is, the range of grid points involved in each integration step overlapped the last five-sixths of the range for the preceding step. It was found that the solution stabilized for a number of grid points greater than 140 and remained stable up to at least three hundred grid points. The number of grid points used in the final solution, which had to be a multiple of six, was 144. The first six values of $\underline{v}_z$ were computed using the NC-6 formula on a grid scale six times finer than the main grid. The flow integral (73) was calculated by normal application of the NC-6 formula. The velocity profile was calculated for a 50°C. temperature difference across the annulus and a mean temperature of 45°C. The final values of the adjustable constants were

$$\underline{dp/dz} = -824.872$$

and

$$\underline{C} = -51.9150.$$

The value of dp/dz corresponded to the static fluid pressure gradient of toluene at 45.5°C.

DIFFUSION PROBLEM

The molecular weight and temperature dependence of the diffusion coefficient D for the polystyrene in toluene were needed for a solution of the diffusion equation [Equation (30)]. Literature data at 25°C. for molecular weights from 18,000 to 2,700,000 (54-57) give a relation

$$D_o = 3.02 \times 10^{-4} M^{-0.56} \tag{78}$$

where D_o is the diffusion coefficient at infinite dilution of polystyrene in toluene in the ordinary units of sq. cm./g.

The temperature dependence of D_o may be derived in the following manner. The familiar Einstein equation for free diffusion is

$$D_o = RT/f_o \tag{79}$$

where R is the gas constant and f_o is the molecular frictional coefficient. According to Flory (58), f_o is proportional to the size of the polymer in solution and the viscosity of the solvent. The size of the coiled polystyrene molecule in solution is not very dependent on temperature, and therefore the temperature dependence of f_o may be assumed proportional to that of η_o, the solvent viscosity, which is given by Equation (77). The resulting equation for D_o becomes

$$D_o = 3.45 \times 10^{-5} T/M^{0.56} \exp(1050/T) \tag{80}$$

where M is the molecular weight and T the absolute temperature.

Using the above expression for the diffusion coefficient, the differential equation describing the diffusion process in the column [Equation (30)] was solved by means of the Runge-Kutta method applied to two simultaneous first-order equations. The experimental values of the infinite dilution extinction coefficients were assumed and the thermal diffusion coefficient $\underline{D}'$ was adjusted until the necessary boundary conditions were satisfied. The magnitude of the initial value of $\underline{P}$ did not affect the solution.